Production of Aligned

Short-fibre Composites

MRes Science and Engineering of Materials

By Nicola Jameson

Word count: 14,846

1st September 2012

School of Metallurgy and Materials

College of Engineering and Physical sciences

The University of Birmingham

Abstract

This study investigated a manufacturing process to align short-fibres using a custom-made fibre chopper system. With this technique, continuous waste fibres are chopped, aligned and deposited onto an adhesive substrate to produce aligned short-fibre prepregs. Experimental methods were developed to address issues associated with calibration, a blade inspection criteria and the optimisation of producing parameters to achieve at least 60% fibre alignment in the prepreg.

In order to ensure that the quality and the consistency of the chopped fibre ends were maintained, a criteria was developed to specify when the blade or the fibre chopper should be replaced. This production technique was used to manufacture 8-ply composites using the aligned short-fibre prepregs. Continuous fibre prepregs were also used to manufacture reference composites for comparison purposes. Non-destructive testing via visual inspection and ultrasonic c-scanning was used to determine the quality of the composites.

The physical and mechanical properties of the composite were established using conventional test methods.

The main conclusions reached were:

(i)   The fibre-chopper-based technique developed in this study was capable of producing aligned glass and carbon short-fibre prepregs.

(ii)   The degree of fibre alignment was approximately 70%.

(iii)   The fibre volume fraction was found to be approximately 60%.

(iv)   The Young's Modulus of the aligned glass short-fibre composite was 33 GPa ; in comparison, the corresponding value for the continuous fibre composite was 39 GPa

Acknowledgements

Firstly, I would like to thank my parents and family for their incredible support through my education, sporting activities and social events. I love them all very much and will forever be thankful for all they have done for me in my life to date and the future.

The exceptional network of friends I have made through school, University and sport have left lasting memories and their support has been second to none.

As a student at the University of Birmingham I am happy to say that I have had some incredible times and experiences over the duration of my studies which I will never forget.

I must also show my appreciation to my supervisor Professor Gerard Fernando who has provided support and guidance as well as bringing new ideas into the research.

Finally, I would like to thank all the members of the Sensors and Composites group who have provided an input into my research whether it was in the laboratory or the office. I am thankful for the help and enjoyment they provided as part of the research group.

Table of Contents

1   Introduction

It is well known that fibre-reinforced composites have high strength-to-weight and stiffness-to-weight ratios. Other significant benefits of composites are their fatigue resistance dimensional stability, durability and corrosion resistance. The reinforcing fibre can be in continuous or short forms. The properties of short-fibre composites depend strongly on the microstructural parameters such as the degree of fibre alignment and the fibre volume fraction.

The proposed implementation of EU legislation in the composite industry requires that 85% of composite waste must be recycled and reused by 2015 [1]. Consequently there is an urgent need to develop techniques to reuse, recycle or redevelop waste prepregs and composites. This will reduce the current disposal rate of waste fibre, fabrics, prepregs and composites, as 95% are presently buried in landfill sites in the UK [1]. The increase in demand to improve recyclability of waste fibres has led to the development of techniques to recycle waste preforms and composites including methods to align and produce short-fibre thermosetting composites. The current composite recycling efforts are dominated by two main techniques: (i) the prepregs are ground, chipped, or flaked into a powder of a specified size and distribution that can be used as filler material in polymers; and (ii) the continuous fibres are chopped into short-fibres and are processed to produce sheet-moulding or dough-moulding compounds.

It is generally recognised that the mechanical properties of fibre reinforced composites (FRC) are superior in the direction of the fibres, the relative fibre volume fraction and the degree of fibre orientation. Furthermore, in the case of short-fibre composites, increasing the degree of

fibre alignment and the fibre volume fraction will lead to an increase in the physical and mechanical properties.

A sponsor associated with the project utilises carbon fibre to over-wrap aluminium cylinders using filament winding. The product specification dictates the manufactured product should not contain any 'fibre joints'. Therefore, the last 10-20m of a bobbin or creel are disguarded. Obviously, the development of techniques to utilise this waste will accrue significant commercial, economical and environmental benefits.

This study presents a novel technique to recycle waste E-glass and carbon continuous fibres for the production of aligned short-fibre prepregs. End-of-spool carbon and glass fibres were used as the source materials. The production of aligned short-fibre prepregs required the following: (i) design and construction of a fibre chopper; and (ii) design and construction of a conveyor belt system to house the fibre chopper and an adhesive film.

2   Aims and Objectives

The aims and objectives of the current work were as follows:

(i). To develop a technique to enable glass and carbon fibres to be chopped and deposited in an aligned fashion on an adhesive backed substrate.

This was achieved by modifying a commercially-available fibre chopper. The fibre chopper was adapted to combine the chopping process and the ejection trajectory. Thus it was possible to deposit the chopped fibres in a controlled manor on to a conveyor belt with an adhesive backing.

(ii). To calibrate the output of the custom modified fibre chopper.

Here the chopped fibres were deposited onto an analytical weighing balance which was connected to a data acquisition system. The rotation speed of the fibre chopper was controlled by the applied voltage; the output of the fibre chopper, conveyor belt and traverse were calibrated as a function of the applied voltage.

(iii). To manufacture "reference" composites using a hand lay-up technique.

In order to enable comparison between the continuous fibre and short-fibre composites (manufactured using the fibre chopper) reference composites were made involving end-of-spool glass and carbon fibres. These fibres were hand-laid up on an adhesive film and laminated to give an 8-ply laminate followed by processing in an autoclave.

(iv). To characterise the physical and mechanical properties of the reference continuous-fibre and the aligned short-fibre composites.

The continuous fibre and short-fibre composites were characterised and the following properties were determined: fibre alignment, density, fibre volume fraction, void content, tensile strength, failure strain, Young's Modulus, flexural modulus and short-beam strength.

3   Thesis Overview

Section 1 introduces composites and the need to increase recyclability.

Section 2 details the aims and objectives for the project.

Section 3 shows the overview of the thesis.

Section 4 presents an overview of the literature in the following areas: Composites, fibre reinforced polymer composites and short-fibre composites.

Section 5 details experimental procedures used in the manufacture of the continuous fibre and short-fibre composites. Also involved in this section is information relating to the fibre chopper system calibrations, quality control and material testing procedures.

Section 6 reports the results combined with the discussion of the completed testing procedures.

Section 7 presents a summary of the main achievements and conclusions reached.

Section 8 contains recommendations for future work.

Section 9 contains additional information in an appendix.

Section 10 lists all references used in this report.

4   Literature Review

4.1   Composites

The principle characteristics of a composite material is that they have three main constitutes that are fundamental to their performance. First is the reinforcement which can be continuous fibres, short-fibres or particulates. The second is the matrix which secures the reinforcements in position and transfers the applied load to the fibres. The matrix also offers a degree of protection to the reinforcement. The third component is the interface which is the region between the fibre and the matrix. It is necessary to understand the individual constitutes as their structure forms an important factor in determining the properties of the composite. Fibre-reinforced polymer composites (FRPC) are increasingly used in industrial sectors because they offer unique properties such as: low density, high strength characteristics, high modulus, superior corrosion resistance and higher fatigue properties [2].

4.1.1   Preforms

Preforms are generally available as chopped strand mat, woven fabrics, prepregs, stitched fabrics or braided components [3]. The fibre is an important constituent in a composite as this is the main load-bearing component. The fibre normally occupies 30% - 70% of the composite volume. The fibres are generally treated with sizing agents as this improves the bonding between the matrix [3]. The most common fibres used in polymer matrix composites are glass, carbon and aramid. Common matrix materials include epoxies, polyesters and polyamides [3].

4.1.2 Reinforcements

Table 1 provides a summary of the mechanical properties for specified fibre types. The choice of fibre and its specific properties are selected to complement a specific matrix; the addition of fibres in different volume fractions and orientation allow composites to be customised for specific applications.

Type of Fibre	Tensile Strength (GPa)	Failure Strain (%)	Young's Modulus (GPa)	Density (g/m^3)
E-glass	2.4	3.0	73	2.6
S-glass	3.4	3.9	86	2.5
Carbon HS	3.5	1.5-2.2	220-240	1.8
Carbon HM	3.5	1.3-2.0	290-300	1.8
Carbon UHM	3.4-5.5	0.7-1.0	350-450	2.0
Aramid	2.0-3.0	4.4	60	1.4

HS: High Strength, HM: High Modulus, UHM: Ultra High Modulus

Table 1 Summary of physical and mechanical properties for selected reinforcing fibres [3].

4.1.2.1 Glass fibres

Glass fibres are based on silica (SiO2) with additions of oxides such as calcium and sodium [3]. There are many classifications of glass fibres: E-glass (electrical) fibres are the most commonly used and have good strength, stiffness and electrical properties. C-glass (corrosive) fibres have lower strength but are better suited to corrosive environments whilst S-glass (strength) fibres have higher strength than E-glass fibres but are more expensive [3]. AS-glass (alkaline resistant) fibres have an increase of use in specific environmental conditions. The general advantages of fibre glass include low cost, high tensile strength, high

chemical resistance and excellent insulating properties [4]. The fibre itself is regarded as an isotropic material [3]. When fibres are uniform and parallel to each other the optimal strength of E-glass fibres can be achieved by this alignment [3]. Manufacturers of E-glass fibres are reported to generate approximately 40 tons of waste glass-fibres each week. Therefore, the ability to utilise these waste fibres will avoid the need for them to be deposited in land fill sites (as they are currently).

4.1.2.2 Carbon fibres

Carbon fibres are an anisotropic material and they are used extensively in aerospace, motor racing and top-of-the-range sporting goods. Carbon fibre composites are increasingly being used in new manufacturing applications where the cost of the material can be secondary to design considerations such as increased performance, high strength and reduced weight [5]. Carbon fibres have the disadvantage of lower impact strength than aramid and glass fibres but have a higher fatigue resistance [3].

4.1.3   Matrix

Two classes of resins that are used as the matrix material in FRPC are thermoplastics and thermosets. A thermoplastic resin melts or softens when heated above a specified temperature and turns into a glassy state when cooled. In a thermosetting resin, the curing or cross-curing process is irreversible, where the curing is commonly achieved through the application of heat. Table 2 presents a comparison of the properties of thermoplastic and thermosetting matrix materials. Other curing methods include photo-curing, electron beam and microwave processing [6]. Different resin systems are used depending on the applications, where polyesters, vinyl esters and epoxies probably account for 90% of all thermosetting resin systems used in structural composites [3].

Type of Matrix	Tensile Strength (MPa)	Failure Strain (%)	Young's Modulus (GPa)	Density (g/m^3)	Heat distortion Temperature (°C)
Thermoplastic					
PEEK	90-170	50	3.6	1.26-1.32	150-200
Polypropylene	20-40	300	1.0-1.4	0.9	80-120
Nylon 6.6	60-70	40-80	1.4-2.8	1.14	120-150
Thermosets					
Epoxy	40-80	1.0-20.0	2.0-5.0	1.1-1.4	50-200
Polyester	40-90	2.0	2.0-4.5	1.2-1.5	50-110

Table 2 Mechanical properties of different matrices [3].

4.1.3.1   Epoxy resin systems

With reference to Table 2, it can be seen that the epoxy resins used in composites have lower material properties than the fibres.

Epoxy resins systems are used extensively in the automotive, electrical and appliance applications. Epoxy resins can be cured at temperatures from 5 °C to 180 °C [3], depending on the refractivity of the functional groups and the choice of curing agent. The cure rates can be formulated to meet the required processing characteristics. Curing agents that are typically used in epoxy systems are amines and anhydrides. Table 2 highlights the advantageous properties of epoxies showing low shrinkage [3] during cure. This reduces the internal stresses and ensures the retention of dimensional tolerance after processing. The other advantages of epoxies include high electrical insulation, good chemical resistance, adhesive strength, mechanical properties and pot-life [3].

4.1.4   Interface

The interface is the region between the fibres and the matrix. It is difficult to access the interface region using analytical techniques because it is generally said to be in the region of 2-10 nm. However, the region of the interface is known to have significant bearing on the properties of the fibre reinforced composite [7].

4.2 Fibre reinforced polymer composites

Increased demand for higher performance applications using FRPC has led to the development of innovative manufacturing techniques [10]. Some of the key advantages of composites over other engineering materials are highlighted in Table 3. Carbon fibre reinforced polymer composites (CFRP) are characterised to have a significantly higher modulus and strength [8] than glass fibre composites.

Material	Density (g/m^3)	Young's Modulus (GPa)	Tensile strength (MPa)	Fracture toughness (MPa √m)
Wood	0.6	16	80	6
Metal (mild steel)	7.8	208	400	140
Construction ceramic (concrete)	2.4	40	20	0.2
Rubber	1.2	0.01	20	0.1
Carbon fibre composite	1.5-2	250-390	220-270	100

Table 3 Physical and mechanical properties of specified materials [3] [9].

Depending on the component, it can be a challenge for manufacturing methods to meet the required specifications, fibre distribution, production costs, mirco-structural quality and surface-finish. The processing routes must be adapted in order to achieve the most desirable physical and mechanical properties [10]. There are three common manufacturing techniques used in producing impregnated continuous fibre composites, with many variations and patented techniques. The following section presents a review of selected manufacturing techniques for fibre reinforced polymer composites:

(i) Pultrusion

The process of pultrusion involves continuous pulling of fibres through a resin bath and then into a heated mould, sees Figure 1. The increased temperature inside the mould cures the matrix with the end product showing a constant cross-section structural shape this can be then cut to the desired length.
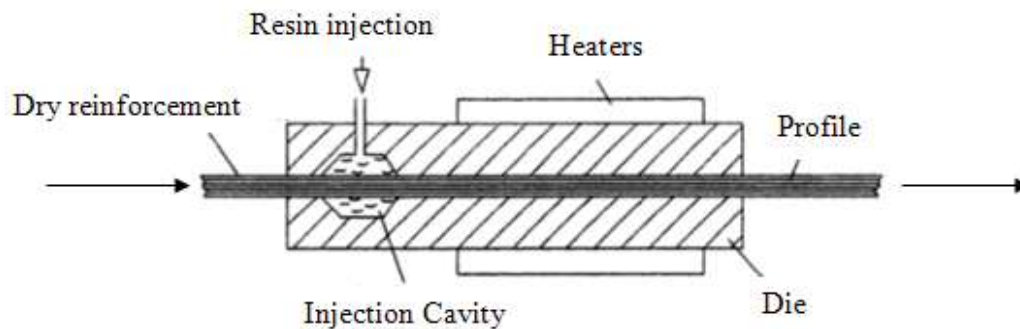
Figure 1 A schematic illustration of a typical pultrusion resin-injection die impregnation [10]

(ii) Wet-filament winding

A schematic diagram of wet-filament winding is shown in Figure 2. The resin impregnated continuous fibres are wound around a mandrel to produce circular or polygonal shapes. After winding, the part is cured in an oven and the composite is extracted from the mandrel.
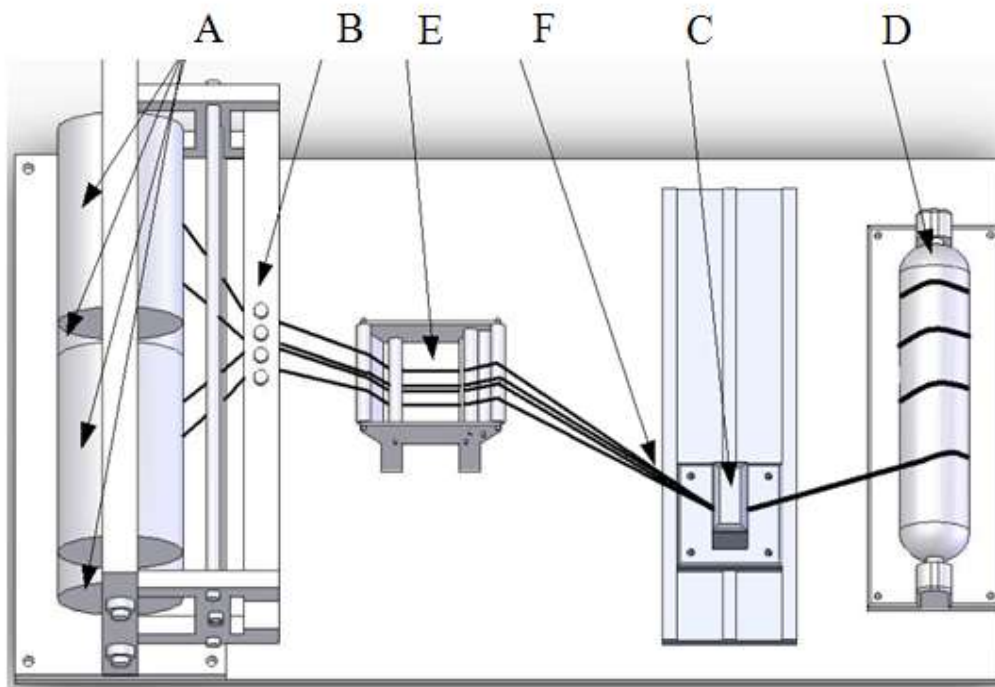
Figure 2 Schematic illustration of the conventional wet-filament winding technique [11]. Labelled are the key components of the system:(A) Fibre creels, (B) Tensioning system, (C) Traverse, (D) Mandrel, (E) Resin bath and (F) Fibre bundles.

(iii) Hand-lay-up

In this manufacturing technique, the prepreg or fabric is laid manually on a mould surface, where fabrics are used. The resin system is applied manually and rollers are used to aid the impregnation process. The advantage of the hand- lay-up process is that different layers of different fibre orientations can be made to the desired part thickness and shape [12] hence offering more isotropic properties. A schematic illustration of the reinforcing layers on a mould with a gel coat is shown in Figure 3. After laminating the preform it is cured in an autoclave. The schematic of the autoclave is shown in Figure 4 illustrates the set-up of parts prior to cure using a combination of heat, pressure and vacuum. The vacuum removes air and volatile components while the part is consolidated; heat and pressure are applied for curing. Rollers are used to aid the impregnation of the fabrics and also to consolidate the laminated layers.
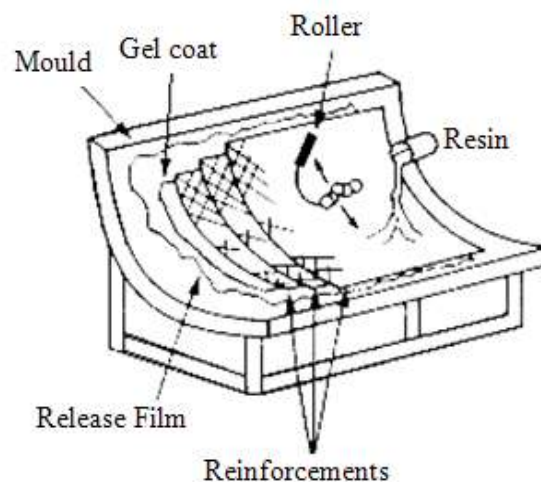
Figure 3 A schematic illustration of the hand lay-up process [12].
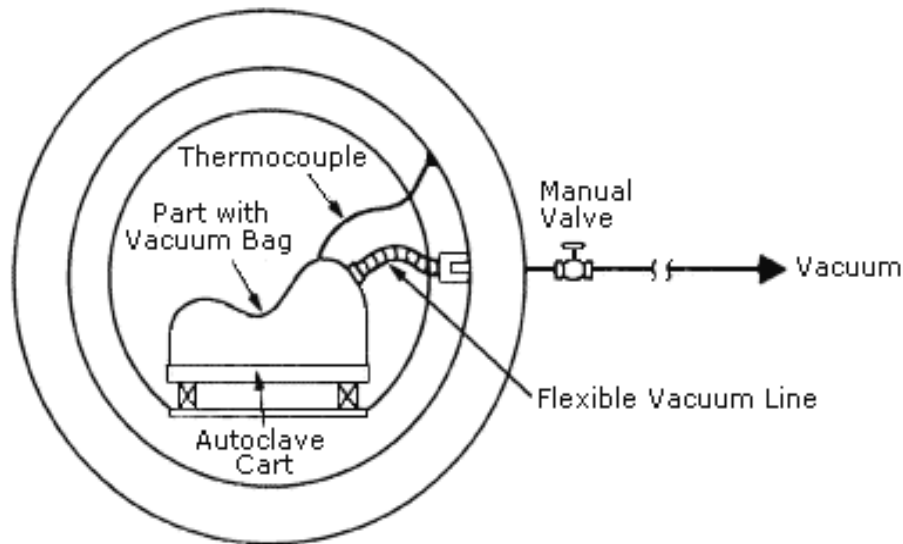
Figure 4 A schematic illustration of a vacuum bagged part place in an autoclave for cure [12].

4.2.1   Matrix cracking

Matrix cracking is localised and generally the initial failure mode and if severe enough can lead to delamination of the plies and eventual failure of the laminate. The energy required for matrix cracking is relatively low, for a brittle carbon / epoxy composite the energy needed could be as low as 0.4 J [13].

4.2.2   Fibre fracture

With reference to short-fibre composites, fibre-ends are common damage initiation sites due to the large stress concentrations [14]. A study by Choi and Takahashi (1992) [25] found it is more logical to consider the tensile strength to be a function of the total number of fibre ends within a sample volume, rather than to consider it to be a function of fibre length. The increase in strain of a composite leads to more cracks progressively forming at the ends of any shorter and/or more misaligned fibres.

4.2.3 Fibre pull-out

In a typical composite, crack initiation occurs from a weakness in a sample. If the stresses are large enough and frictional forces are exceeded, this can result in the fibre being completely pulled out of the matrix [15]. Fibre pull-out is the point where the fibre slides away from the matrix at the fibre-matrix interface, if the crack continues to grow along the length of the fibre it is pulled away from the surrounding matrix. The micrograph in Figure 5 clearly shows the fibre pull-out of a 25% fibre volume fraction, short carbon fibre/ polypropolyene composite.

Figure 5 Scanning Electron Miscopy micrograph of tensile fracture surface of a short-carbon fibre polypropylene composite [32].

After the crack propagates through the fibres, the energy release rate in the specimen is higher than the fracture toughness causing an unstable 'crack jump', until the elastic energy in the specimen is released to a new fibre that stops the crack. The new fibre stabilises crack propagation, and the fracture toughness increases again. The sequence of stable vs. unstable propagation is repeated as the crack grows. It has been shown that initially this cracking can be accommodated by load transfer to adjacent fibres which "bridge" the cracked region. Final failure occurs when the extent of cracking across the weakest section reaches a critical level and the matrix can no longer support the increasing load [25]. Choi and Takahashi (1992) further calculate the tensile failure of short-fibre composites of the stress difference between the interior and the surface of samples. The stress values found in the interior are considerably larger than those on the surface. The failure mechanisms reported that tensile cracks were likely to be formed at the fibre ends of the specimen surface with the cracks growing into the matrix.

4.2.4   Delamination

Delaminations in FRPC are commonly caused by defects introduced during manufacture or impact damage. Dependant on the initiation point of delamination within a material there can be two modes of delamination. If the initiation point is near to the surface of the sample, local delamination can occur, where plies above and below the initiation point split. Global delamination is a caused by internal delamination where plies move in the same direction, if the composite is under compression loading this can result in the composite buckling [15].

4.2.5 Fatigue

Short-fibres offer a potential advantage in terms of fatigue behaviour because they are able to retard crack propagation, by the fibre ends acting as crack arrestors or they divert the crack in a different direction. Curtis *et al*., (1978) [16] used injection moulded samples of short-fibre reinforced polyamide-6 to find the effect of fibre length on material properties and failure characteristics. The level of reinforcement is increased by using a high fibre volume fraction. The test specimens with longer fibres showed greater fibre alignment in the loading direction. These factors lead to higher strength but this is limited by a reduction in failure strain, which appears to follow an inverse relationship to any increase in fibres. Final failure of the samples occurred from an accumulation of cracks in critical cross-sections. This 'weak' area of the material showed that fibres which bridge that section are unable to continue to support the load and fracture [16].

4.3 Short-fibre composites

The use of short-fibre composites have steadily increased, where material cost in the U.S.A have passed \$4.3 billion in 2008 [17] for applications from high-performance automotive components to consumer goods. Short-fibre reinforced polymer composites are very attractive over continuous fibre composites in the following areas [23]: (i) lower fabrication costs; (ii) greater feasibility for mass production; (iii) reduced cycle times; (iv) yield mechanical properties (such as stiffness) to continuous fibre composites; (v) simplistic fabrication of complex parts; (vi) better scales of economy, and (vii) drapability over complex shapes [18].

4.3.1 Mechanical properties

Mechanical properties of composites depend on variables such as: fibre types, fibre lengths, orientations and architecture. Short-fibre composites are typically used for non-primary applications due to lower mechanical properties which are achieved from these composites. However short-fibre composites can approach levels similar to that of continuous fibre composites if: fibre orientation and fibre length is controlled; significantly optimising these critical factors as well as the fibre content and fibre to matrix adhesion [19].

When a load is applied to any composite, the forces at the fibre and matrix are relative to the specified material. Equation 1 describes stresses carried by the fibre and matrix for an applied stress to continuous fibre composites. This relationship is also known as 'Rule of Mixtures' [3].

$$f\sigma_m + (1-f)\,\sigma_f = \sigma_A \qquad\qquad \text{Equation 1}$$

where f is the fibre volume fraction, σ_m is the matrix stress, σ_f is the fibre stress, and σ_A is the applied stress.

It is apparent that as a composite is exposed to internal or external stresses the performance of the material compensates the applied force. Towards the fibre ends the shear stresses increase due to the great shear loads placed on the fibre matrix interface. Figure **6** graphically represents the magnitude of stresses at the fibre ends in relation to the fibre mid-point.
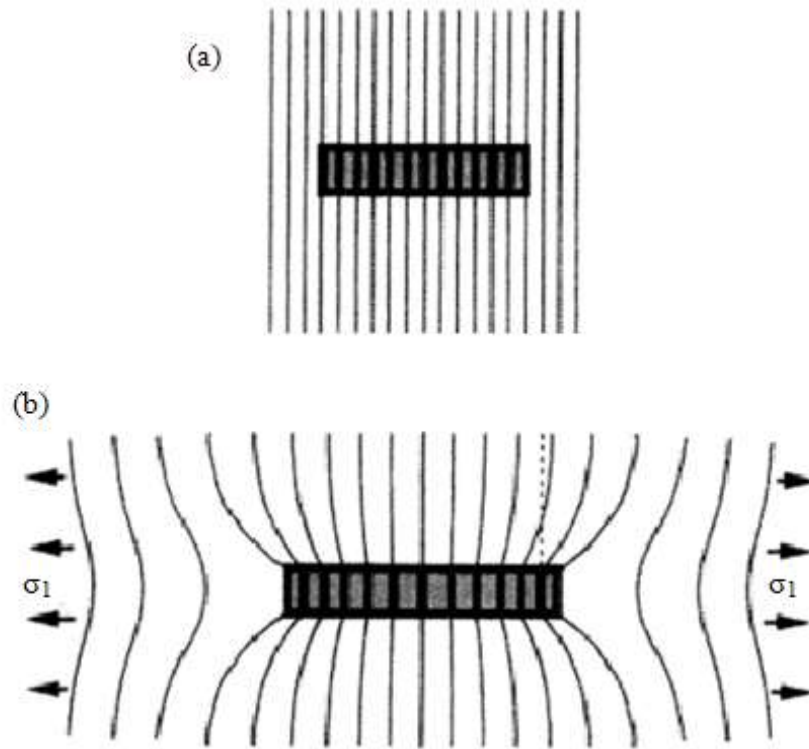
Figure 6 Schematic illustrations of (a) unstressed system and (b) axial displacements introduced on applying tension across the length of a fibre [3].

To predict the mechanical behaviour of short-fibre composites [20]: (i) the elastic behaviour is considered by using unidirectional continuous fibres; (ii) the composite strength is more dependent on mean fibre length or mean fibre aspect ratio than on fibre volume fraction and (iii) the composite modulus is more dependent on fibre volume fraction than on the mean fibre length.

A relationship between failure strain, fibre volume fraction, fibre length and the fibre radius determines the tensile strength of the composite [32]. Harper *et al*., (2009) [31] reported that the orientation of fibres was a function of fibre length and tow size, with longer fibres (115 mm) showing greater alignment [31]. Further improvements in the degree of alignment were said to be possible by using a larger tow because of its higher mass per chopped fibre bundle, where by fibre movement was reduced [21] [31]. Flemming *et al*., (1995) [22] established that the short-fibre length needed to be optimised to give the required material properties for the application, due to the increased stress concentration at fibre ends, but also provide scope for flexibility during manufacture.

4.3.2   Fibre length distribution

Unlike the stiffness, it is accepted that the tensile [23] and flexural [24] properties of short-fibre composites will not be equivalent to their long-fibre counter-part due to increases in shear-stress at the ends of the short-fibres [3]. However as far as the Young's Modulus is concerned, the performances of short-fibre composites are comparable to those in long-fibre composites. Choi and Takahashi (1992) [25] found through microscopy inspection, the failure mechanisms in short-glass fibre reinforced polyethylene-terephthalate were caused by tensile cracks at the fibre ends which grew into the matrix. However, analysis of the interior of the composite showed greater shear yielding and shear cracking along the fibre length direction, at the fibre-matrix interface, with growth of shear bands around the fibre ends. As the fibre aspect ratio increased, the interior shear stresses cause a larger shear failure. Therefore short-fibres are less effective at bearing a load placed on the composite [25] where the stress profile may not be fully developed throughout the short-fibre length [25].

21

Short-fibre composite parts manufactured using spray lay-up, are generally cheaper and quicker to manufacture than those containing continuous fibres, because of the labour-intensive hand lay-up methods and production rates used to produce these composite parts [46]. Tsuji *et al*., (1997) [26] investigated the drapability of uncured unidirectional short-fibres and continuous fibres, where the drapability was defined as the tip deflections, per minute, of a short-fibre reinforced composite cantilevered beam. The authors' findings indicate that uncured short-fibre composites increase the ability to be draped, so more complex and varied shapes can be manufactured, but there is a decrease in longitudinal modulus.

4.3.3   Fibre volume fraction

Short-fibre reinforced composites show an increase in the stiffness and strength properties when compared to un-reinforced materials. Fu *et al*., (2000) [32] found that the greatest mechanical property improvements are obtained with a fibre volume fraction of 25%, in an aligned orientation, using fibres lengths greater than 800 μm.

The volume fraction that any strengthening effect of the fibres is observed is known as the 'critical' fibre volume fraction [27]. This value is used to describe the minimum volume fraction that is necessary for the fibres to carry the applied load with a low proportion of the stress applied to the matrix [3].

With reference to short-fibre composites, a high fibre volume fraction can have an adverse influence the failure mode and is a key factor in determining the material properties [28][31][32]. This problem can be overcome to some extent by increasing the fibre length as it will reduce the number of fibre ends; a primary initiation site for failure [29].

4.3.4 Fibre alignment methods

Within the composite, the short-fibres can be orientated in a random or aligned fashion. It has been reported that randomly orientated preforms offer high drapability [30] but present the most variability in mechanical properties [31]. On the other hand, aligned fibre composites are said to give consistently better mechanical properties [20][32][33]. Therefore, fibre alignment is critical in order for short-fibre composites to exhibit mechanical properties that approach those exhibited by continuous fibre composites.

In order to determine the degree of fibre alignment in a composite careful analysis with respect to fibre position, orientation and distribution is essential. It is well-known that when an inclined or off-axis fibre is viewed in the transverse plane, an elliptical image is seen where the aspect ratio determines the angle, θ to the surface normal. The position of the elliptical profile in relation to a reference axis can be used to determine the orientation of the fibre. As seen in Figure 7, the two angles, θ and ϕ, specify the orientation of each fibre with respect to the dominant y-axis. Where the *z*-axis for these materials is the main fibre direction and θ is the angle between the projection of the fibre image in the *x-y* plane and the *x* axis. These two angles; θ and ϕ, are all that is needed to describe the 3D special orientation of a fibre [34].
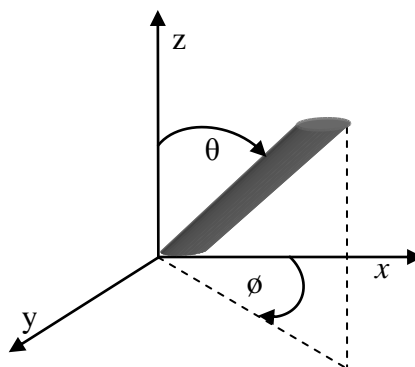
Figure 7 Definition of the fibre angles θ and ϕ to the main fibre direction in the z-axis [35].

Figure 8 can be used to consider the elliptical shape and intersection method, to calculate the misalignment angle ø, with respect to an aligned fibre in the vertical θ plane [35]. Micrographs of polished fibre-ends can be used to derive two-dimensional analysis to calculate the fibre alignment [36]. A single section dimensional method may have drawbacks if a wide orientation distribution of short-fibres is present [34]. However using the shape intersection method (Equation 2) the fibre cross-section in Figure 8 can be used to determine the misalignment angle ø:

$$\text{ø} = a \cos (B/A) \qquad \text{Equation 2}$$
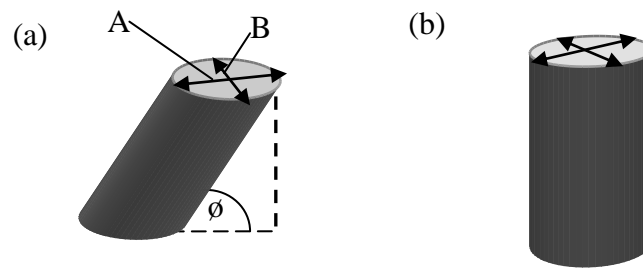
Figure 8 Schematic illustration to show off-axis and aligned fibres; (a) represents an off-axis fibre with a misalignment angle ø, where θ is defined as the major axis; A is the major radius and B is the minor radius of the ellipse, respectively; and (b) an aligned fibre in the θ plane with 100% orientation at 90° to the horizontal plane.

A recent study by Harper *et al*., (2009) [31] investigated the levels of alignment that could be achieved using a spray alignment technique, the mechanical properties that could be attained from these composites was also investigated. It was reported that larger tow sizes tended to prevent misalignment because they were less susceptible to 'disturbances'. Smaller tow sizes were reported to yield higher in-plane properties due to greater levels of fibre homogeneity across the preform. This was said to reduce the magnitude of the stress raisers at the fibre bundle ends. Thus it was claimed that a much higher ultimate strength could be

achieved [31]. The authors showed that inducing fibre alignment could increase both the tensile stiffness and tensile strength of the plaques when compared with random fibre architectures; the tensile stiffness and strength increased by 206% and 234%, respectively. This was apparent when there was a high concentration of aligned fibres (fibre aligned ±10˚) in the loading direction. When compared to a continuous unidirectional composite the maximum stiffness and strength retention obtained were 83% and 31% respectively. Aligned short-fibre composites show similar or increased compressive mechanical properties, when compared to continuous fibre composites, but fail to reach the same value of tensile strength and stiffness, even at 100% orientation [31].

Although superior and more predictable properties can be achieved when using aligned short-fibres as opposed to random short-fibres, there is a major problem with producing composites with aligned short-fibres throughout the material and at even spacing. The following section presents a brief review of the methods already attempted in previous studies to align short-fibres. Current methods to align short-fibres include: hydrodynamics [46], extrusion [37], electrostatics [38], magnetics [39], spray techniques [21], injection moulding [40], compression moulding [41], converging flows [42], centrifugal force [43], vibration [44] and vacuum drums [45].

4.3.4.1   Hydrodynamics

Fluid or hydrodynamic alignment techniques are used to create aligned short-fibre composite parts. This works by suspending the fibres in a highly viscous liquid and alignment is achieved by accelerating the mix of fibres and liquid through a converging nozzle. This forces the fibres to follow the fluid streamlines. This technique is normally used in injection moulding and extrusion. It was reported by Kacir *et al*., (1975) [42] that hydrodynamic methods have the potential for aligning more than 90% of fibres in the range of +/-15°.

Papathanasiou *et al*., (1997) [46] describe the theory behind fluid alignment. They stated that the fibres in the fluid cause a difference in the velocity fields. The velocity on the surface of the fibre, as it moves with the fluid, induces a mismatch and disturbs the surrounding fluid which causes the fibres to rotate. The thinner the fibre, the smaller the velocity mismatch so the fibre rotates slower out of the aligned orientation. A fibre with a high-aspect- ratio was said to be slow to leave an aligned orientation but quick to realign itself once it drifted out of alignment. Therefore fibres with a high-aspect-ratio will be easier to align in a preform, because they spend a large amount of time aligned within the flow, where most of the fibres align themselves along stream lines [46]. The degree of alignment is also thought to be a function of fibre length, with shorter fibres being easier to align in the shear flow of the fluid.

Guell and Graham (1996) [47] investigated fibre alignment using hydrodynamics. A plastic rod (0.16 cm diameter) was passed numerous times in a single direction to achieve fibre alignment of chopped and milled carbon fibres in an epoxy resin system. They reported that the simple motion of the rod being manoeuvred through the slurry was sufficient to induce the fibres into an aligned orientation. Aligning the short-carbon fibres resulted in 90% higher stiffness and an increase of 100% to tensile strength, when compared to randomly orientated fibre composites. These results were in agreement with the predictions acquired from a computer model developed using boundary element computational analysis [46]. In addition, Guell and Graham [47] found the alignment of fibres had a smaller effect on the ultimate strain than the randomly aligned fibres suggesting the aligned fibres exhibit linear stress-strain behaviour right up to fracture. These findings showed the 'aligned' samples had a higher tensile strength and a modulus whilst the ultimate strain was lower.

Fara and Pavan (2004) [48] studied the effects of fibre orientation on the fracture of short-fibre composites, they found that that matrix fracture and fibre de-bonding were a result of low values of fibre orientation while fibre breakage and fibre pull-out were observed in highly orientated composites.

4.3.4.2 Extrusion

Calverty *et al*., (1997) [49] investigated the effect of using extrusion freeform as a method to produce composite structures. The short-fibre carbon composites were manufactured using a syringe and a hot-plate to assist in the curing. It was found that as the length of the fibres increase from 85 μm to 220 μm, an increase in the modulus of 4.0 GPa to 5.3 GPa occurred respectively. It reiterates the relationship that longer fibres show a significant improvement to the mechanical properties [21] such as there is an increase of the modulus, decrease of yield strain while no significant relationship was apparent with the yield stress.

A study by Sanomura and Kawamura (2003) [50] examined the fibre orientation distribution, fibre length and Young's Modulus of extruded short-fibre reinforced polypropylene where the stiffness was predicted using the model by Cox, Fukuda and Kawada [51]. The authors showed that more fibres could align parallel to the extrusion direction by increasing the extrusion ratio. The orientation of extruded fibres was almost uniform throughout the section showing that the control of fibre orientation can be easily achieved by means of ram extrusion. The high fibre orientation caused a greater stiffness which could be improved with increasing the extrusion ratio.

Flemming *et al*., (1996) [22] developed a technique to align short-carbon fibres in prepregs using a two stage process. Carbon fibres were suspended in a thermoplastic supporting liquid and pressed through nozzles onto a sloping rail where the first stage of alignment was achieved. The mixture then flowed onto a rotating cylindrical mandrel and here the final alignment occurred. Figure 9 illustrates the claimed final alignment with an approximate accuracy of ±4°; this is much better than previous hydrodynamic methods of alignment. They reported tensile stiffness and strength retentions relative to continuous fibres to be 94% and 80%, respectively.
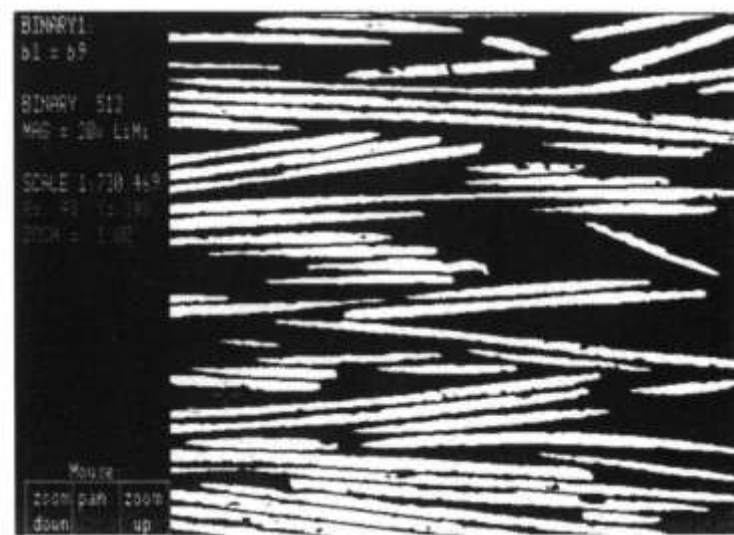

Figure 9 Micrograph of aligned short fibre prepreg [22].

Flemming *et al*., (1996) [22] found there are some disadvantages with using injection moulding and extrusion methods for aligning short-fibres. In the injection moulding and extrusion process fibres are often mixed with the polymer before passing through the screw-extruder, this can cause fibre breakage during processing, which can significantly reduce the length of the fibres in the final product. The mean fibre length was found to decrease linearly with increasing fibre volume fractions and injection speeds because of fibre breakage. A major problem with any hydrodynamic process to be successful is the fibre

concentration must be very low and the fibres dispersed completely in the liquid to prevent any blockages occurring at the injecting nozzle.

Peng *et al.*, (1999) [52] used a slurry-based writing technique to produce aligned short-fibre composites. They reported that it was possible to produce a short-fibre composite component with a 90% degree of fibre alignment with a fibre volume fraction of 18%.

4.3.4.3   Electrostatics

Electric field-based methods rely on the fibre being conductive or this can be achieved by applying coatings such as acidic salts. Electrodes positioned under a moving belt are used to align the fibres in the direction of the electric field lines.

Chirdon *et al.*, (2006) [53] used electrostatics to align short glass fibres (120 μm long and 15 μm diameter) in resin. A mix of resin and fibres were poured into a cell with aluminium strips glued on the inside which acted as the electrode. 6 kV was applied to the aluminium electrode for 60 seconds. The resin was cured under UV light while still subjected to the electric field. Figure 10 shows the degree of alignment achieved using this process.
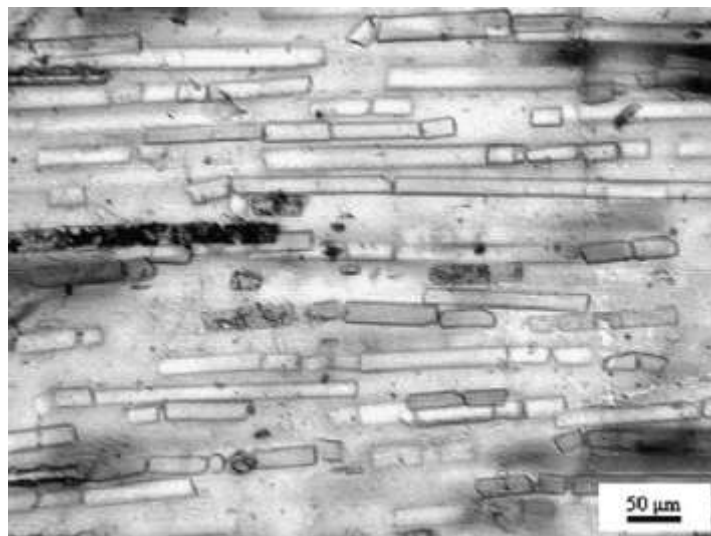

Figure 10 Optical micrograph of a composite aligned by an electric field [53].

4.3.4.4 Magnetics

Yamashita *et al*., (1989) [39] used a magnetic field to achieve alignment of nickel coated short-graphite fibres in an unsaturated polyester resin. In particular they determine the critical fibre volume and looked at the effect the fibre volume fraction had on the control over the orientation of fibres. Their findings showed that the fibre orientation could be controlled if fibres were coated uniformly with a thin ferromagnetic material. It was demonstrated the critical fibre volume fraction increases rapidly with a decrease in the fibre-aspect-ratio, but once the fibre volume is too high the fibre movement becomes limited due to the interaction of the fibres. It is important for a high strength composite that the aspect ratio of the fibres is high. Therefore they introduced ultrasonic vibrations to the fibres with the magnetic alignment; see Figure 11. The authors found that the fibres would detangle making alignment much easier, so increasing the fibre volume fraction. This experiment focused on the through-thickness alignment of particles and therefore control of fibre orientation for large components will need further investigation.
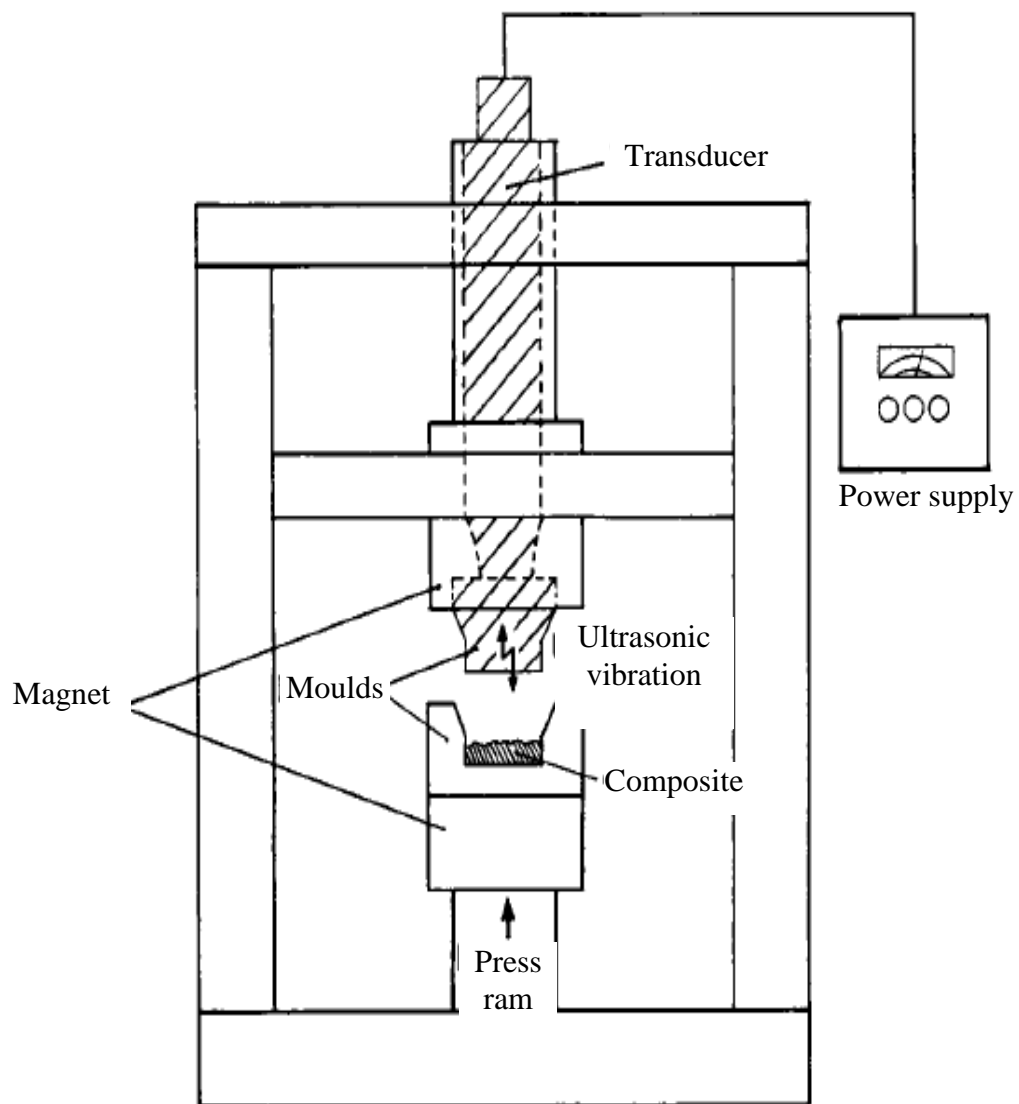
Figure 11 Schematic drawing of the combined magnetic and vibration apparatus

used to align short graphite fibres [39].

4.3.4.5   Spray techniques

Harper *et al.*, [21] [31] [14] produced a preform by using a robot-mounted mechanical chopper head, which sprayed carbon fibres and a polymeric, powdered binder onto a mould, see Figure 12. Airflow was passed through the tool to secure the deposited fibres in place. Once the spray had covered the mould, the other side of the mould was lowered to compress the preform in order to control the thickness. The preform was extracted from the mould and transferred to a separate part moulding station for the injection of liquid resin to produce the final composite part. The effectiveness of the vacuum holding the fibres has a reduced effect on the top layers of fibres so the alignment tends to decrease as the through-thickness dimension increases.
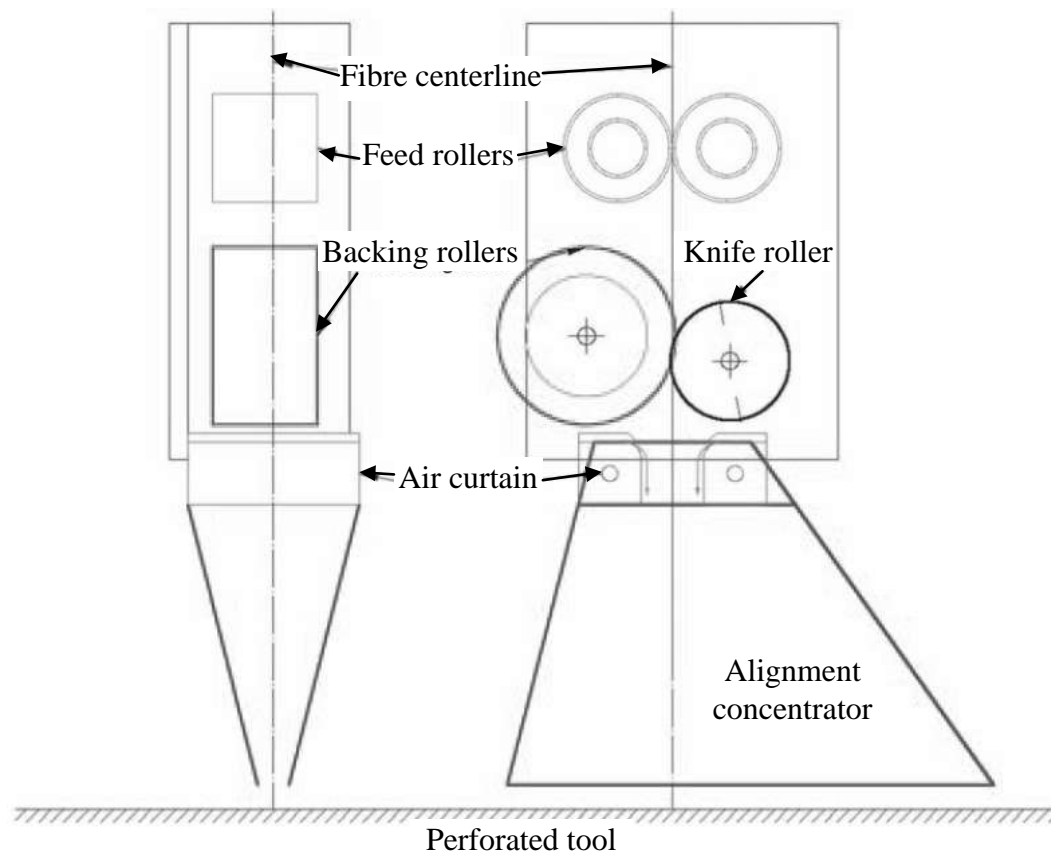
Figure 12 A schematic illustration of the short-fibre spraying/chopping method [31].

4.3.4.5.1 Mechanical properties of aligned short-fibre composites

Over the past 40 years detailed research into the manufacture of aligned short-fibre composites has seen huge improvements to the quality, control and versatility of such techniques. It is clear that the methods available are effective at producing short-fibre composites with some fibre alignment. Table 4 summarises different short-fibre alignment techniques accompanied by their physical and mechanical properties. The comparison between manufacturing processes shows the interaction between fibre length and fibre material, and the impact they have on the material properties.

Author	Year	Fibre type: CF- Carbon GF-Glass	Manufacturing process	Young's Modulus (GPa)	Tensile strength (GPa)	Failure strain (%)	Fibre volume fraction (%)	Fibre length (mm)
Dodworth [54]	2009	CF 6K tow	Spray deposition and compression	-	0.60	-	50	37
Harper *et al.*, [21]	2008	CF 24K tow	Directed preforms-spray technique	36.9	0.13	-	31.7	28.5
		CF 24K tow		62.8	0.31	-	33.8	115.5
		CF 6K tow		33	0.25	-	33	28.5
		CF 6K tow		36.6	0.46	-	36.6	115.5
Turner *et al.*, [55]	2007	CF	Hydrodynamics	13	0.16	-	30 to 60	12
Hassan *et al.*, [56]	2004	GF	Injection moulded	1.25	0.0012	0.74	23	12
Fu *et al.*, [32]	2000	GF	Extrusion compounding and injection moulding	8.8	0.05	1.2	25	0.15-0.3
		CF		15	0.059	0.5	25	0.15-0.4
Calverty *et al.*, [49]	1997	CF	Extrusion	4	0.07	1.8	15*	0.085
		CF		5.3	0.076	1.5	15*	0.22
		CF		5.9	0.062	1.1	20*	0.085
		CF		7.5	0.064	0.9	20*	0.22
Guell and Graham [47]	1996	CF	Hydrodyamics	5.82	0.0017	0.38	0.17	0.015
Flemming *et al.*, [22]	1995	CF	Fluid flow	10	1.1	-	50	3

*weight fraction

Table 4 A table summarising the physical and mechanical properties of short-fibre alignment techniques.

5 Experimental

5.1 Materials

5.1.1 Reinforcements

E-glass fibres and carbon fibres were used as the reinforcement materials in the production of continuous fibre and short-fibre composites.

Four different fibres were used for the production of continuous fibre composites: (i) carbon fibre T700 (Toray); (ii.) out-of-shelf-life pre-impregnated carbon fibre*; (iii) E-glass fibres (PPG Industries) 1200 TEX**; and (iv) E-glass fibres (PPG Industries) 2400 TEX.

*Confidential

**TEX is the mass, in grams, of 1 km of fibre strand.

E-glass fibres 1200 TEX and carbon fibre T700 were the selected materials to manufacture into short-fibre composites using the fibre chopper system.

5.1.2 Matrix

The matrix material for the composites manufactured in this study was HexPly 913, an epoxy resin system with a low-temperature cure cycle, supplied by Hexcel. Manufacturer's reported that the material had a tensile yield strength of 65.5 MPa and a tensile modulus of 3.39 GPa.

5.2 Manufacture of continuous fibre laminates

The continuous-fibre 8-ply laminates were produced using a hand lay-up technique. Figure 13 shows a schematic illustration of adjacent fibre tows which cover an area of the resin. The fibre tows were placed manually on the resin system. The resin film was approximately 0.45 m x 0.16 m. The number of fibre tows used per ply was between 25-40 dependent on the reinforcing material.

Figure 13 A schematic illustration of the placement of the fibre tows over the resin material.

5.2.1 Differential scanning calorimetry

The glass transistion temperature (Tg) of the out-of-shelf-life pre-impregnated carbon fibre was assessed using a differential scanning calorimetry (Diamond DSC, ParkinElmer, UK). Small sections of prepreg were placed in an aluminium DSC pan and the sample was subjected to a temperature ramp from 30 °C to 250 °C at 40 °C/minute.

5.3 Short-fibre prepreg manufacturing process

A commercially available fibre chopper was purchased from Fibreglast (USA) and custom-modified whereby the pneumatic motor was placed by an electric motor from a cordless screw driver (Argos Value Range 12V).

5.3.1 Fibre chopper

Figure 14 illustrates the fibre chopper that was used for cutting the continuous fibre tow into lengths of approximately 25 mm. The fibre tow was drawn from a bobbin and directed through a rubber anvil and a brass feeder-roller before led to a six-blade chopping head mechanism. The fibre chopper was driven at a set voltage. The three components were individually cog driven from the dominant chopper head component, see Figure 15.
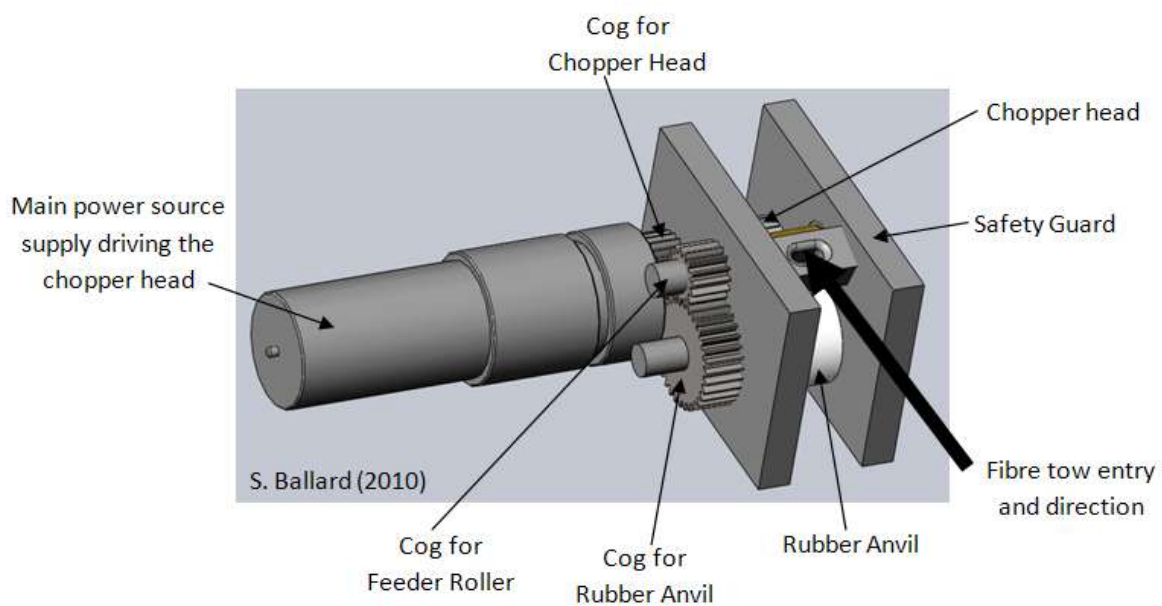

Figure 14 A systematic diagram to show the custom-designed fibre chopper.

The fibre chopper was mounted on a computer-controlled traverse platform. Once cut, the fibres fell directly on to a conveyor belt covered in the adhesive resin film. To obtain optimum fibre coverage on the resin film, light pressure was applied to the chopped fibres as they were delivered to the resin film by a small (10 mm diameter and 30 mm long) rubber roller. The speed at which the conveyor belt rotated was altered in relation to the chopping speed. Once the short-fibres were delivered to the resin film, the traverse drive mechanism was used to achieve full fibre coverage over the resin.

Feeder roller cog

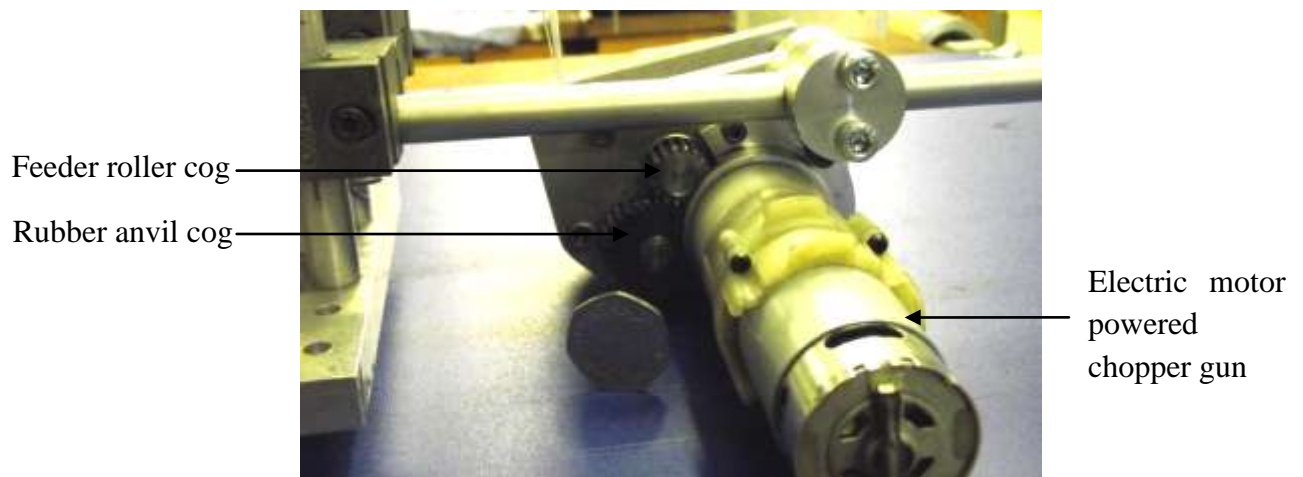Rubber anvil cog

Electric motor powered chopper gun

Figure 15 Photograph of the cogs and electric motor powered chopper gun used in the fibre chopper system.

5.3.2 Voltage-control system

Figure 16 shows the dual power supply that controls the voltage to the electric motor powered gun in order to drive the rotating blade component. The equipment was controlled manually to give a fibre throughput depending on the speed of the traverse and conveyor belt systems respectively.

Figure 16 The power supply (EX354D Dual power supply) used to drive the fibre chopper.

5.3.3 Conveyor belt

A 1.6 m long and 0.45 m wide polyurethane belt was purchased from Conveyor Lines Ltd. The schematic illustration of the conveyor belt system in Figure 17 shows the basic set-up of two Perspex rollers to aid in a uniform rotation of the belt.
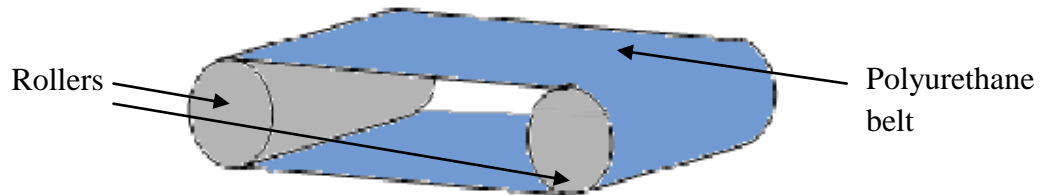

Figure 17 A schematic illustration of the conveyor belt system using two rollers and a polyurethane belt.

The conveyor belt speed was controlled using a dial setting from an EX354D Dual power supply. This could be adjusted from 0 to 99.9 arbitrary units, where higher values increase the speed of the belt. The static charge created by the rotation of the belt inhibited fibre alignment; therefore the fibre chopper was earthed using appropriate materials and connections.

5.3.4 Traverse system

The traverse device (Rexroth) shown in Figure 18 was controlled using software IdEasy provided by the manufacturer. The programme was capable of a range of speeds and accelerations. The speed and acceleration of the traverse device were input manually in the software. The traverse device was able to travel a maximum distance of 0.6 m but for the purpose of the fibre chopper system a maximum distance of 0.35 m was used.
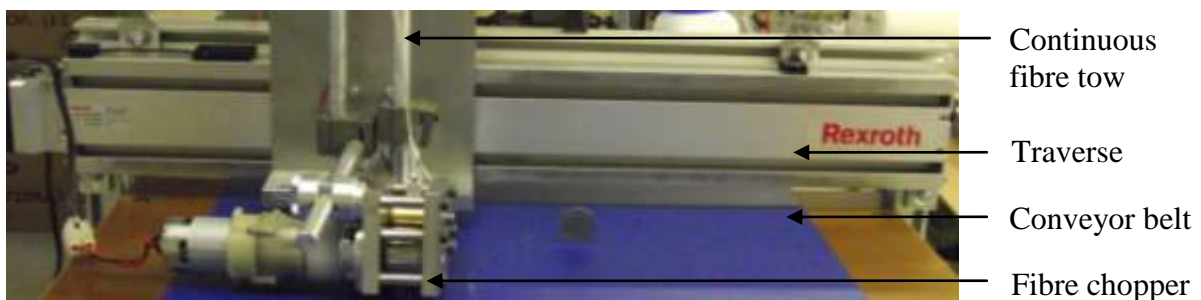

Figure 18 A photograph of the traverse system with the fibre chopper attached.

5.3.5 Unwinder

A fibre bobbing unwinder (1xPX REWIND-253-09) supplied by Pultrex was used to provide the fibre chopper with continuous carbon fibres at a constant delivery rate. Depending on the fibre chopper rate, the unwinder gradually accelerated until the required unwinding speed could be maintained.

5.4   Calibration of the fibre chopper and conveyor belt system

The following sections describe the parameters that were calibrated with regard to the fibre chopper and the conveyor belt system.

5.4.1 Fibre deposition rate

The fibre deposition rate (grams/minute) was measured using the following procedures. Glass fibres and carbon fibres were chopped individually and delivered for 30 seconds onto analytical weighing balance (Ohaus, New Jersey) using LabView software and a data acquisition system. The chopper was initially set at 3 V, and was increased at increments of 0.5 V, up to 6.5 V. This was repeated five times at each voltage and the results were averaged.

5.4.2 Chopper speed

A digital photo tachometer and reflective strips were used to calibrate the individual revolutions per minute (rpm) of the feeder roller, rubber anvil and chopper head. Values were varied from 3 V to 6 V in 0.5 V increments. The relative speeds of the above mentioned items were recorded three times at each voltage setting and the results were averaged.

5.4.3 Conveyor belt system

The dial setting on the EX354D Dual power supply was calibrated to determine a linear speed per setting. Eight test settings ranging from 10-80 were used, with three trials for each dial setting. Equation 3 was used to calculate the rotation speed of the conveyor belt system:

$$\text{Speed (metres/second)} = \frac{\text{Distance (metres)}}{\text{Time (seconds)}} \qquad \text{Equation 3}$$

5.4.4 Traverse system

The traverse system was calibrated to determine the accuracy of the traverse speed per setting. Seven speeds from 1 mm/sec to 30 mm/sec were used and three trials were performed per speed. Equation 3was used to calculate the speed over a 0.1 m section of the traverse system.

5.4.5 Angle of the chopper head

The chopper head was adjusted to identify the optimal position to achieve maximum alignment. The angle of the chopper head varied from 0° - 40° relative to the conveyor belt where that delivery of short-fibres occurred. Visual inspection and a digital camera positioned 30 cm from the conveyor belt were used to analyse the trajectory of fibres.

5.5   Short-fibre prepreg production

Two carbon fibre composites and two glass fibre (prepregs) laminates were produced using the fibre chopper. From the calibration experiments, settings were determined to achieve optimal coverage of aligned fibres. Eight equal sections were cut (165 mm x 400 mm) from the prepreg to make the eight plies.

5.6   Composite manufacture

With reference to the continuous fibre laminates manufactured in section 5.2 and the short-fibre prepregs produced using the settings summarised in section 5.5 an additional layer of the resin film was applied to each ply illustrated in Figure 19.
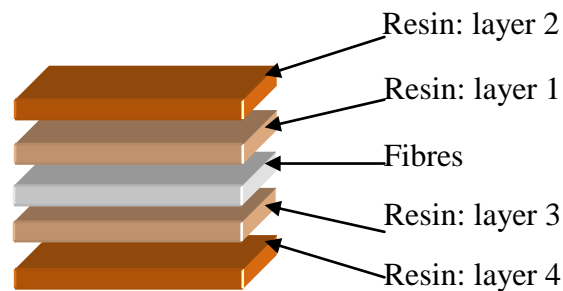

Figure 19 A schematic illustration of a single laminate structure, composed of a single layer of fibres sandwiched between four layers of resin.

Each laminate was aligned with the one below it and consolidated to make an 8-ply prepreg. Each of the 8-ply prepregs were de-bulked using a 'vacuum-bag' process within an autoclave for 30 minutes; this consolidated the fibres and resin together under vacuum. The composite was cured in an autoclave using the cure schedule recommended by the manufacturers.

5.6.1 Autoclave

The autoclave (Leeds and Bradford Boiler Company) used in the production of the composites followed a set programme; detailed as followed in Table 5:

Target Temperature (°C)	Temperature ramp rate (°C/min)	Duration at target temperature (mins)
125	2.0	110
50	2.0	1
0	1.0	0
Target pressure (bar)	Pressure ramp rate (bar/min)	Duration at target pressure (mins)
1.38	0.14	2
48.27	0.14	135
1	0.07	1

Table 5 A summary of the cure schedule for the production of composites.

5.6.2 Short-fibre prepreg alignment

Short-carbon fibre and glass fibre prepregs (350 mm x 230 mm) manufactured using the fibre chopper system were divided into six equal sections (100 mm x 100 mm) and individually photographed using a digital camera. Each section was enlarged to scale where misaligned fibre bundles were identified using visual inspection followed by a superimposed box outline. Figure 20 illustrates the box outline method used to analyse the angle of the fibres bundles, which were then placed in four categories: 0°>5°, 5°>10°, 10°>15° and >15°. The twelve sections of prepreg were analysed where the weight of resin and backing paper were taken into account before determining the total number of fibre bundles.
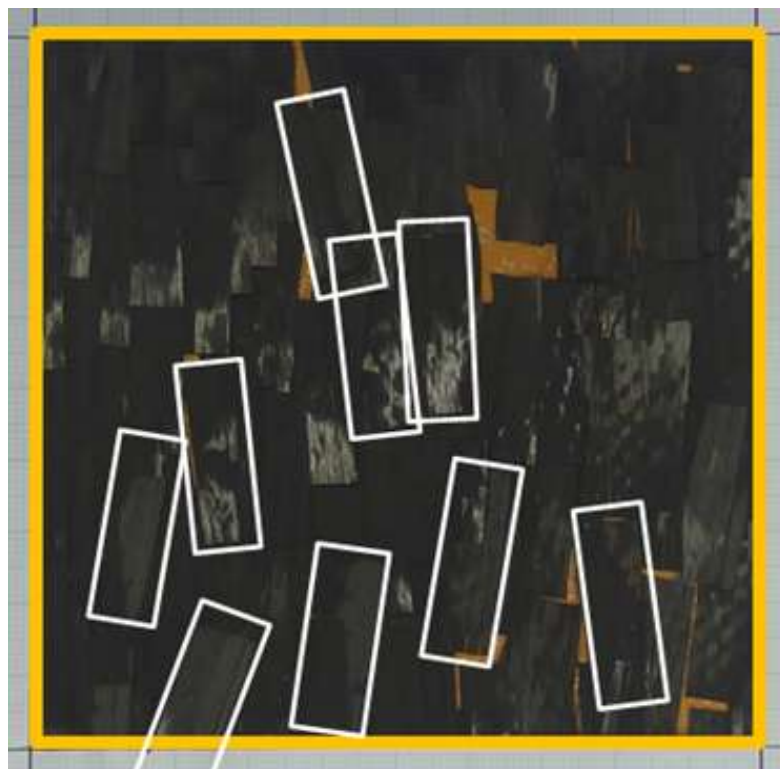

Figure 20 Photographs of carbon-fibre prepreg section with highlighted box outlines to analyse fibre alignment.

5.6.3 Short-fibre prepreg coverage

The fibre coverage was quantified using individual ply images taken using a digital camera and a superimposed grid (5 mm x 5 mm). Each square was inspected visually to evaluate the fibre coverage, an example of which is shown by Figure 21. If a square in the grid was occupied by 50% or more of resin, the square was contrasted with an alternative colour. All squares were included to find the average resin content of each ply and as a complete 8-ply prepreg.
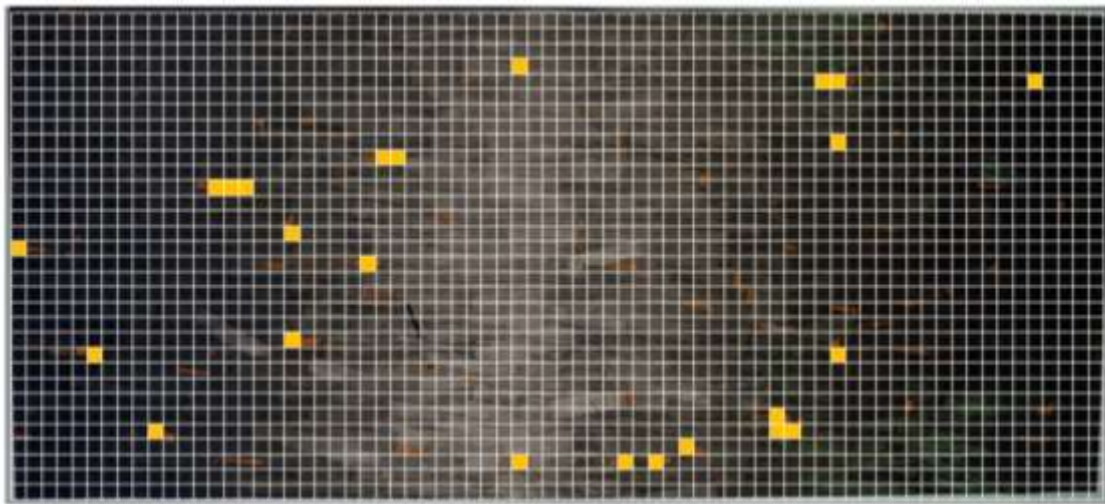

Figure 21 A photograph of a carbon fibre ply and superimposed grid used to quantify the fibre coverage.

5.7   Quality Control

5.7.1 Macro imaging

Photographs using a digital camera and back-lighting were used to characterise continuous fibre composites. Both glass fibre 1200 TEX and glass fibre 2400 TEX were imaged using this procedure to detect any visual flaws or features visually.

5.7.2 C-Scan

C-scans of the continuous fibre and short-fibre composite plates were taken using software Ultrawin. The C-scan used ultrasonic waves to determine the quality of the plate by measuring the amplitude of the reflecting waves. Each scan was performed at a rate of 10 cm/second and optimal gate settings. Gate settings were operator dependant where a colour intensity scale (0-100%) provided the resulting plate quality.

5.7.3 Scanning Electron Microscopy

Scanning Electron Microscopy (Joel 6060, SEM) was used to investigate the fibre-end quality, blade quality and fractography. The settings were adjusted and controlled to provide optimal images. The fibre samples were sputter coated with gold to prevent the accumulation of electric charge on the specimen during inspection in the SEM.

5.7.4 Optical Microscopy

Image analysis, using a Swiss, axioskop-2 microscope, investigated the integrity of the chopper blade, fibre alignment and fibre volume fraction. Microscope software Axiovision 4.6 was used to capture the images at appropriate magnifications.

5.7.4.1   Chopped fibre end -face quality, blade inspection and blade replacement

SEM was performed to inspect the quality of out-of-shelf-life carbon fibres. This study focused on the surface-quality and fibre-ends cut using a fresh blade. Further analysis investigated the glass fibre-ends and the effect of the cutting rate where the fibre chopper was set between 2-8 V.

SEM images and optical microscopy compare the amount of damage to used and new chopper blades, inspecting side and top-down profiles. To maintain a high quality of the chopped fibre-ends the relationship between the chopper setting and blade rotation was used to establish a criteria to replace the blade.

5.8   Test methods

The continuous-fibre and short-fibre composite plates were characterised to determine their physical and mechanical properties; the number of samples per test and material are summarised in Table 6.

	Continuous fibre 8-ply composite				Short-fibre 8-ply composite			
	Carbon fibre	Out-of-shelf-life carbon fibre	Glass fibre 1200 TEX	Glass fibre 2400 TEX	Carbon fibre 1	Carbon fibre 2	Glass fibre 1	Glass fibre 2
Fibre alignment	78*	78*	78*	78*	78*	78*	78*	78*
Density	5	5	5	5	5	5	5	5
Fibre volume fraction	30*	30*	5	5	30*	30*	5	5
Tensile	5	5	7	7	7	7	-	7

*frames used by image analysis

Table 6 A summary of the number of samples used for characterising the continuous composites and short-fibre composites.

48

5.9   Physical properties

5.9.1 Composite fibre alignment

Three samples with dimensions of 20 mm x 20 mm were taken from continuous fibre and short-fibre eight-ply composite plates. The samples were potted in Epofix resin, polished to 0.25 μm using a Buehler automatic polisher, and imaged using optical microscopy explained in section 5.7.4. To investigate the alignment, each sample was divided into 26 equal sections and an image was taken from the centre of each section; a total of 78 frames. Only whole fibres in each frame were included where the individual fibres were categorised as aligned or off-axis as seen by Figure 22. In this report Equation 4 was used to determine whether a fibre was off-axis:
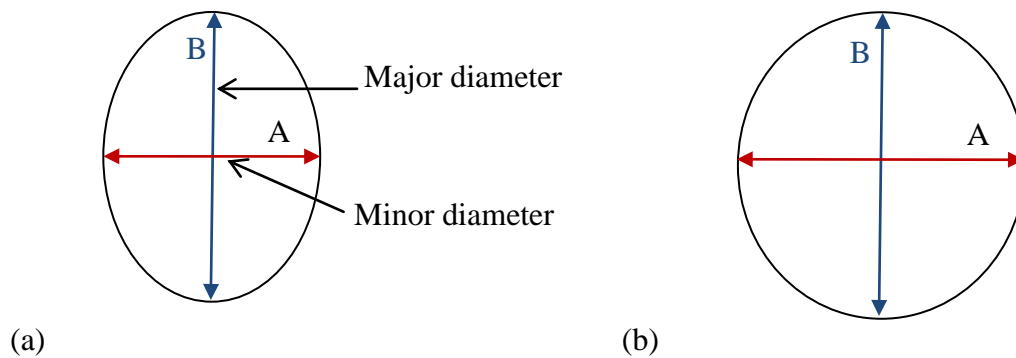

(a)   (b)

Figure 22 A schematic illustration of the cross section of (a) an off-axis fibre
and (b) an aligned fibre.

$$A + \tfrac{1}{4} A < B$$

Equation 4

where A is the minor diameter and B is the major diameter of the ellipse.

5.9.2 Density

Density measurements of five samples (20 mm x 20 mm) were found using an analytical weighing balance (Ohaus). Each sample was weighed in air (weight) and distilled water (buoyancy), with reference to the water density, to find their relative density using Equation 5:

$$\frac{\text{Mass of sample in air (g)}}{\text{Sample buoyancy (g)}} \text{ x density of test liquid = sample density (kg/m}^3)$$

Equation 5

5.9.3 Fibre volume fraction

5.9.3.1   Glass fibre composites

Five samples of dimensions 20 mm x 20 mm were cut from the continuous fibre and short-fibre 8-ply glass fibre composites were used to calculate the fibre volume fraction and void content in accordance with ASTM D2584 [57] and ASTM D2734 [58] respectively. This was calculated using the resin burn-off weighing method, where the resin of the sample was burnt-off at 565˚C for 3 hours and left to cool in the oven overnight.

5.9.3.2   Carbon fibre composites

Optical microscopy and image analysis detailed in Section 5.7.4 were used to characterise the fibre surface volume fraction of the continuous fibre and short-fibre carbon composites. An automated measurement programme wizard used to determine the fibre area per frame by selecting individual fibres. In total, 30 frames were used per material, at X50 magnification. The colour contrast between the fibre and the matrix determined an area percentage, where the values were averaged.

5.10 Mechanical properties

5.10.1 Tensile strength, failure strain, Young's Modulus

The tensile properties of the composite plate were determined in accordance with ASTM D3039 [59]. Composite specimens (20 mm x 200 mm) were cut from each 8-ply plate. Aluminium end-tabs (20 mm x 50 mm x 2 mm) were adhered at the ends of the composite using Scotch-Weld 9323 adhesive. Figure 23 shows an end-tabbed sample secured in a Zwick 1484 machine. Each sample had a 50 mm gauge length and was tensile tested at a cross-head displacement rate of 2 mm/minute until failure. The mechanical properties (tensile strength, failure strain and Young's Modulus) were calculated using the output from software Testexpert II.
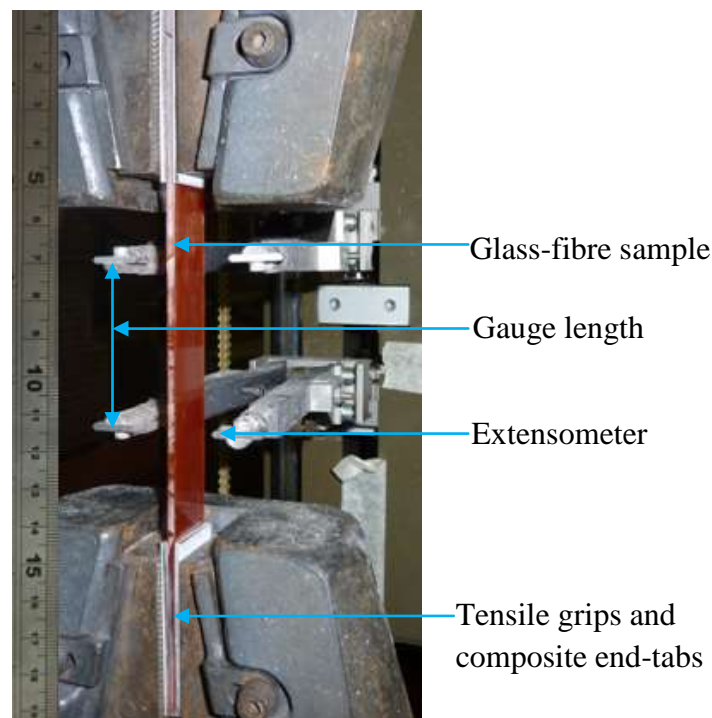

Figure 23 Photograph to show the set-up of a glass-fibre composite tensile specimen.

Visual inspection and macro-imaging were performed on all continuous fibre and short-fibre samples. Fractography using an SEM (Joel 6060) examined representative failed composites investigating transverse, longitudinal and surface sections of common failure features.

6   Results and Discussion

6.1   Short-fibre composite

6.1.1   Calibrations of the fibre chopper

6.1.1.1   Fibre deposition rate

Figure 24 shows the fibre deposition rate for carbon and glass fibres. Co-efficient of determination (R^2) values of 0.99 was obtained for both materials with the exception of the case where the fibre chopper was operated at 6.5 V. This difference was due to the error introduced in collecting the chopped fibres in a specified time at the faster chopping rate. Overall the data presented in Figure 24 shows that the fibre deposit had a low variation and the error bars plotted are negligible. The fibre delivery rate can be used when adjusting parameters to produce a composite with a high fibre volume fraction. With reference to Figure 24, the difference in slopes for the two fibre type was due to the variation in the density with each fibre type. As expected the material with the higher density (glass fibre) showed a steeper slope. Other possible contributing factors include: differences in the tension and friction between the fibres and the surface of the fibre chopping device.
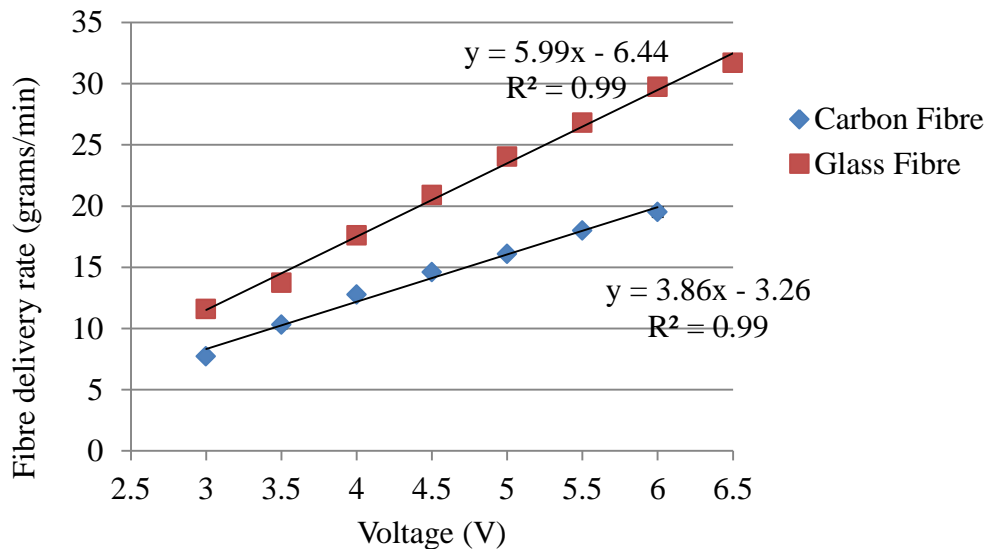

Figure 24 The delivery rate of carbon and glass fibres using the fibre chopper system.

6.1.1.2   Chopper speed

The tachometer was used to estimate the revolutions per minute (rpm) of the feeder roller, rubber anvil and chopper head at various applied voltages. As expected Figure 25 shows that the rotation speeds for each rotating component increased with a higher voltage. As predicted the smaller diameter feeder roller had a greater rpm than the rubber anvil and chopper. The R^2 value of 0.99 was observed for all of the components confirming a low error between the rotation rate and the applied voltage. It can be seen there was a positive linear relationship with all three components, which confirms the feed rate was effective at delivering continuous fibres to the chopper head at a constant rate.
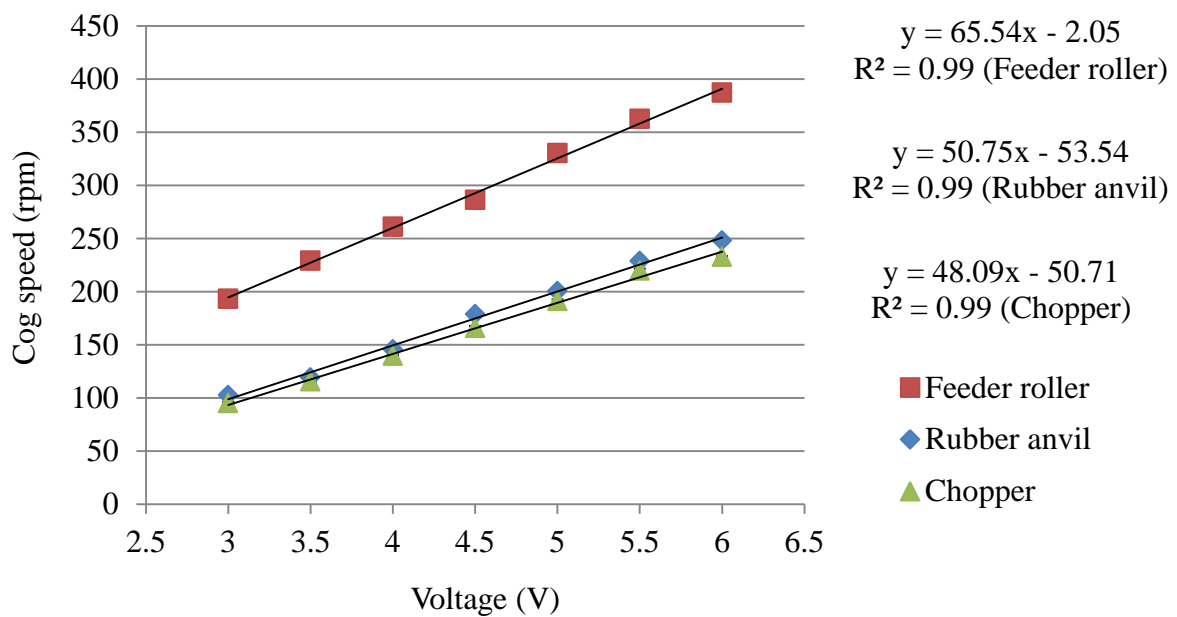

Figure 25 Graph showing the revolutions per minute of the feeder roller, rubber anvil and chopper head at voltages 3 V- 6 V.

6.1.1.3 Conveyor belt

The conveyor belt calibration results presented in Figure 26 show a positive linear correlation between the conveyor belt setting and the speed, which is expressed by the linear trend value R^2 of 0.99. The calibrated conveyor belt speed ensured control is achieved in respect to the fibre delivery rate and length of the short-fibres.
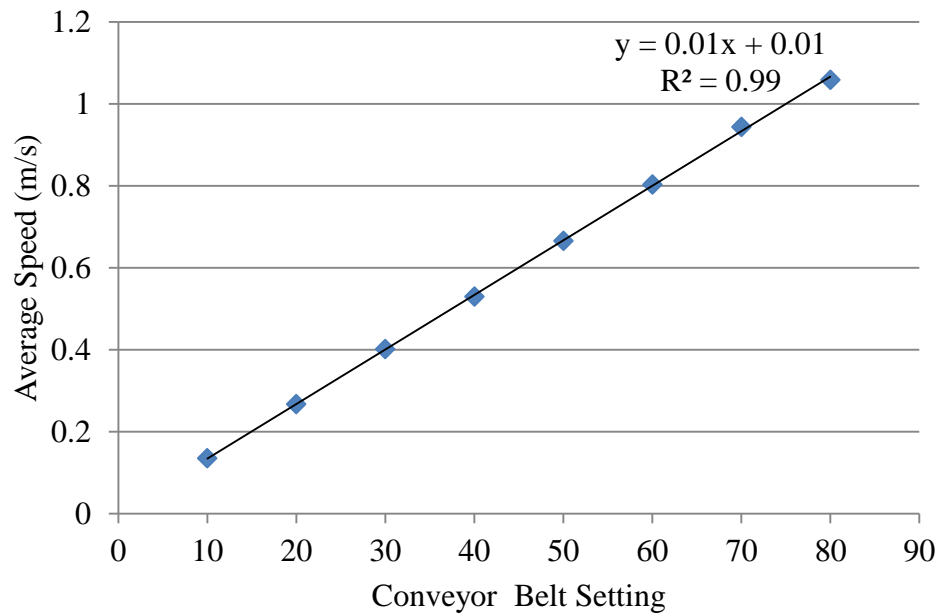

Figure 26 The calibration of the conveyor belt setting against an average speed over three trials.

6.1.1.4   Traverse system

Figure 27 shows the relationship between the set traverse speed and the measured speed. An optimum traverse setting was dependent on the delivery rate, conveyer belt speed and the width of the fibre bundles. A positive linear relationship was present between the set and measured speeds where the error bars are negligible.
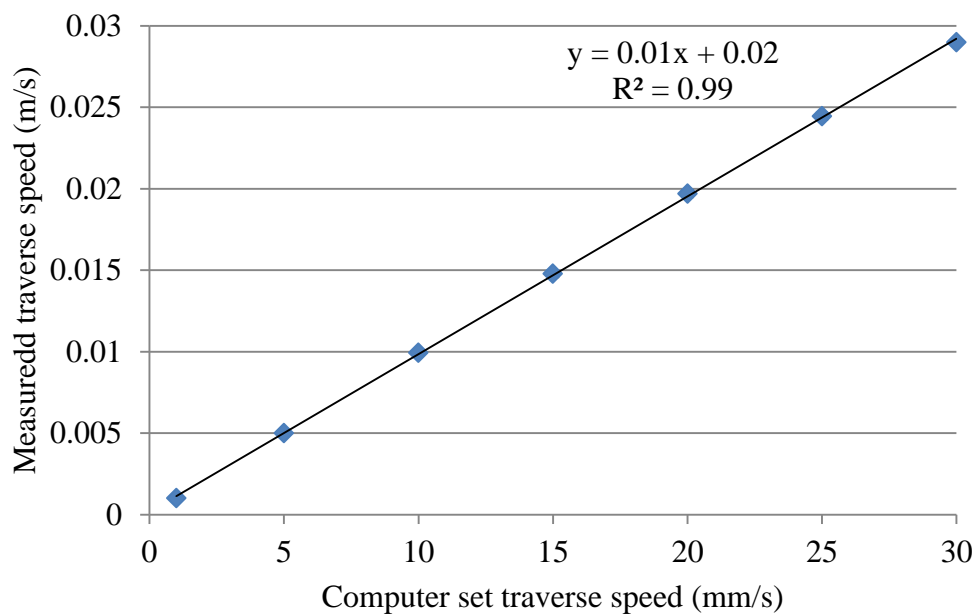

Figure 27 A graph showing the relationship between the set and measured traverse speeds.

In summary, the fibre delivery rate, cog rotation, conveyor belt and traverse all correlate in a positve linear relaitionship, as expected. The reliabilty of these results can be used to calculate an estimated range of setting values and speeds depending on fibre materials, fibre lengths, fibre widths and the rate of production required.

6.1.1.5 Angle of chopper-head

The motion of the chopper blades force the fibres to be deposited onto the belt at an angle. Figure 28 presents the variation of carbon fibre alignment with a change in angle of the chopper head relative to the conveyor belt. Visual inspection determined that the maximum degree of alignment was achieved by setting the chopper head to an angle at approximately 25° for both carbon fibres and glass fibres. The adjustment of the chopper head created the fibres to flow following a natural alignment process. Inevitably with a change in speed or material these characteristics may alter and adjustment will need to be made accordingly.
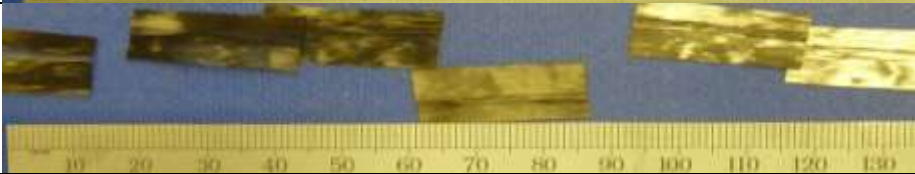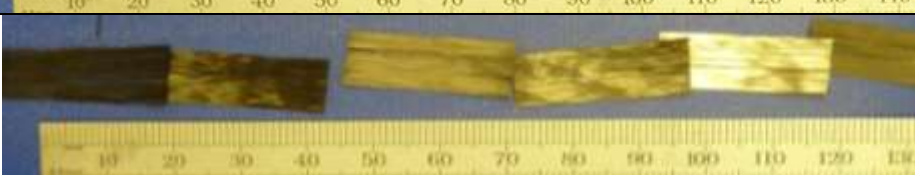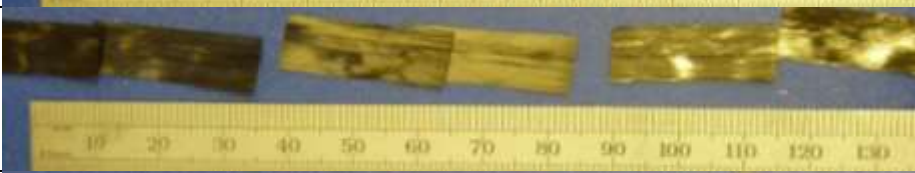
Angle of the fibre chopper head	Images of chopped carbon fibre bundles delivered to the conveyor belt
0°	
10°	
20°	
25°	
30°	
40°	

Figure 28 Photographs of short-carbon fibres delivered to the conveyor belt at various chopper head angles in relation to the conveyor belt.

6.2   Production of short-fibre composites

Optimal processing parameters such as the chopper speed, conveyor belt setting, traverse speed and fibre unwinder setting were used to produce aligned short-fibre prepregs. The calibrations and visual analysis enabled the settings in Table 7 to produce an aligned short fibre prepreg. The control achieved meant that reliable production of carbon-fibre and glass-fibre prepregs could be achieved.

Parameter	Glass fibre	Carbon fibre
Chopper speed (V)	5.75	3.5
Conveyor belt setting	17.8	14.5
Traverse speed (m/s)	0.00033	0.0005
Unwinder setting	n/a	50

Table 7   Processing parameters used for short-fibre prepreg production using the fibre chopper system.

6.2.1   Fibre alignment in the prepreg

A typical micrograph of fibre alignment for carbon fibres are shown by Figure 29. Each category is demonstrated where an average of the fibre alignment of carbon and glass short-fibre prepregs are summarised in Table 8. The analysis showed the overall fibre bundle alignment at <5° was found to be 79% for glass fibre and 89% for carbon fibre, respectively.

Angle (°)	Glass fibre 1	Glass fibre 2	Carbon fibre 1	Carbon fibre 2
0>5	77	81	90	88
5>10	4	6	6	5
10 >15	5	3	1	3
>15	1	10	2	5

Table 8 Table to show fibre alignment obtained in two carbon fibre and glass fibre prepregs.
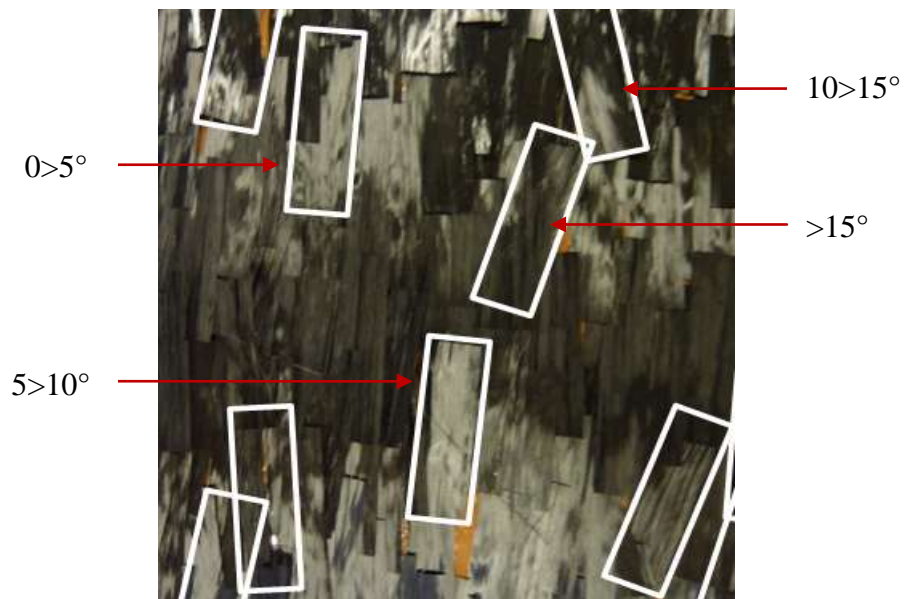
Figure 29 A micrograph to represent the fibre alignment using the fibre chopper system.

Figure 30 shows the fibre chopper system can produce highly aligned short-fibre prepregs. Glass fibre prepregs reported a greater misalignment but overall the variability was low for both materials over two separate prepregs. In conclusion, the fibre chopper can produce prepregs with at least a 75% fibre alignment.

Figure 30 A micrograph to show the quantification of angles for carbon-fibre lengths.

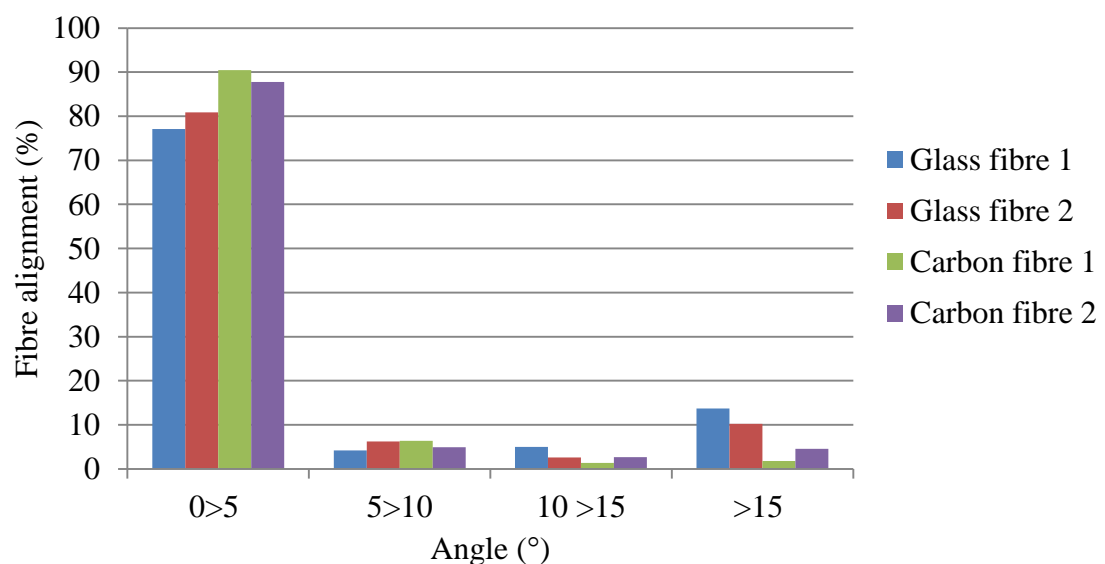Fibre coverage in the prepreg Table 9 shows each of the eight plies and the amount of occupied squares of resin compared to fibres. Average prepreg fibre coverage with respect to resin in a single ply using carbon fibre was 98.74% and 97.11% for glass fibre.

Ply Number	Carbon Fibre coverage (%)		Glass Fibre coverage (%)	
	Prepreg 1	Prepreg 2	Prepreg 1	Prepreg 2
1	98	99	98	96
2	98	99	98	96
3	99	99	98	97
4	98	99	97	97
5	99	99	97	97
6	99	99	97	97
7	99	99	97	98
8	98	99	96	97
Average	98	99	97	97
SD	0.64	0.20	0.83	0.62

Table 9 A table summarising fibre coverage and averages for carbon and glass fibre prepregs.

Figure 31 shows favourable fibre coverage of 99 ± 0.7 % and 96 ± 0.3 % can be achieved for carbon fibre and glass fibre composites, respectively. The low variation in fibre coverage shows the fibre chopper can produce prepregs with a high fibre volume fraction. This will benefit the material properties as a greater percentage of fibres occupy the resin matrix.
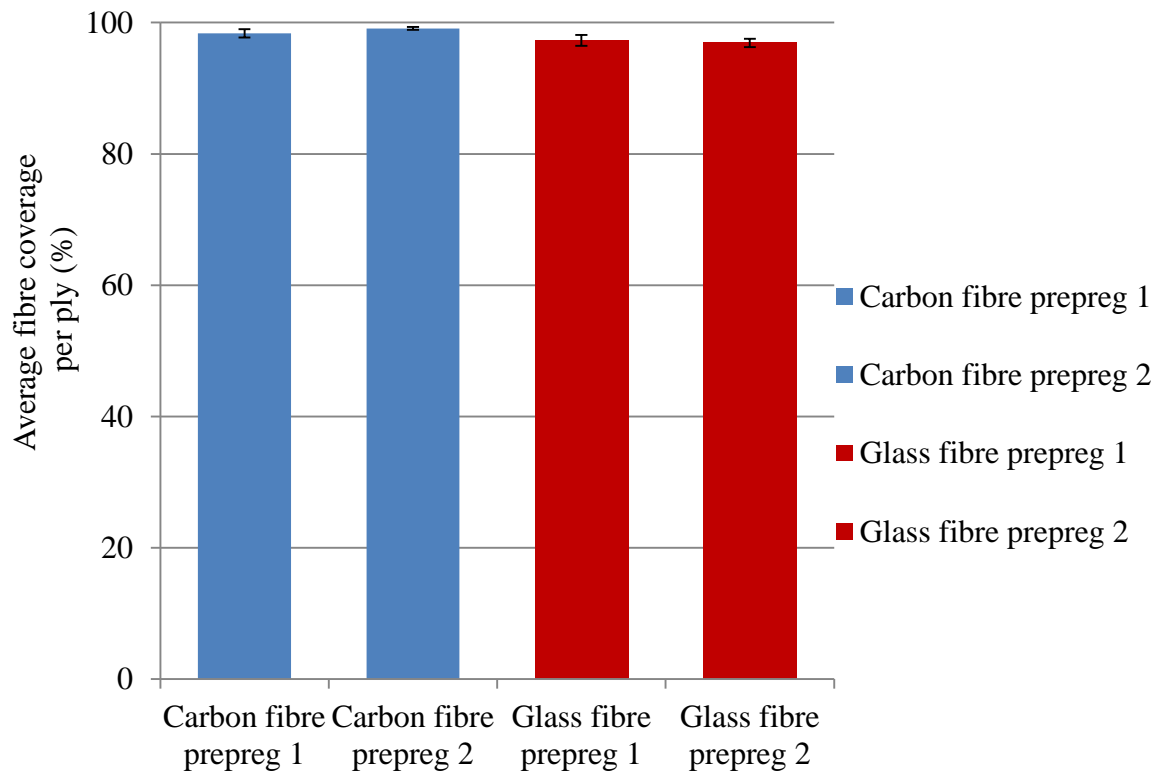
Figure 31 A graph to show the fibre coverage of the short-fibre prepregs manufactured by the fibre chopper.

6.3 Production of continuous fibre composites

6.3.1 Differential scanning calorimetry

Figure 32 shows the glass transition temperature (Tg) of out-of-shelf-life carbon fibre to be 160°C. To ensure matrix integrity during manufacture, Hexply 913 resin remains a suitable material due to the reduced curing temperature at 125°C.
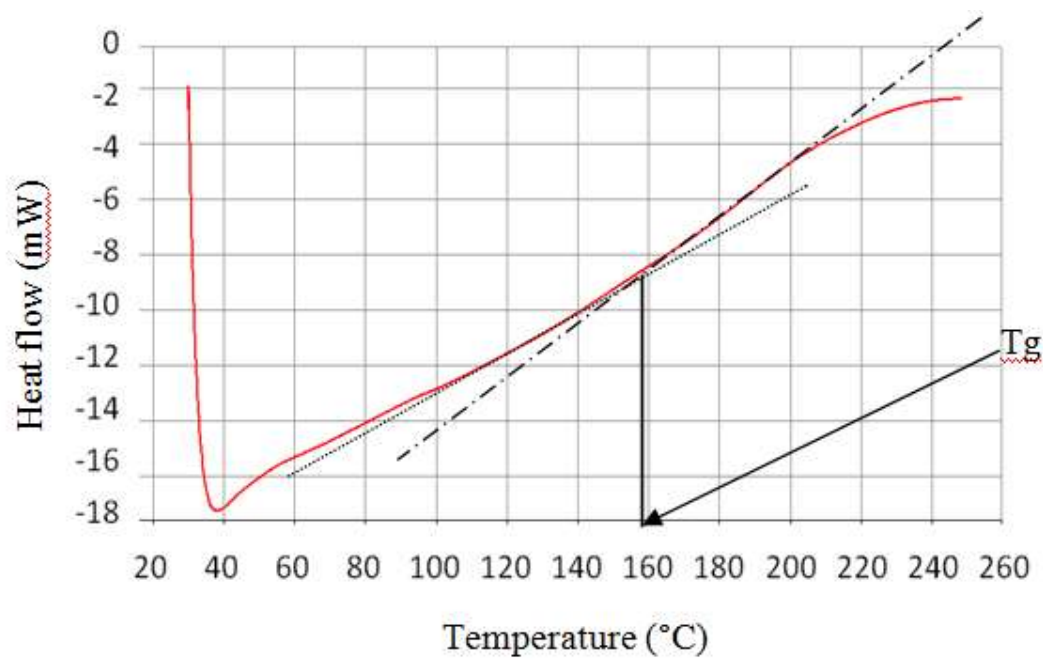
Figure 32 Differential Scanning Calorimetry trace of the out-of-shelf-life carbon fibre, highlighting the glass-transition temperature.

6.3.2 Macro imaging

Figure 33 shows back-lit images of the continuous glass fibre composite plates. Both images show a unidirectional fibre structure with a high fibre volume fraction. The glass fibre 2400 TEX composite appeared to show 'waves' of fibres; these sections are likely to be caused by a lack of matrix resin due to the larger fibre tow, so unimpregnated fibres are apparent.

(a)

(b)

Figure 33 Image of continuous 8-ply glass fibre composite (a) 1200 TEX and (b) 2400 TEX.

6.4   Quality control

6.4.1   C-scans

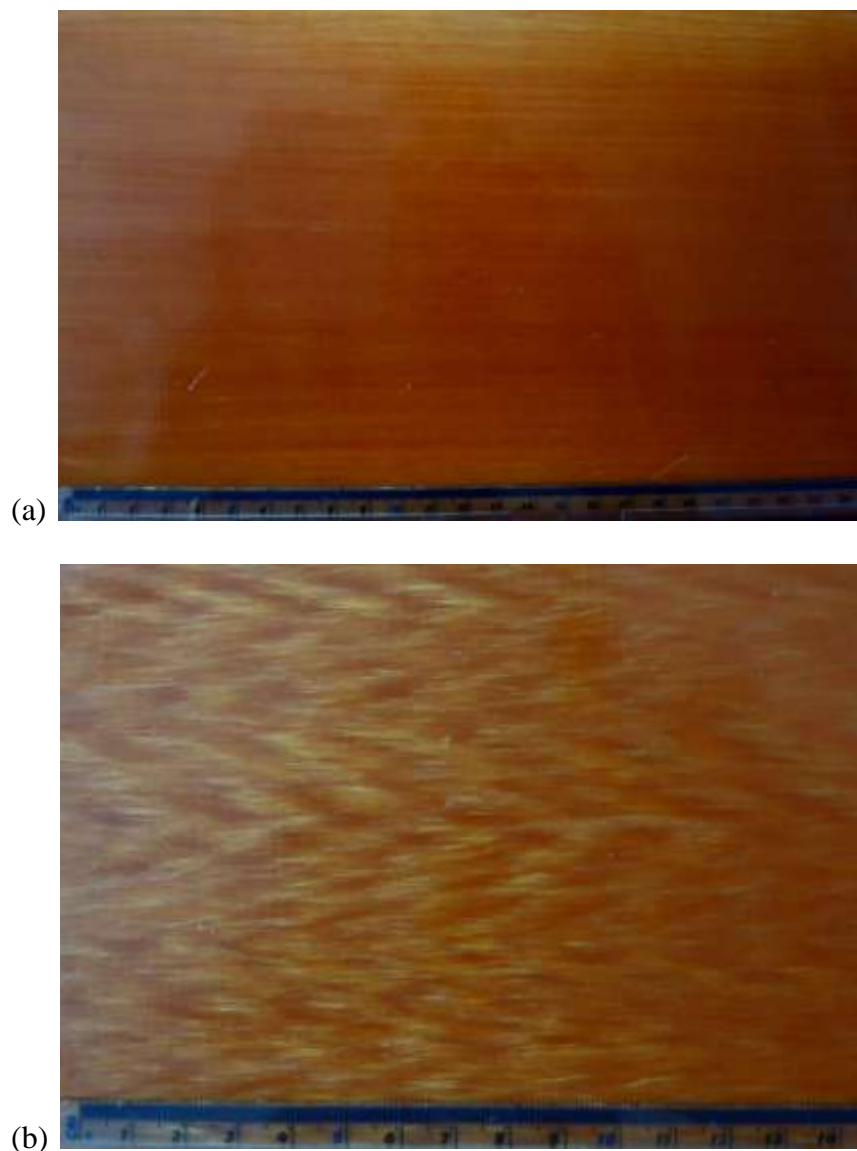Figure 34a-c show C-scan images of the continuous fibre composites; glass fibre 1200 TEX, glass fibre 2400 TEX and carbon fibre respectively. The left y-axis scales are the percentage of detected ultrasonic waves within the predetermined gate setting. The x-axis and right y-axis show the dimensions, in centimetres, of the C-scan performed.   The largest black rectangle shows the section of the composite used for mechanical testing. While the numbered sections of the composite and the arrows indicate sections used for image analysis and their polished faces respectively. The C-scan images use a colour scale where blue region indicate the bottom of the C-scan tank, due to the lower reflected signal in this region. The green areas show 100% ultrasonic wave detection (reflected signal), therefore high amplitude of reflective waves was measured. The red regions indicate possible flaws in the composite; these may include voids, lack of resin content, reduced fibre volume fractions, scratches or an uneven surface quality. Both of the continuous glass fibre plates were in a post-cure state where sample edges show a greater degree of variability.

(34a)

(34b)

(34c)
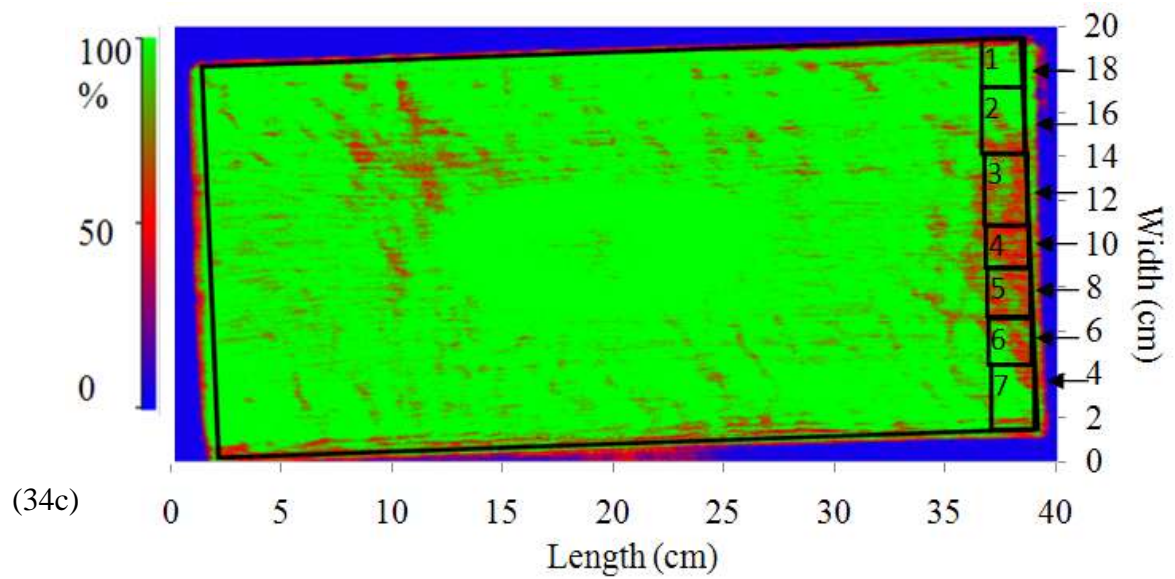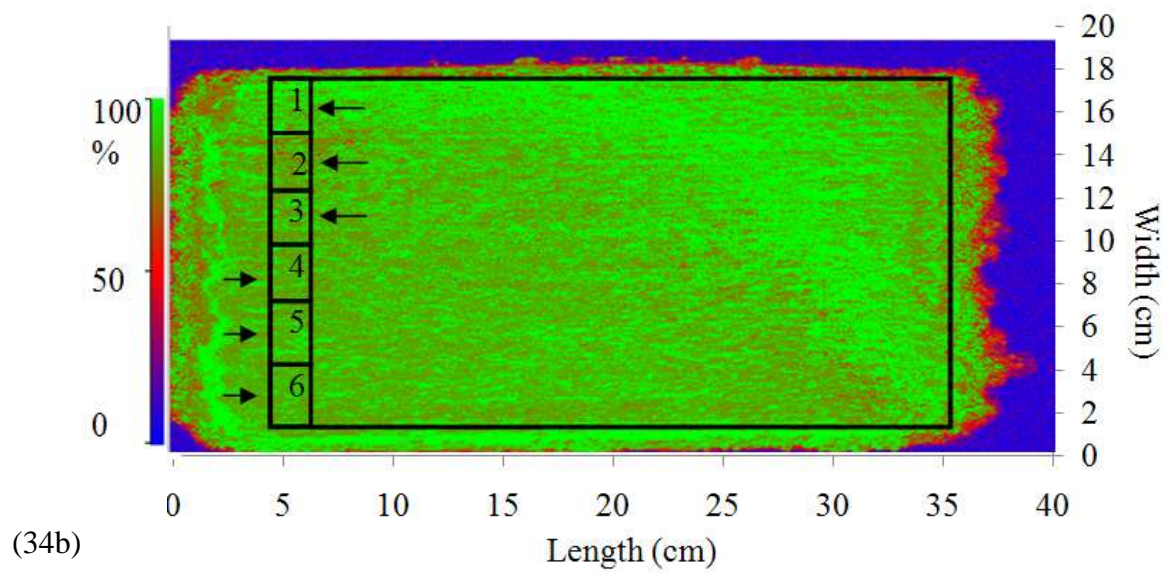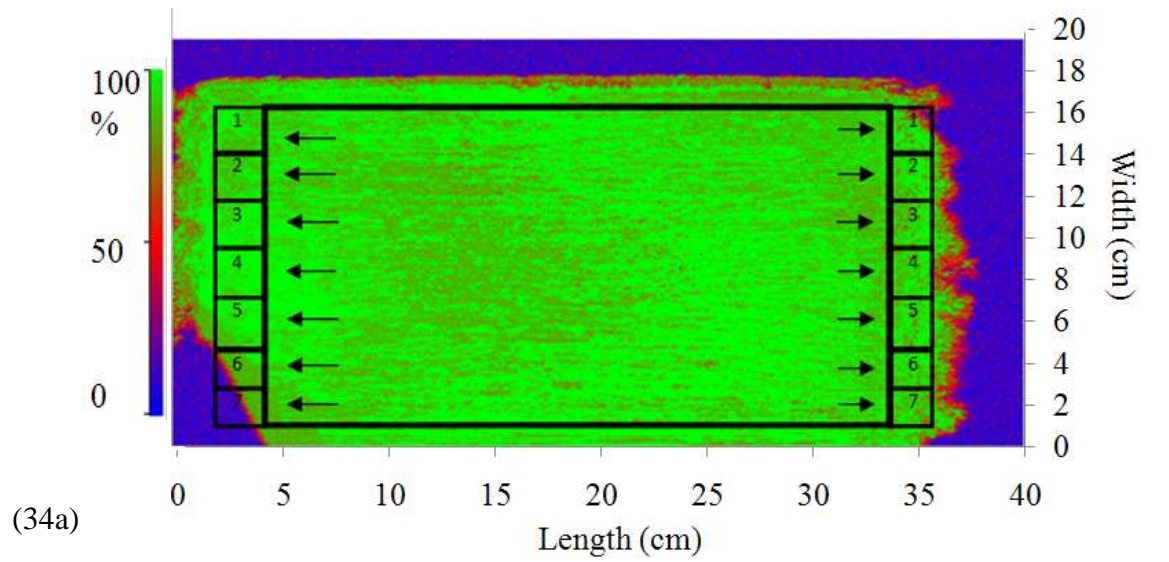
Figure 34 C-scan images of continuous fibre composites (a) glass fibre 1200 TEX,

(b) glass fibre 2400 TEX and (c) carbon fibre.

Quality control of the short-fibre composites are shown by the C-scans in Figure 35a-b. The colour intensity scale shows that all the composite plates had minor defects where the majority of each plate showed a high reflected signal. Therefore, the images presented show the quality of the composite plates to be comparable to the continuous composite plates.

(35a)

(35b)
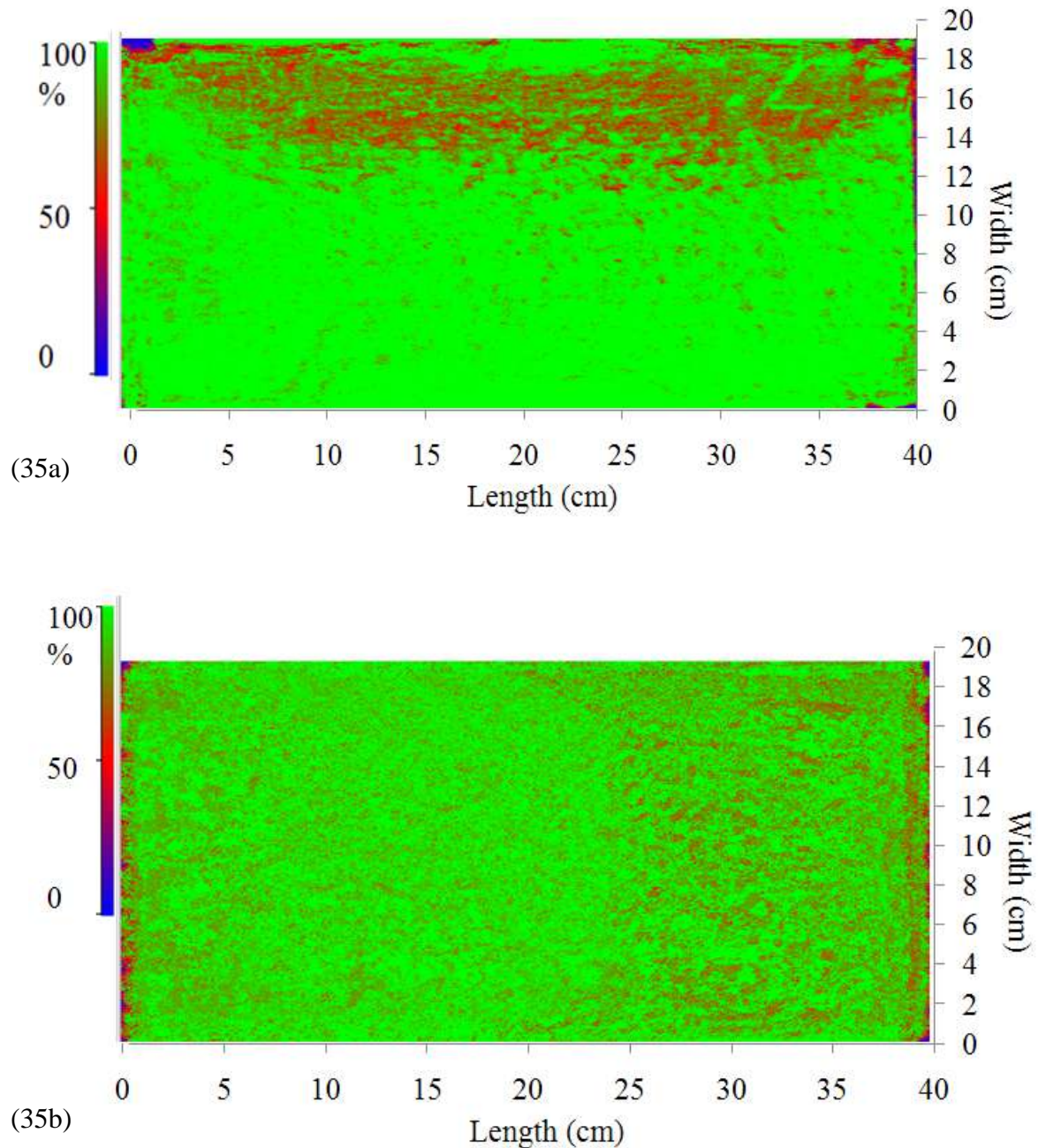
Figure 35 C-scan images of short-fibre composites manufactured using the fibre chopper system (a) glass fibre and (b) carbon fibre.

The ultrasonic C-scan was only capable of showing damage in a plane perpendicular to the emitted pulses to give an integrated picture of the overall damage which does not identify the through-thickness location of the damage. The C-scan technique is useful in identifying the location of the damage and defects. Further investigation to the damaged and undamaged areas used image analysis where Figure 36a-b compares two different transverse section from the continuous carbon fibre sample. The sections selected were determined from the C-scan in Figure 34c, where one represents a higher measure of the reflected wave amplitude (sample 1) and a second of a low amplitude (sample 4).

(36a)

(36b)
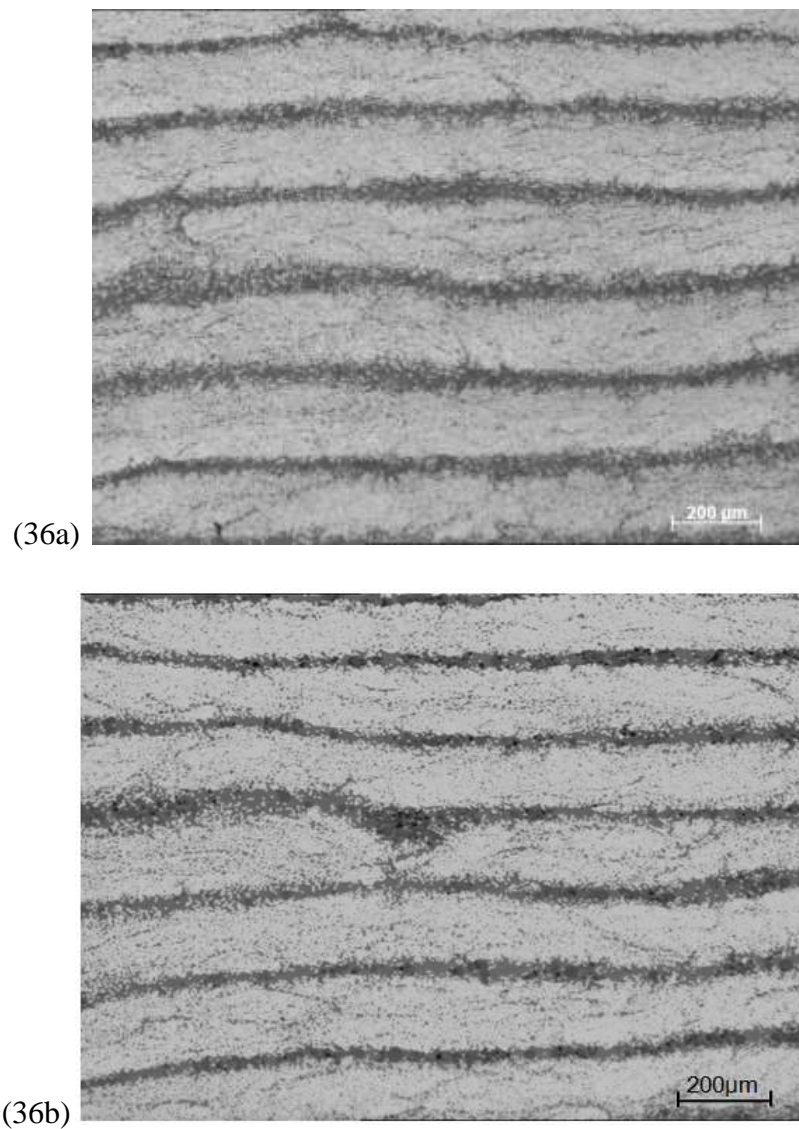
Figure 36 Image analysis showing carbon fibre composite samples of (a) high reflected signal strength (sample 1) and (b) low reflected signal strength (sample 4).

The micrograph and enlarged region shown in Figure 37 confirm the darker sections are occupied by resin and are not voids. The difference in colour intensity of the two samples were analysed to quantify resin content as a value where Figure 38 uses micrograph analysis and software to quantify the resin rich areas. Increased resin content appears to correspond to a lower reflected C-scan signal. The difference between the resin content is summarised in Table 9. The lower detected signal strength shows a higher resin content by an average of 3% in the small sample area compared to a high reflected signal strength. This is further justified by the reduced wave amplitude at the edges of the composites plates, especially in the post-cure state.

(37a)

(37b)
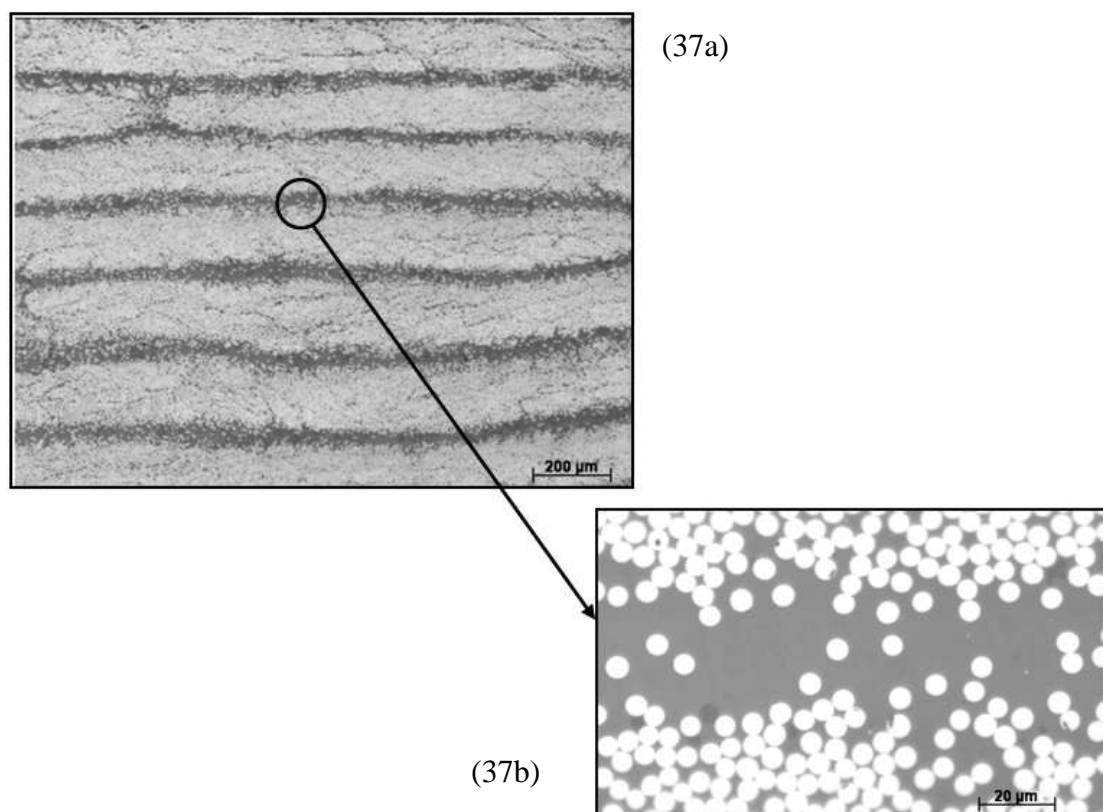
Figure 37 (a) Micrograph showing the cross-section through a continuous carbon fibre composite, (b) magnified image showing the resin-rich region.

With reference to Figure 38a-b, image analysis was used to quantify the resin rich areas. Where a greater resin content receives a lower reflected signal and therefore shows as red during the C-scan.

(38a)

(38b)
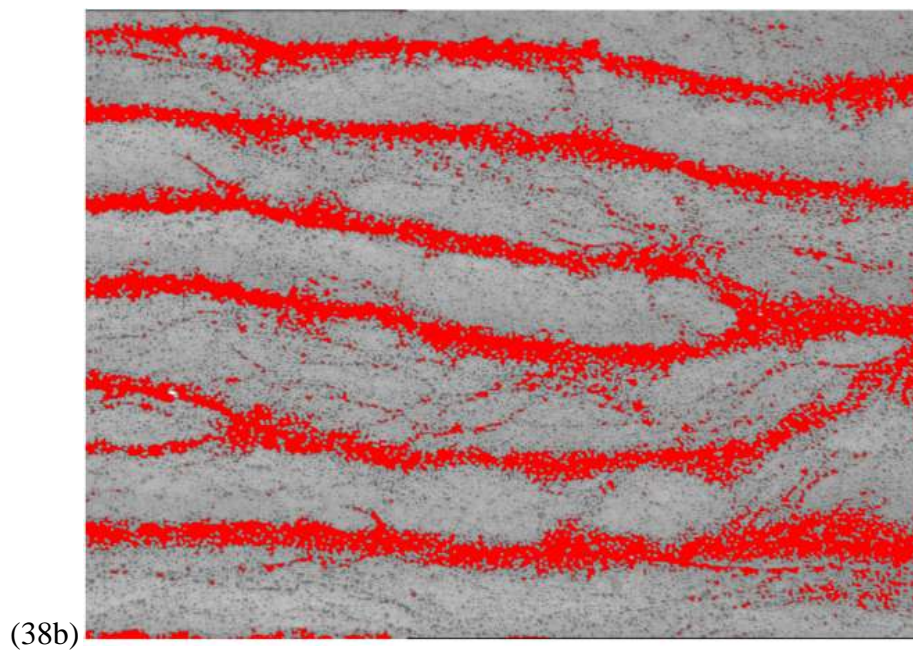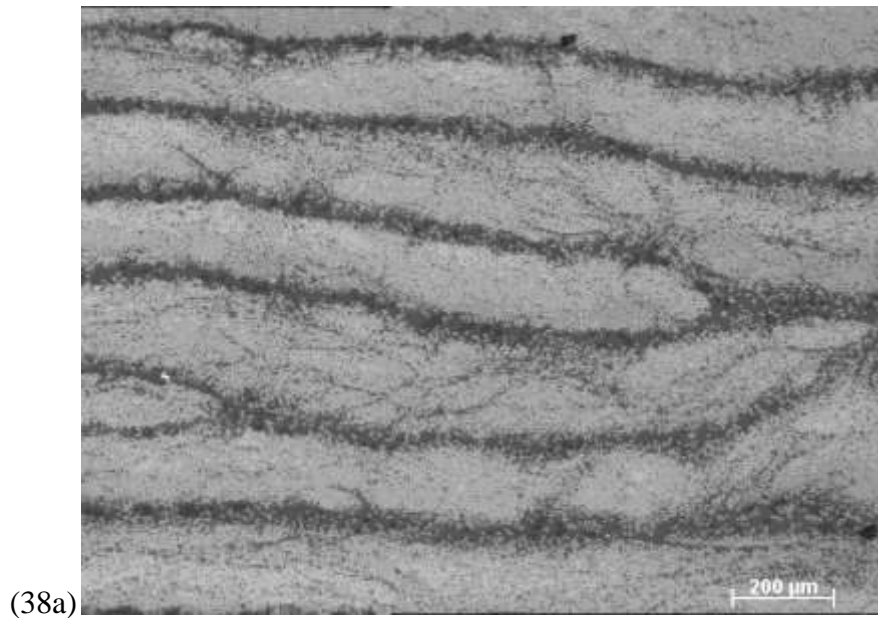
Figure 38 Micrographs comparing the same cross-sectional image of (a) Continuous carbon fibre composite and (b) computer selected regions of resin.

6.4.2   Scanning electron microscopy

6.4.2.1   Blade inspection and replacement

It was found that the difference in blade quality from a used blade to a new blade is transferred to the chopped fibre-end quality [60]. Figure 39 and Figure 40 compare fibre ends cut with a used blade and a new blade, respectively. There was increased fragmentation and fibre-end damage shown on fibres chopped by a used blade when compared with a new blade. Exploring the images of fibre-ends show a clean-cut section approximately a third of the fibre cross-sectional area and the remainder of the fibre is fractured. The roughness of the fibres in Figure 39 implies that the fractured surface of a fibre-end cut with a used blade is more extreme compared with fibre-ends cut using a new blade. It appears that the fibres are forced to fracture under the pressure between the blade and the rubber anvil, causing increased damage to fibre-ends at increased speeds. Consequently there is a reduction in fibre-end quality from a used chopper blade with an uneven edge and at a higher chopper setting.
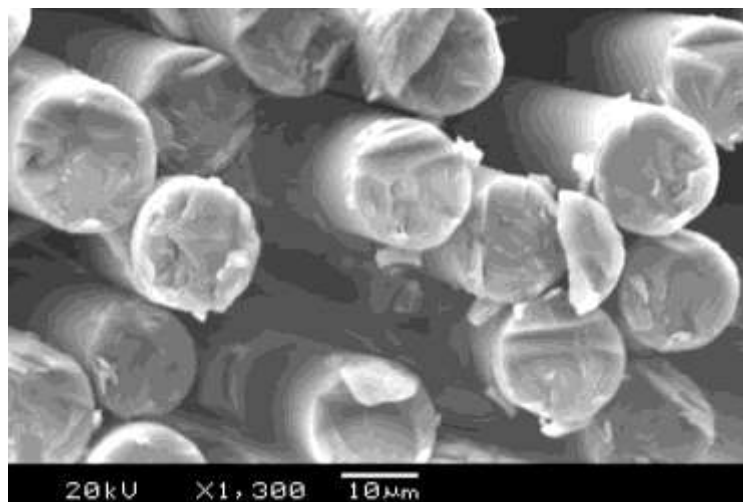
Figure 39 An SEM image of fibre-ends chopped by a used blade.
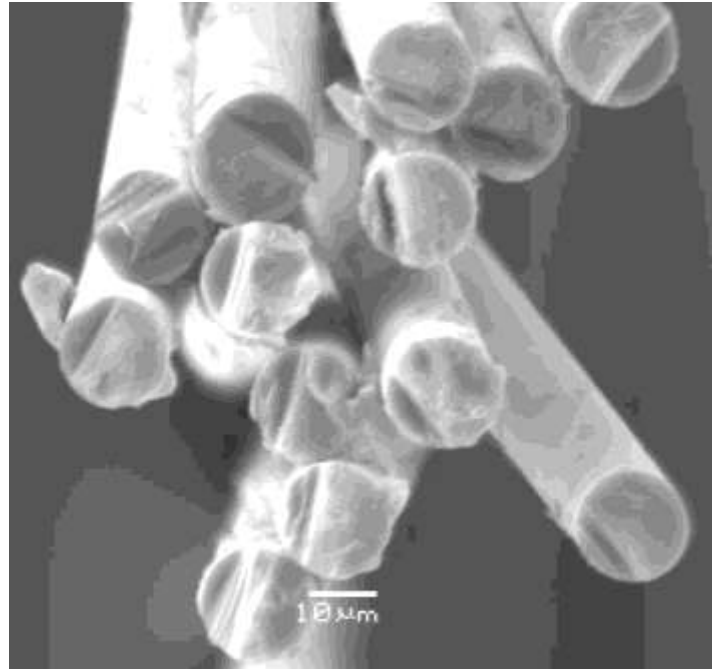
Figure 40 An SEM image of fibre-ends chopped by a new blade.

A criterion for blade replacement has been determined in order to produce high quality fibre ends. By investigating the wear of blades from a top-down view using SEM, Figure 41 shows an increase to blade wear width of the used blades. A large difference in blade wear width of 30 µm is apparent between a used blade and a new blade, as seen in Figure 41. To ensure the fibres are not subject to the degree of damage observed by the used blade it is important to replace blades. To determine the point of blade replacement Equation 6 was used. By maintaining the quality of the blades it will increase the repeatability to produce a high quality prepreg made by the fibre chopper system.

$$\text{Used blade wear width} = 2Wn \qquad \qquad \text{Equation 6}$$

where Wn is the blade wear width of a new blade before any fibres are chopped.
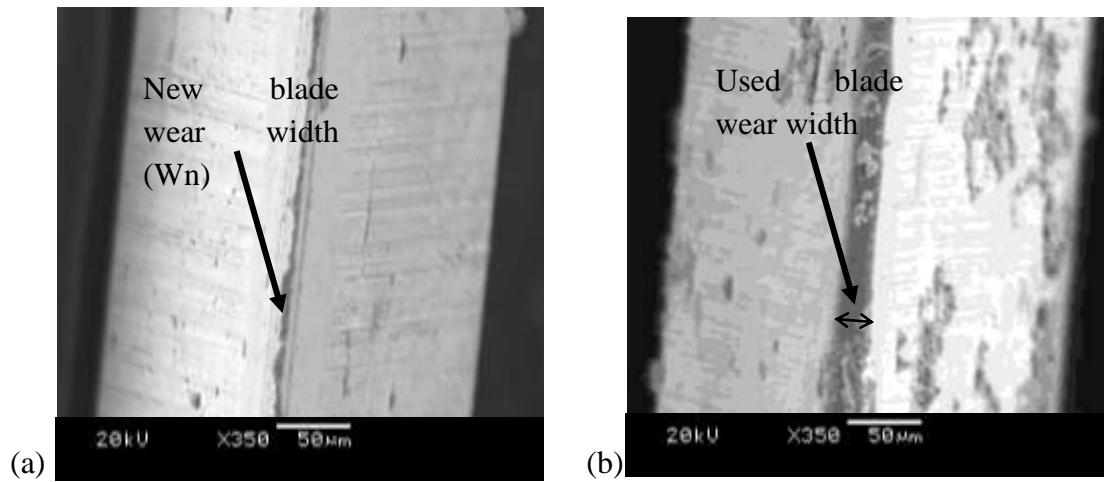
Figure 41 SEM images showing the blade width of (a) a new blade and (b) a used blade.

The process of removing blades for inspection can be time consuming and problematic. The results of the blade rpm show a positive linear correlation to the chopper setting. During the manufacture of prepregs the voltage, number of blades and duration are all variable depending on the material, prepreg size and fibre length. Equation 7 can be used to estimate the life cycle of blades before replacement is advised:

$$\frac{d(54.819c - 53.342)}{N} \geq 9000 \qquad \text{Equation 7}$$

where d is the duration of time the chopper is used (minutes), c is the chopper setting (voltage) and N is the number of blades in the chopper head.

6.4.2.2   Fibre-end quality

Figure 42 images the surface of the out-of-shelf-life carbon fibre using SEM. The image shows a surround of resin around each fibre, creating a bond between the fibres and the resin matrix.
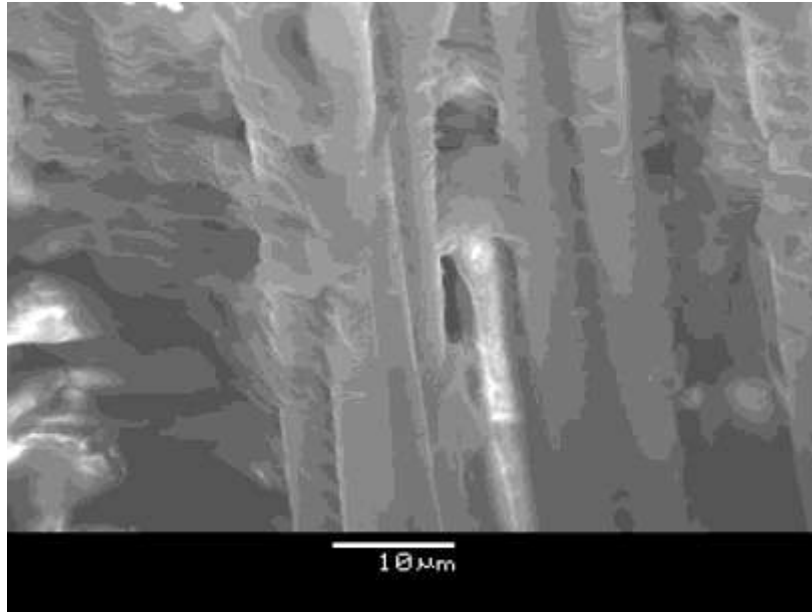
Figure 42 Micrograph of the out-of-shelf-life carbon fibre ends and the fibre surface quality.

SEM images of out-of-shelf-life carbon fibre ends and carbon fibre ends both show large a volume of debris and damage seen in Figure 43a-b. The different fibres exhibit a contrast in debris type, where a greater debris size is present in the out-of-shelf-life carbon fibres. The larger debris volume of the out-of-shelf-life carbon fibres occurred from the fracture of the pre-impregnated resin that surrounds the fibres. The debris at the fibre ends is created by the blade force applied to the fibres. The pre-impregnated fibres are tougher to cut using a single blade so greater force was required. The difficulty to cut the out-of-shelf-life carbon fibre meant this material would be unsuitable for use in the fibre chopper as a high torque between cogs would be required. Consequently, carbon fibre was used as the reinforcing material for the production of short-fibre composites using the fibre chopper.

(43a)

(43b)
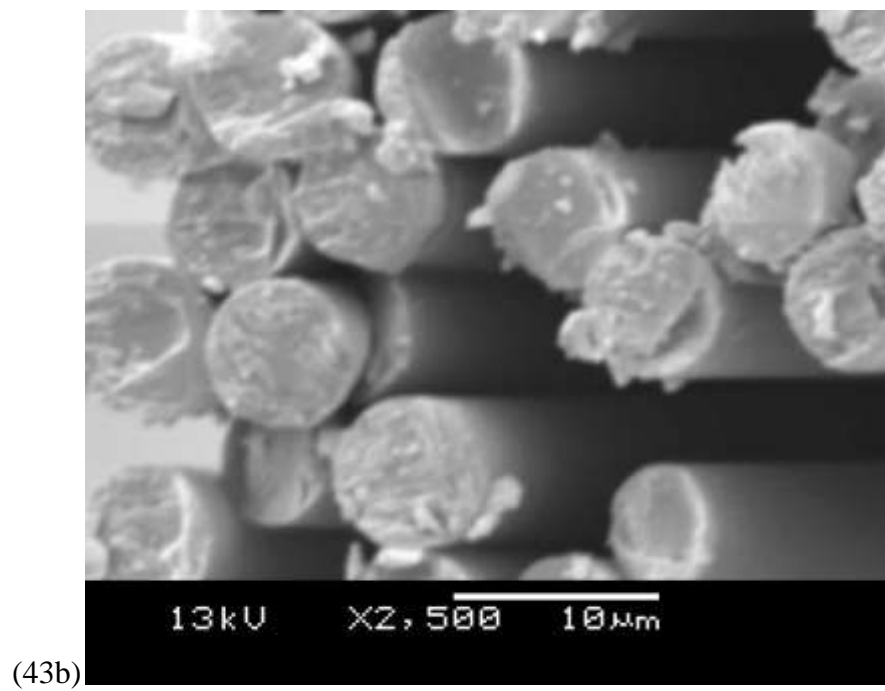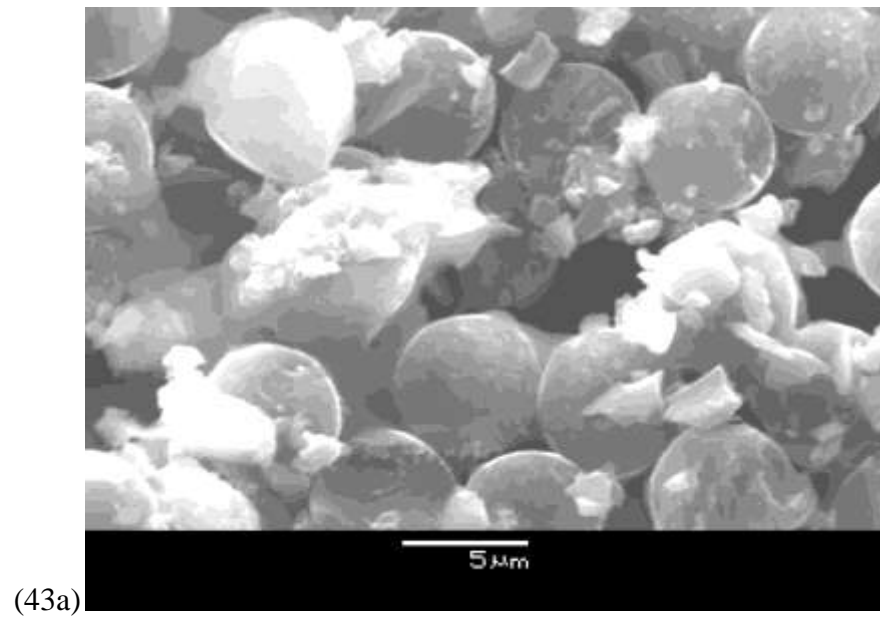
Figure 43 SEM images of fibre ends after a clean-cut using a blade (a) out-of-shelf-life

carbon fibre and (b) virgin carbon fibre.

74

6.5 Test methods

Physical and mechanical testing provides a quantitative measure for the comparison of material properties between continuous fibre and short-fibre composites. The results of the short-fibre composites can be compared to alternative alignment methods for short-fibres as well as the continuous reference composites produced using the same materials and production process. In total eight different materials in this report have been manufactured and produced, these have been labelled as: (i) continuous glass fibre 1200 TEX, (ii) continuous glass fibre 2400 TEX, (iii) continuous carbon fibre, (iv) continuous out-of-shelf-life carbon fibre, (v) short-glass fibre 1, (vi) short-glass fibre 2, (vii) short-carbon fibre 1 and (viii) short-carbon fibre 2.

6.5.1   Fibre alignment

Figure 44a-d provide high quality micrographs to identify the fibre alignment of continuous fibre and short-fibre composite samples. Glass fibre composites show comparable images to carbon fibre composites, indicating a clear fibre circumference to determine whether the fibres are aligned or off-axis using the Equation 4 in Section 5.9.1.

(44a)

(44b)

(44c)

(44d)
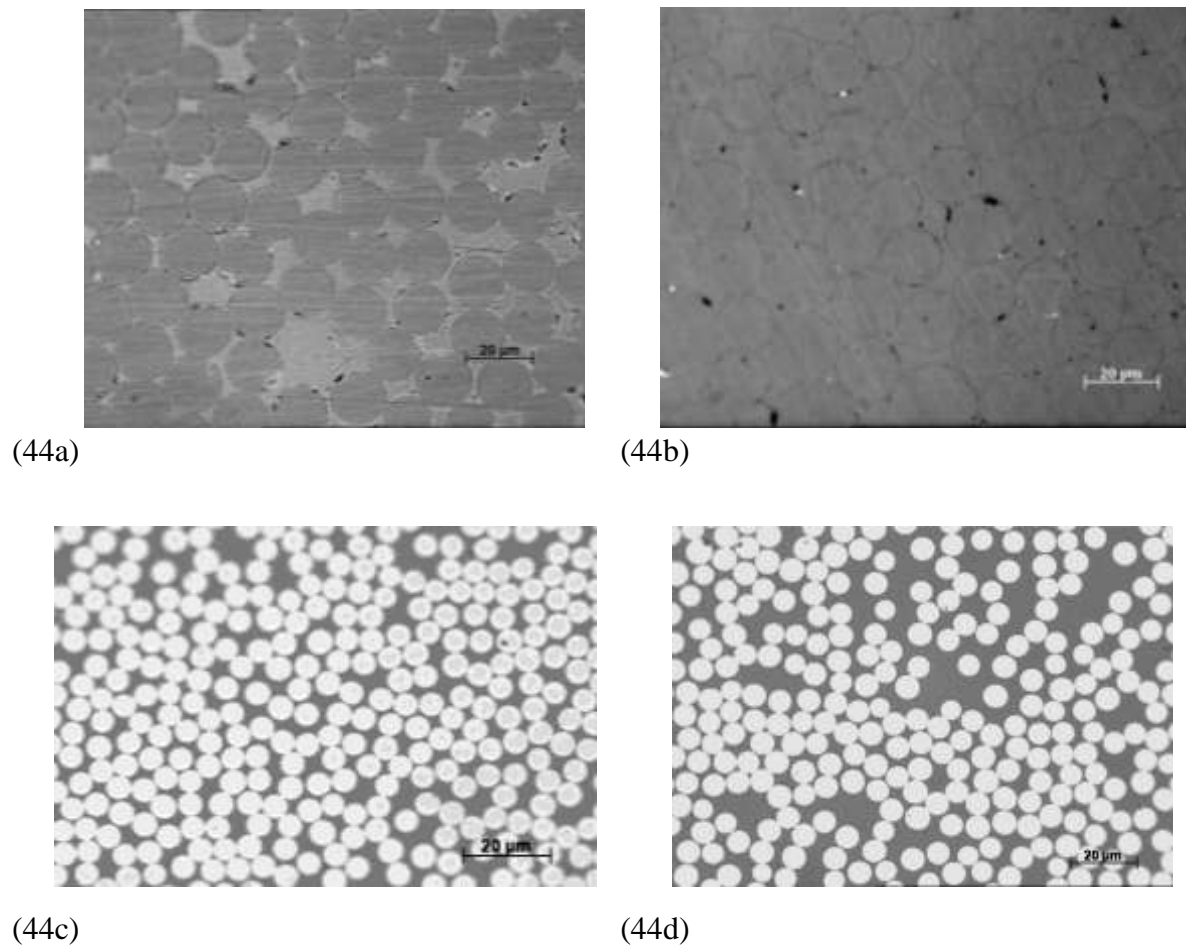
Figure 44 Micrographs of fibres used to categorise fibre alignment (a) continuous glass fibre 1200 TEX, (b) continuous glass fibre 2400 TEX, (c) continuous carbon fibre and (d) short-carbon fibre.

Figure 45 shows a longitudinal section of a continuous carbon fibre composite. The continuous fibre composites all showed a highly orientated composite as seen by the large ellipse of each fibre. The variation of fibre alignment due to fibre chopper manufacture of short-fibre composites is shown in Figure 46. In the case of the short-fibre composite there were scattered regions of aligned and off-axis fibres. Highly aligned fibres are imaged to show a longitudinal length of 400 μm while the greatest off-axis fibres present a longitudinal length of nearer 25 μm. The main reasons for the change in fibre ellipse size can be related to the processes of the fibre chopper, the hand lay-up of composite manufacture and the scale of magnification used. At low magnifications, only a small percentage of the complete composite is analysed making the technique dependant on the samples investigated.
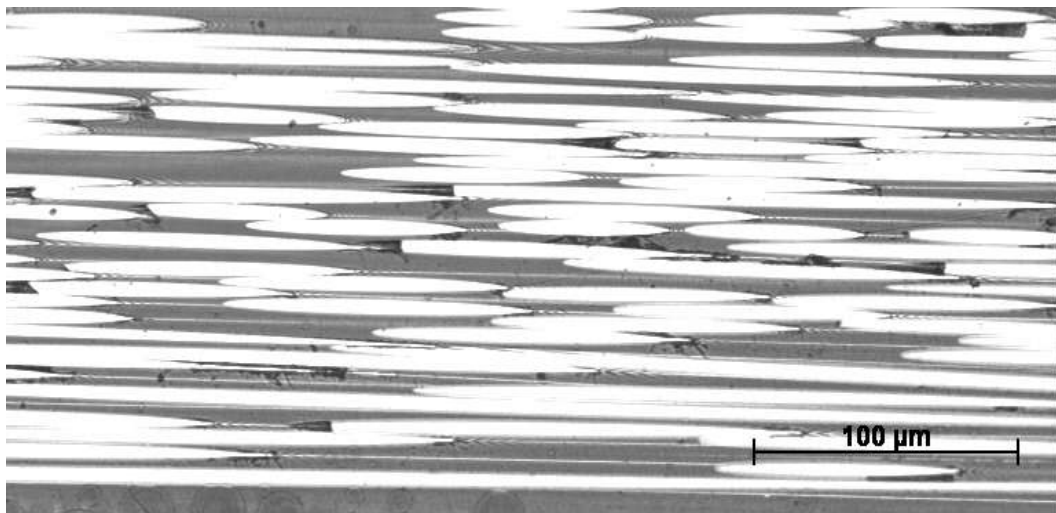
Figure 45 Micrograph showing longitudinal fibre alignment sections of a continuous carbon fibre composite.
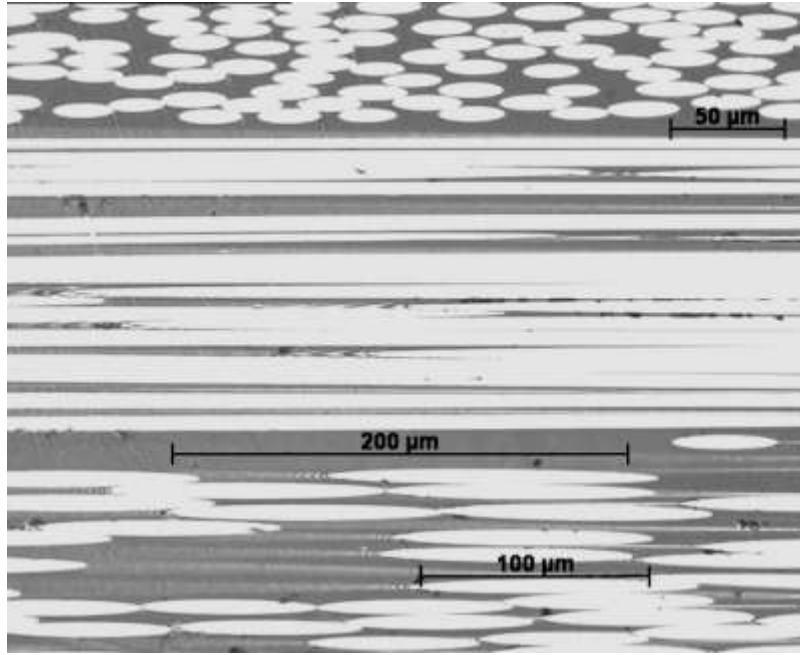
Figure 46 Micrograph of a short-carbon fibre composite through a longitudinal section.

Table 10 compares the fibre alignment between continuous fibre composites and short-fibre composites manufactured using the fibre chopper. The number of fibres per material was dependent upon fibre length and diameter. Typically carbon fibre samples had a greater amount of fibres per frame when using a standardised X50 magnification. The histogram in Figure 47 shows the continuous fibre composites all have 100% fibre alignment which was expected due to the manual hand lay-up of individual fibre tows placed parallel to each other. This shows the hand lay-up method is a successful and reliable approach when aligning each ply of fibres above a subsequent ply. Overall the fibre chopper system has shown it can produce composites with a fibre alignment of 79% and 89% for glass fibre and carbon fibre composites, respectively. It is inevitable that the fibre chopper system will not be able to match those of the continuous fibre composites due to the large number of fibre bundles which are present in short-fibre composites.

Fibre material	Continuous fibre				Short fibre			
	Glass fibre 1200 TEX	Glass fibre 2400 TEX	Carbon fibre	Out-of-shelf -life carbon fibre	Glass fibre 1	Glass fibre 2	Carbon fibre 1	Carbon fibre 2
Number of fibres analysed	4589	3541	7882	4910	3417	3212	3761	3852
Aligned	100%	100%	100%	100%	80% (6.79)	80% (5.11)	89% (8.88)	97% (0.77)
Off-axis	0%	0%	0%	0%	20%	20%	11%	3%

Table 10 A comparison of the fibre alignment of continuous fibre and short-fibre composites

indicating the total number of fibres analysed.
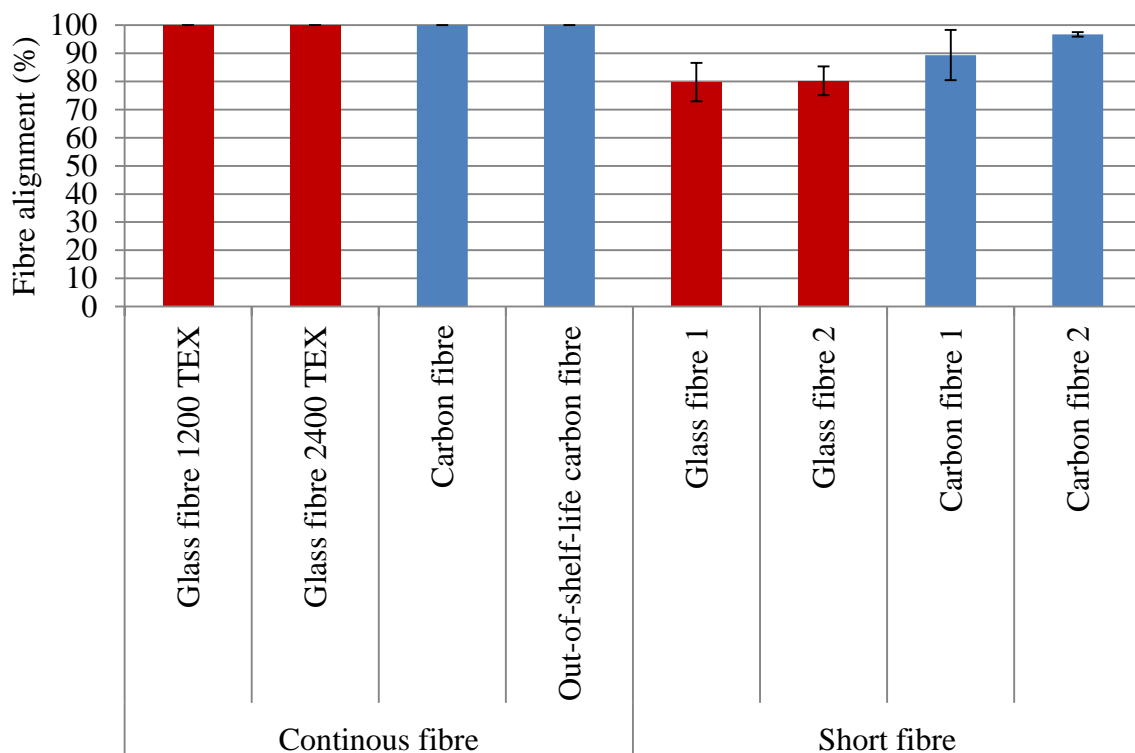
Figure 47 A comparison the fibre alignment of continuous fibre composites and short-fibre

composites.

Figure 48 shows the image analysis method used to quantity fibre alignment is in good agreement with the prepreg fibre alignment results presented in Section 6.2.1.

Conclusions: The initial macro imaging procedure can be used as an effective technique to determine the fibre alignment of short-fibre prepregs. Both materials showed some discrepancies in fibre alignment when comparing the visual inspection and image analysis. The variation is likely to be created by the magnification used in microscopy, where only a small section is analysed, therefore the fibre alignment becomes dependent on the composite section imaged. Overall both methods are in agreement that the fibre chopper based delivery system produces a greater alignment for carbon than glass, both of which exceed a 60% fibre alignment.
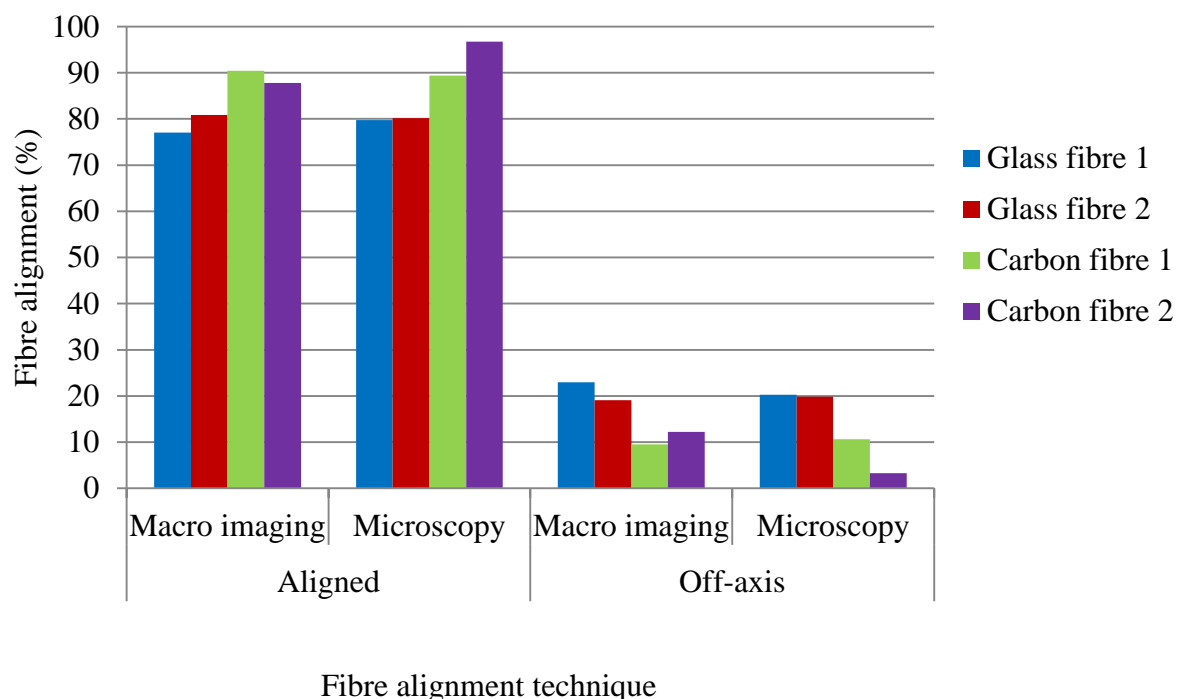
Figure 48 Fibre alignment prepreg techniques comparing macro imaging with microscopy.

6.5.2   Physical properties

Density, fibre volume fraction and void content values were analysed and are reported in the following section. An overview of the physical properties of continuous fibre composites and short-fibre composites manufactured by the fibre chopper are compared in Table 11.

Test	Continuous fibre				Short-fibre			
	Glass fibre 1200 TEX	Glass fibre 2400 TEX	Carbon fibre	Out-of-shelf -life carbon fibre	Glass fibre 1	Glass fibre 2	Carbon fibre 1	Carbon fibre 2
Sample Density (kg/m3)	1941.59 (50.42)	1953.67 (32.87)	1420.22 (31.51)	1428.67 (22.92)	2101.53 (37.73)	2052.05 (38.26)	1599.81 (77.91)	1493.94 (4.69)
Fibre volume fraction (%)	52.46 (3.44)	53.55 (1.35)	64.75 (8.41)	64.03 (8.16)	67.04 (3.00)	63.13 (1.73)	61.75 (6.37)	60.32 (7.19)
Void content (%)	1.9 (0.74)	1.83 (0.44)	n/a	n/a	3.09 (1.99)	2.03 (1.18)	n/a	n/a

Table 11 A summary of the physical properties of glass fibre and carbon fibre composites as continuous fibre and short-fibres composites.

6.5.2.1 Density

Figure 49 shows the density of glass and carbon fibre composites with standard error bars. The results show that glass fibres have a higher density than the carbon fibre. This was expected due to the higher density of glass fibre. It is seen that each material shows comparable density values irrespective of fibre length where the error bars are negligible.
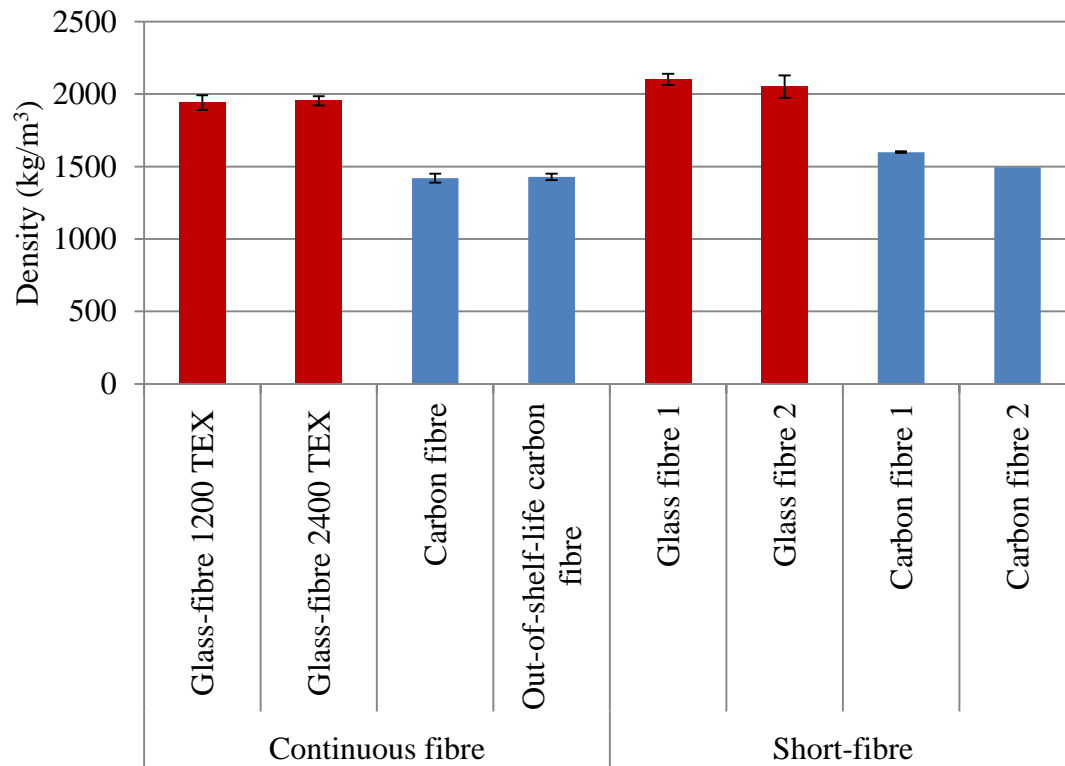
Figure 49 Density of continuous fibre and short-fibre composites.

6.5.2.2   Fibre volume fraction

Different techniques to quantify the fibre volume fraction were used as carbon fibres are unable to be tested using the resin burn off technique due the carbon oxidising. Therefore image analysis based on fibre surface volume fraction was used.

6.5.2.2.1   Glass fibre composites

The resin burn-off technique and simple calculation determined the glass fibre volume fraction, matrix volume and void content for glass fibre composite plates. Figure 50 represents the fibre volume fraction of glass fibre carbon fibre composites, all showing a fibre volume fraction in the range between 50-70%. The short-glass fibre composites showed a void content between 1.8-1.9%. The low void content is a common feature of the autoclave manufacturing process. It was expected that short-glass fibre composites would show a higher fibre volume fraction due to the increased number of fibres present, due to overlapping fibres that occur during the manufacturing process.

6.5.2.2.2   Carbon fibre composites

The fibre surface volume fraction (fibre volume fraction) of carbon fibre composites are also compared in Figure 50. Irrespective of fibre length all of the composites showed a fibre volume fraction of at least 60%. Void content analysis will need further investigation as the microscopy method is limiting to the accuracy of the findings due to the low magnification used over small composite sections.
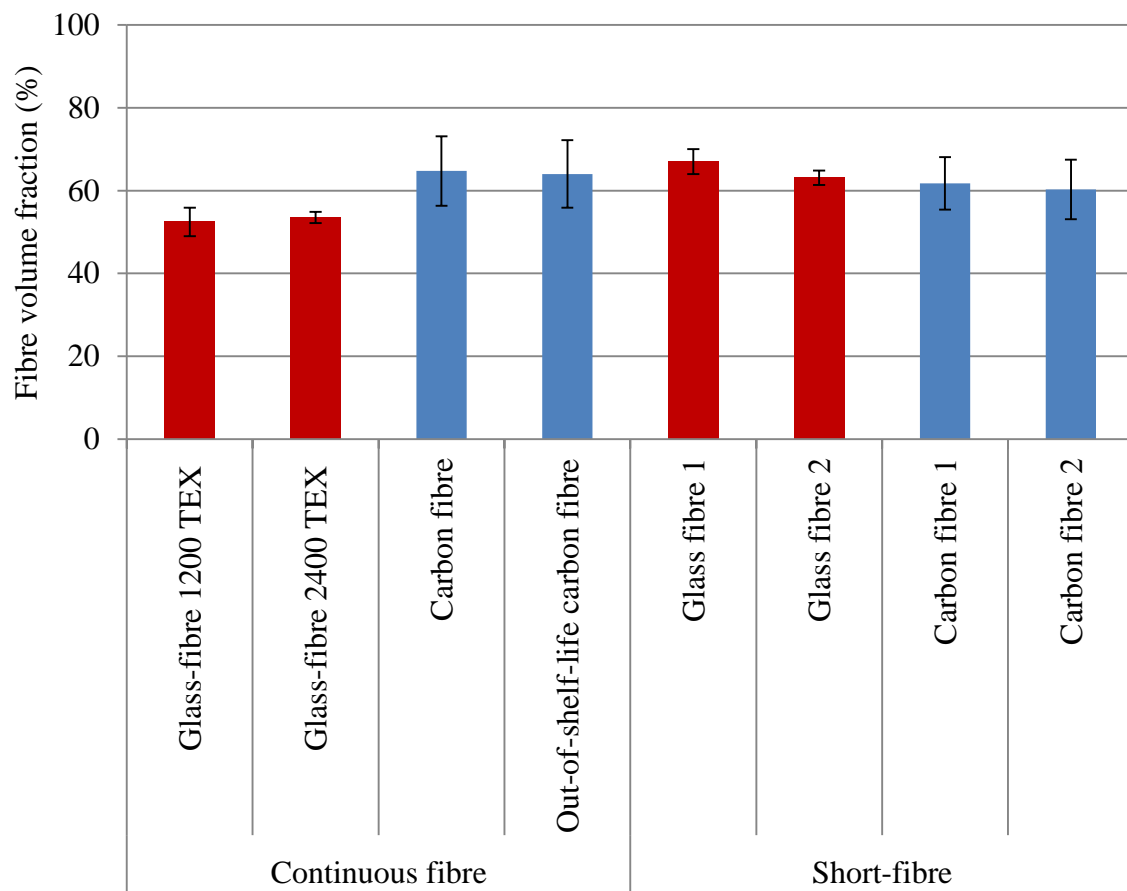
Figure 50 Fibre volume fraction of continuous fibre and short-fibre composites reinforced with glass fibres and carbon fibres.

6.5.3 Mechanical properties

6.5.3.1 Tensile strength

Figure 51 shows the variations of the tensile strength as a function of the composite materials for continuous fibres and short-fibres. Continuous fibre composites made by glass fibre and carbon fibres showed enhanced tensile strength when compared to short-fibre composites, see Table 12. Moreover, it can be seen that the strength of short-carbon fibre composites are higher than those of short-glass fibre composites. This is because carbon fibres have a much higher strength than glass fibres. However, the scatter of the data for short-carbon fibre composites is larger than that for short-glass fibre composites. The reasoning for this are not known at present.

6.5.3.2 Failure strain

The failure strains of continuous fibre composites and short-fibre composites are presented in Figure 52. It can be seen that as the fibre length decreases in the short-fibre composites, the composite failure strain decreases for both glass fibre composites and carbon fibre composites. In addition, the failure strains of glass fibre composites are higher than those of carbon fibre composites. The reduction in failure strain maybe caused by matrix cracking, that forms at the ends of the fibres. Consequently, as the strain is increased, more cracks form progressively at the ends of shorter fibres. Initially this cracking can be accommodated by load transfer to adjacent fibres which "bridge" the cracked region. Final failure occurs when the extent of cracking across the weakest section of a specimen reaches a critical level when the surrounding fibres and matrix can no longer support the increasing load.
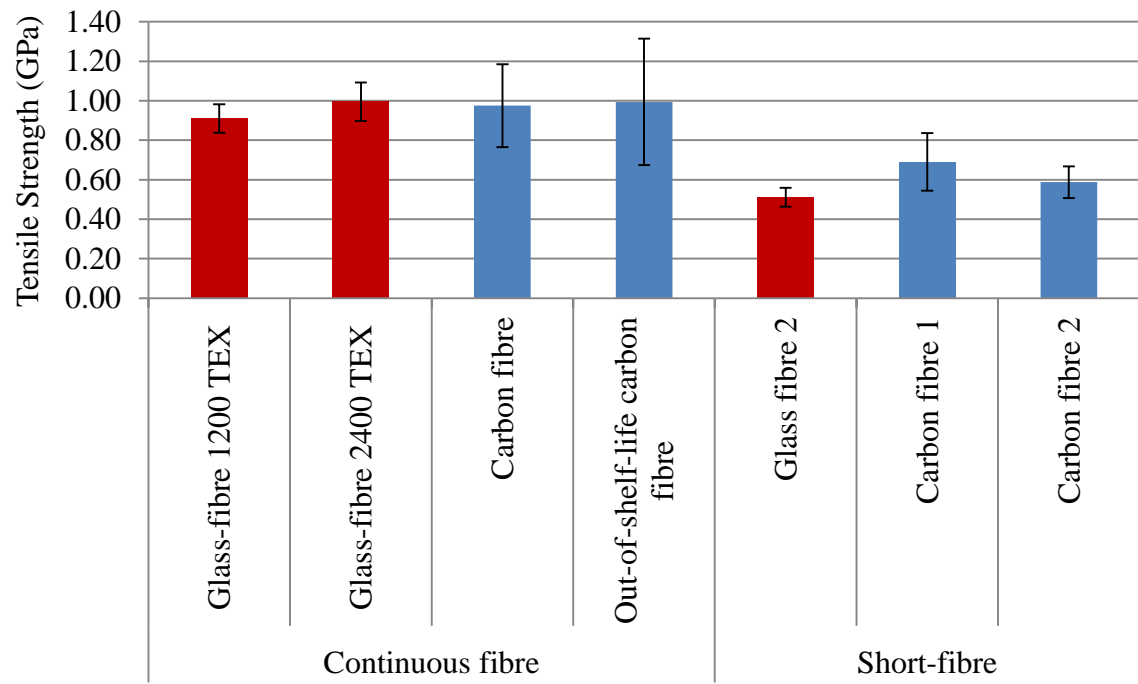
Figure 51 Tensile strength of each composite material manufactured in the study.
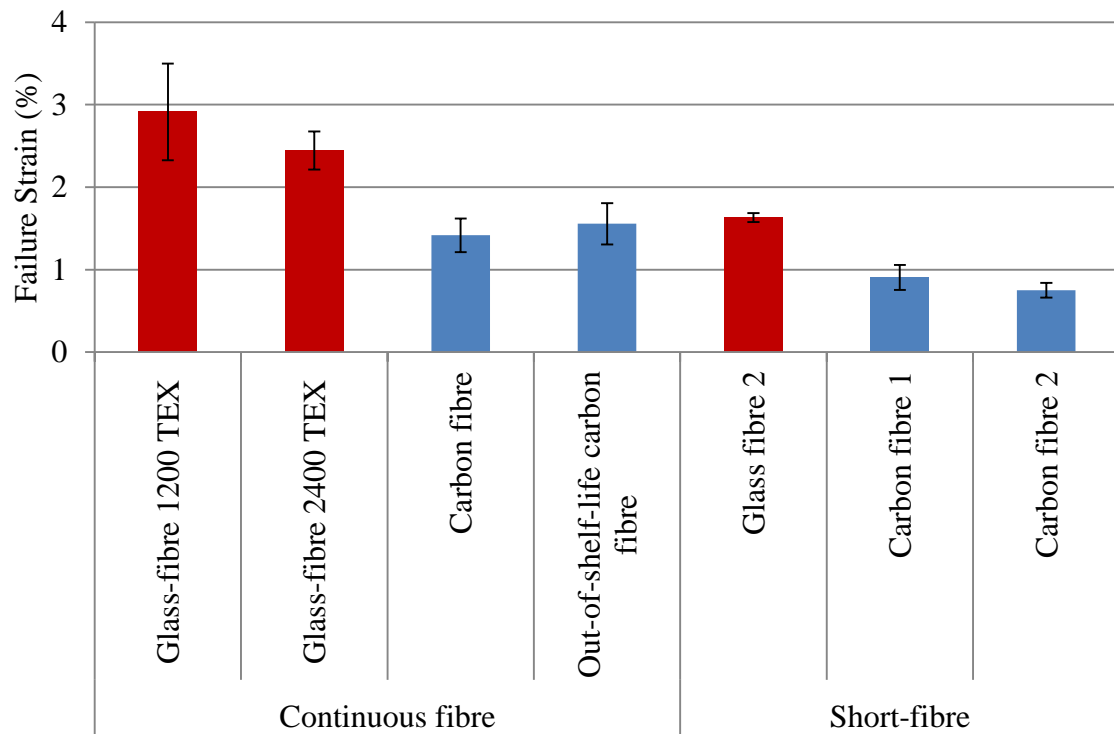
Figure 52 Failure strain of continuous and short-fibre composites.

6.5.3.3   Young's Modulus

The variations of the Young's Modulus of continuous fibre composites and short-fibre composites as a function of fibre length are shown in Figure 53. It can be seen that the modulus of carbon fibre composites are considerably larger. Furthermore the effect of fibre length is insignificant to the Young's Modulus for both carbon fibre composites and glass fibre composites.
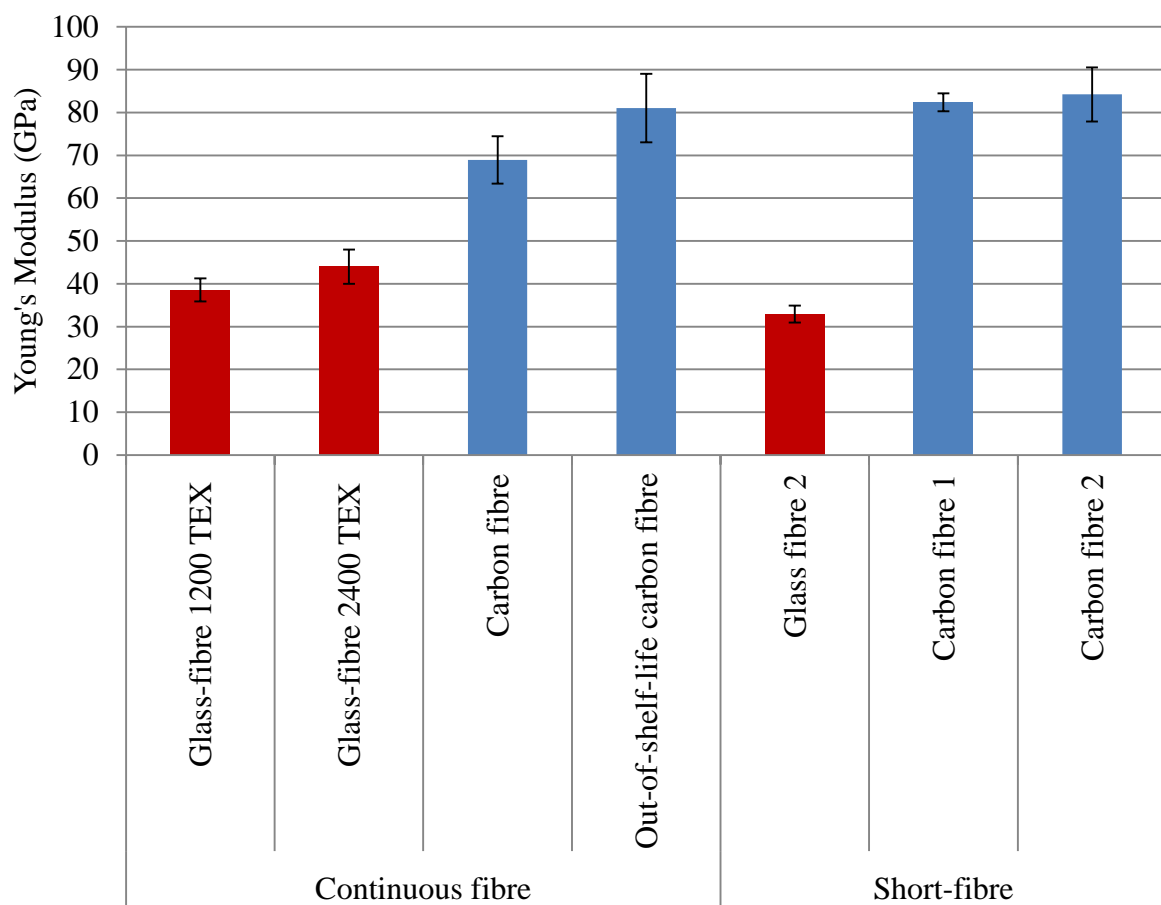
Figure 53 Young's Modulus of continuous fibre and short-fibre composites.

Table 12 summarises the material properties of the continuous fibre and short-fibre composites developed in this study. The resin system and manufacturing techniques were common for all composites manufacture so direct comparison is possible. It is apparent that the composites produced using the fibre chopper system exhibit comparable physical properties to the continuous fibre composites.

It is accepted that the tensile properties of short-fibre composites will not be equivalent to their long-fibre centre-point. The failure strain is closely related to the quality of the chopped fibre-ends. As the number of fibre ends increase, the smaller the failure strain is. This is because of the shear-stress at the ends of the short-fibres. However on inspection of the Young's Modulus, the performance of the short-fibre composite is comparable to that found from the long-fibre composites.

Test	Continuous fibre				Short-fibre			
	Glass fibre 1200 TEX	Glass fibre 2400 TEX	Carbon fibre	Out-of-shelf -life carbon fibre	Glass fibre 1	Glass fibre 2	Carbon fibre 1	Carbon fibre 2
Fibre volume fraction (%)	52 (3.4)	54 (1.4)	65 (8.4)	64 (8.2)	67 (3.0)	63 (1.7)	62 (6.4)	60 (7.2)
Void content (%)	1.9 (0.7)	1.8 (0.4)	n/a	n/a	3.1 (2.0)	2.0 (1.2)	n/a	n/a
Sample density (kg/m^3)	1942 (50.4)	1954 (32.9)	1420 (31.5)	1429 (22.9)	2102 (37.7)	2052 (38.3)	1600 (77.9)	1494 (4.7)
Tensile strength (GPa)	0.9 (0.1)	1.0 (0.1)	1.0 (0.2)	1.0 (0.3)	-	0.5 (0.1)	0.7 (0.2)	0.6 (0.1)
Failure strain (%)	2.9 (0.6)	2.5 (0.2)	1.4 (0.2)	1.6 (0.3)	-	1.6 (0.1)	0.9 (0.2)	0.8 (0.1)
Young's modulus (GPa)	39 (2.7)	44 (4.0)	69 (5.5)	81 (8.0)	-	33 (2.0)	83 (2.1)	84 (6.3)

Table 12 A summary table of the physical and mechanical properties, comparing continuous

fibre and short-fibre composites.

6.6   Failure analysis

6.6.1   Visual inspection

Table 13 compares the failure type, failure area and failure loaction of both continuous and short-fibre glass-fibre and carbon-fibre samples manufactured during the project. Visual inspection showed the continuous samples have brittle fracture laterally, splitting through the sample within the gauge length, inside the grip and at the end of the end-tab region. The failure occurs at vaious locations as the spilt failure type is difficult to locate specific failure regions. The short-fibre composites failed by splitting and in some instantance at an angle. This indicates that fibre delamination may be influenced by mis-alignment of fibres within the sample.   Therefore it reiterates the importance to produce an alignment composite in order to increase the mechanical properties and reduce the probability of failure. All of the short-fibre composite samples failed in gauge area in the middle of the samples.

Material	Failure		
	Type	Area	Location
Continuous fibre composites			
1200 TEX glass fibre	Splitting	End-tab and gauge length	Middle
2400 TEX glass fibre	Splitting	Gauge length	Middle
Carbon fibre	Lateral and splitting	Gauge length	Various
Out-of-shelf-life carbon fibre	Splitting	Gauge length and inside grip	Various
Short-fibre composites			
Glass fibre 2	Splitting and angled	Gauge length	Middle
Carbon fibre 1	Splitting and angled	Gauge length	Middle
Carbon fibre 2	Splitting and angled	Gauge length	Middle

Table 13 Common tensile failure type, area and location of the different composite materials tested.

6.6.2   Fractography (SEM)

The micrographs presented in this section represent typical failure modes that were observed in the various samples when tested. The SEM micrographs of the fracture surfaces of short-fibre carbon fibre composites and continuous carbon fibre composites are shown, respectively, in Figure 54 to Figure 57.

Figure 54 represents a continuous carbon fibre composite that was tested to tensile failure where transverse and longitudinal failure had occurred. Micrographs of the longitudinal failure are shown in Figure 54a where fibres show a 'clean' surface. The matrix damage is more extensive for the continuous fibre composites where greater amounts of debris and transverse cracking have occurred from the delamination.

Figure 54b represents a micrograph of a transverse fracture of the above mentioned carbon-fibre sample. Within the micrograph numerous locations of fibre pull-out are observed. This is due to the increase in load that is placed on the sample before a brittle failure in the transverse direction. Fibre-matrix de-bonding has also been reported where the adhesion between the interfaces of the two materials is unable to maintain adhesion.

The brittle fracture of the matrix was observed in both short-fibre composites and continuous fibre composites which were consistent with the brittle nature of the tensile stress-strain curves for the two types of composites. It can be seen from the micrographs that most fibres are pulled out from the matrix during failure.

6.6.2.1 Continuous carbon fibre composite

(54a)

Matrix cracking

Matrix debris

(54b)

Matrix fracture

Fibre-matrix
de-bonding

Fibre pull-out

(54c)

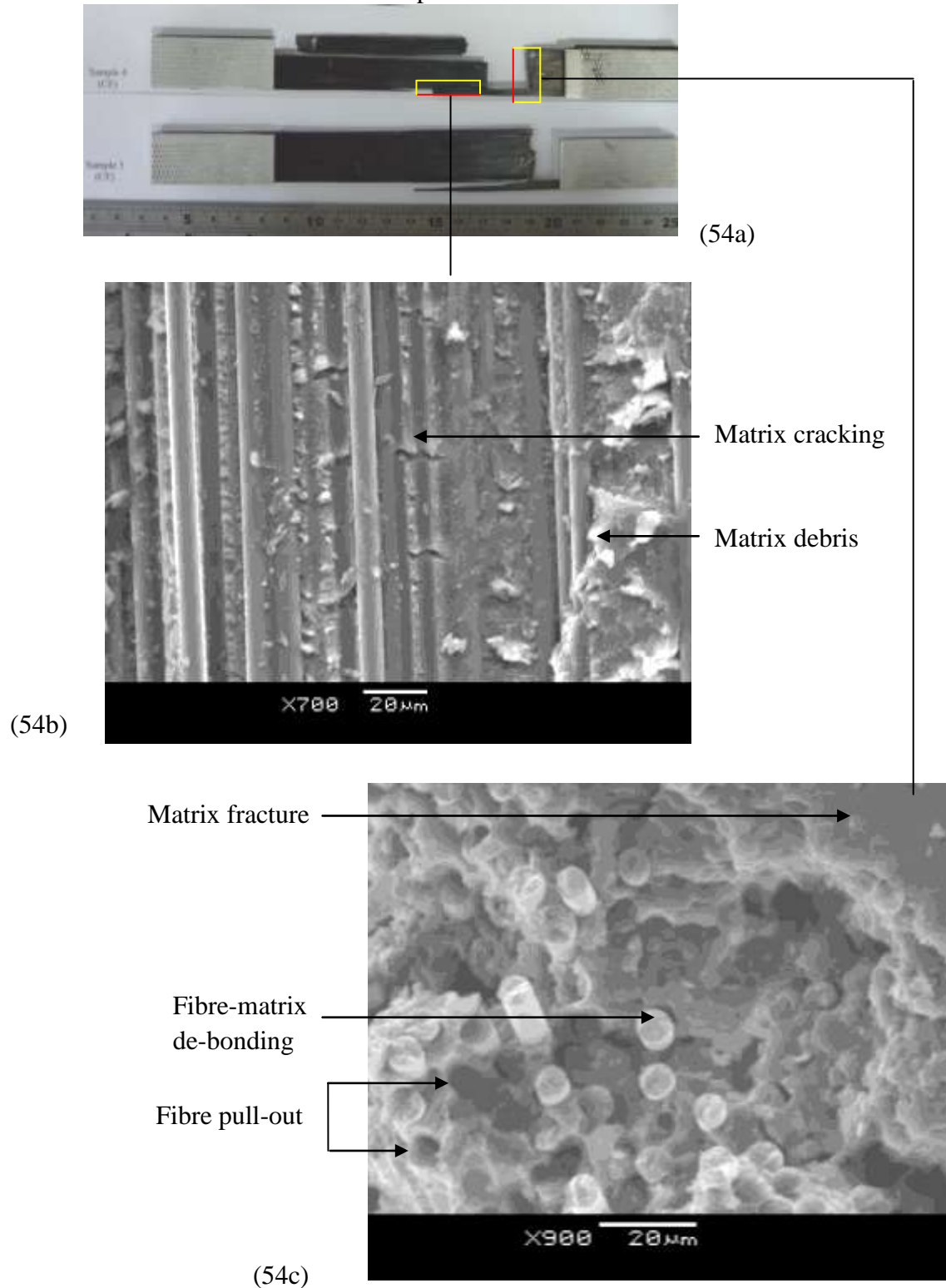Figure 54a Macrographs of a continuous carbon fibre composite with transverse and

longitudinal sections highlighted for microscopic analysis,(b) edge face of longitudinal split,

(c) transverse micrograph.

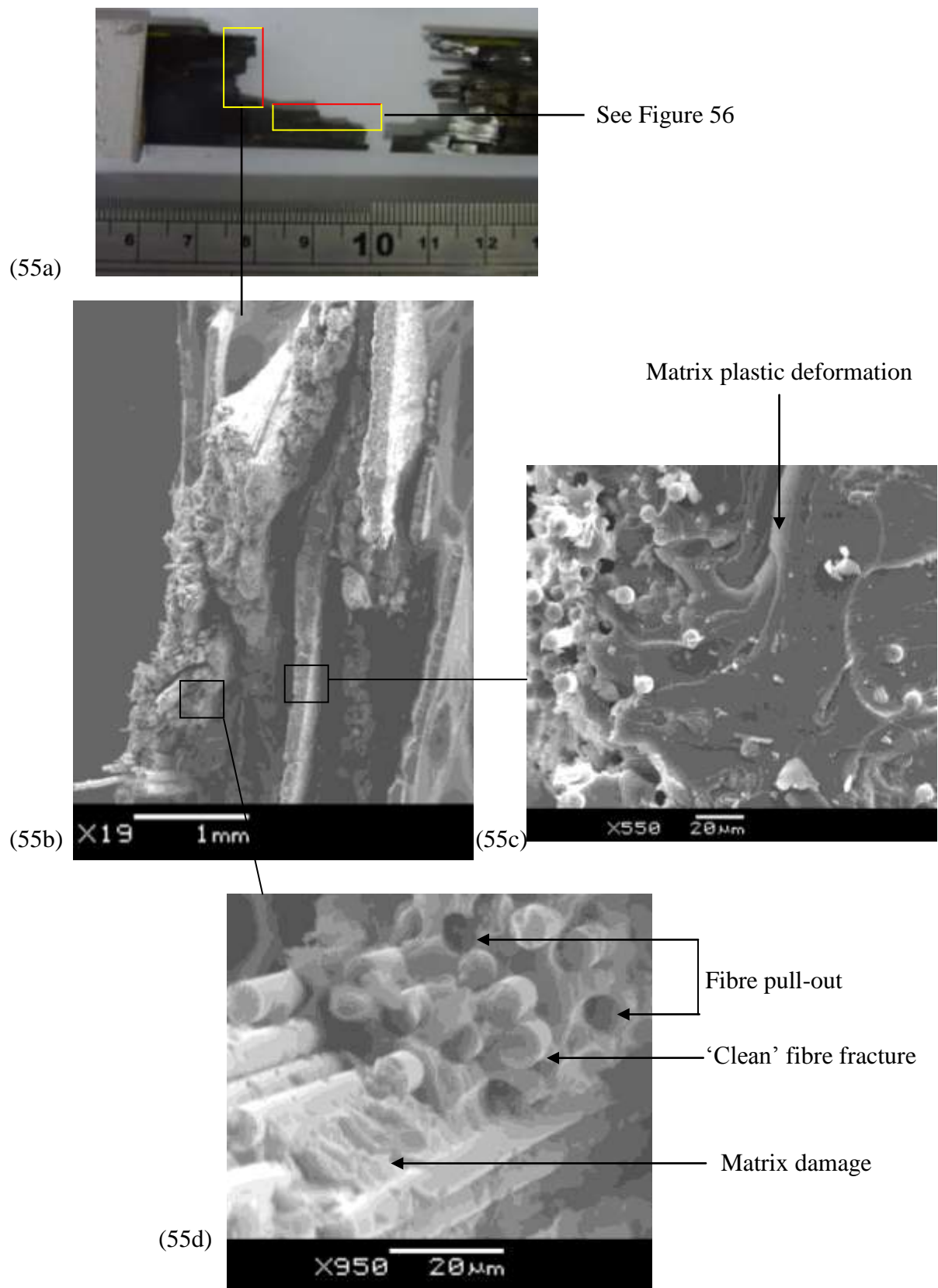## 6.6.2.2 Short-carbon fibre composite

Figure 55a Micrograph of a failed short carbon fibre samples (b) transverse view,

(c) transverse view of laminate and (d) fibre ends at transverse failure.

Figure 55a shows a representative failure of short-carbon fibre composites manufactured using the fibre chopper-based system. Transverse and longitudinal sections were prepared for SEM analysis to inspect the failure modes as a microscopic range.

The transverse section in Figure 55b shows numerous features that are common to this type of failure. Delamination has been highlighted between the different fibre laminates within the composite. The process of delamination maintains each laminate but they became separated by the resin layer that held them in place. The failure mode of delamination is created by the matrix region between the fibre laminates becoming weak during a tensile test and fails to sustain the load it is subject to.

A magnified image of the transverse fibre region, shown in Figure 55c captures fibre pull-out and resin plastic deformation. The resin deformation is likely to be caused by the nature of the tensile test, where the material is put under longitudinal loading before a brittle failure occurs. The large stresses place on the composite samples would expect to fail at regions with a high resin content, end of fibre bundles or across sections with misaligned fibres as these regions would not be able to transfer the load as effectively compared to an aligned, continuous and high fibre volume fraction composite. Fibre pull-out is shown in Figure 55d where a clear hole in the resin is present or fibres are left with little to no resin surrounding them. The weak bonding between the resin and fibres was the cause of this failure characteristic.

The longitudinal failure analysed in Figure 56a-b show larger resin debris for short-fibre composites compared to continuous fibre composites. The matrix deformation in Figure 56a have been caused by the tensile forces. It can be seen that shear matrix failures and hackles have been formed by the brittle manor of failure that is common for composites. Figure 56b shows the fibre fractures observed by the some of the fibres. These cracks are not frequent and they may have already been created during the manufacture and production processes.

(56a)

(56b)
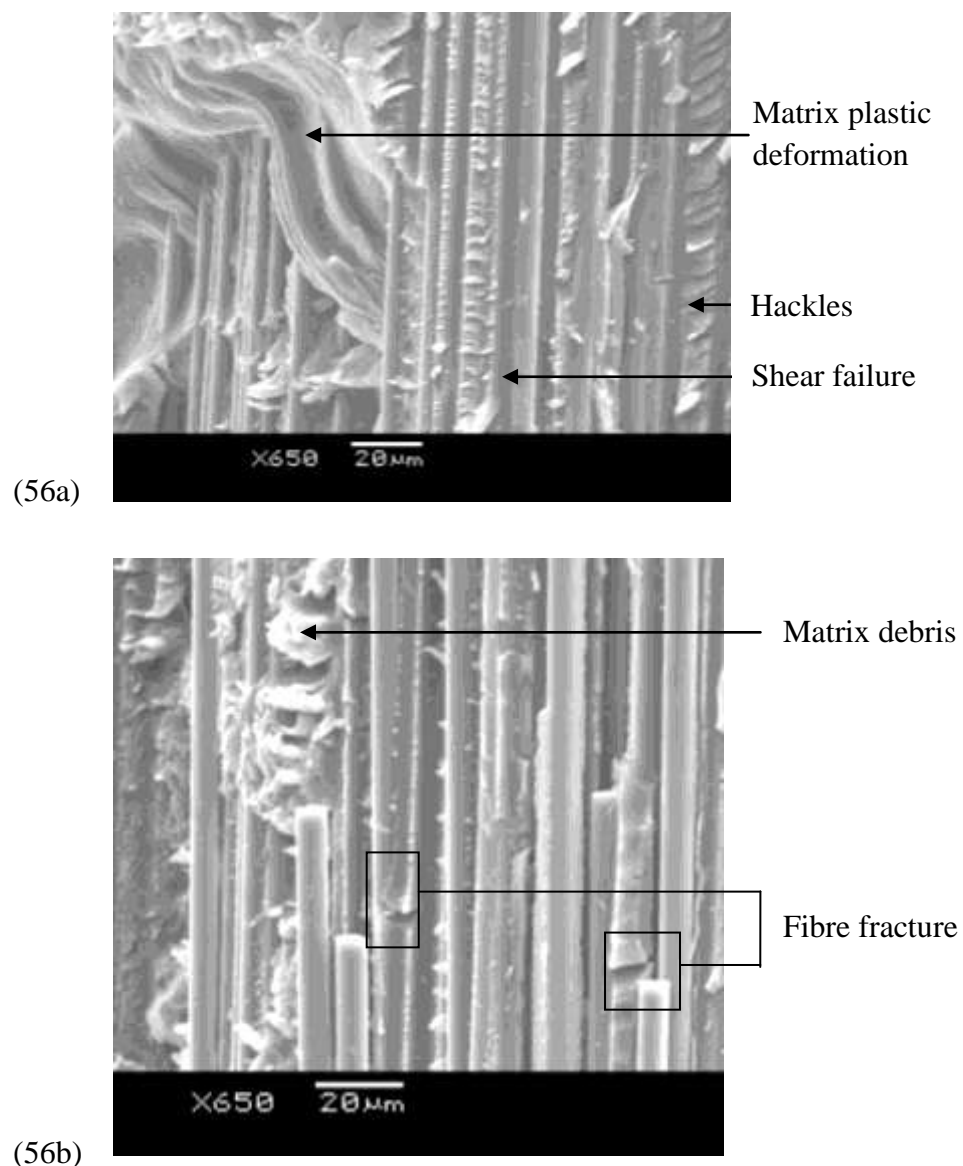
Figure 56 Micrographs of short carbon fibre samples imaged from a longitudinal angle, (a) matrix deformation and (b) fibre fracture.
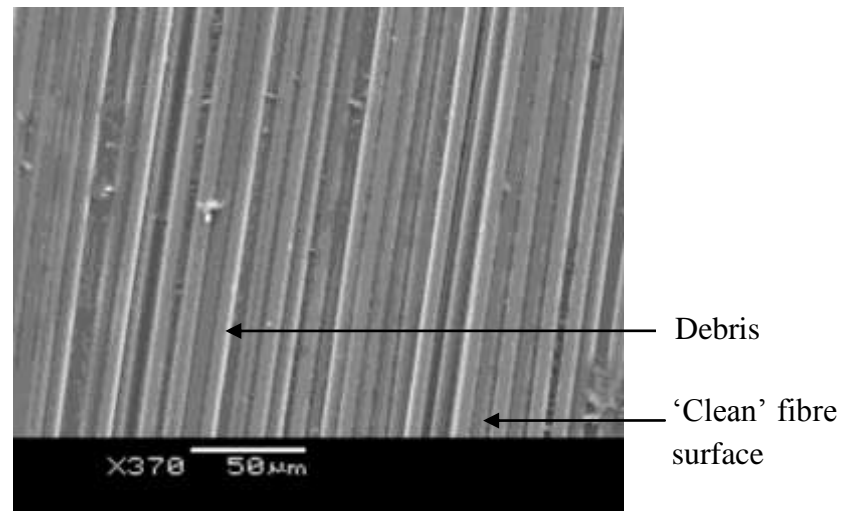
Figure 57 Micrograph of the planar fracture along a short-carbon fibre surface after tensile failure.

Figure 57 shows the planar fracture along the surface of the fibres of a short-fibre composite. The surface micrographs show 'clean' continuous fibres with no fibre fracture. A small amount of matrix debris was present on the surface of the fibres but would be unlikely that this created any fracture as it was created after the fracture of the composite. In conclusion the failure features of the short carbon fibre composites were matrix cracking, fibre pull-out and delamination. The failure initiates from fibre ends; a key characteristic to aligned composites.

7 Conclusions

The study developed a novel method for manufacturing aligned short-fibre prepregs. The fibre chopper technique possesses numerous factors that influence the quality and control of the fibre delivery, orientation and content. Ensuring the greatest control and achieving a compromise between the parameters ensures the composite quality is maintained. Additionally it is apparent by using simple visual analysis methods the fibre chopper can produce glass fibre and carbon fibre prepregs with desirable fibre volume fractions and a fibre alignment of at least 70%.

Based on the findings, control of the parameters is critical to the production of composites with the desired properties. In this report, the quality of the fibre chopper blades were investigated, concluding a used blade causes more debris and damage to the fibre end. Determining regular blade replacement is critical to sustain overall material properties. To ensure the quality of the fibre end is at a most desirable state, a logically approach has been stated to find a balance between blade wear and the point of blade replacement.

The eight-ply short-fibre composites boast comparable physical properties to their unidirectional continuous fibre composite counter-parts. Experimentally determined mechanical properties also compare favourably to alternative short-fibre alignment methods stated in the literature. This suggests that the technique developed in this study is suitable for producing an aligned short-fibre composite.

It was found that the dominate fracture features of the short-fibre composites include fibre pull-out, ply delamination and matrix cracking; common observations in fractured tensile samples with aligned fibres.

Overall the fibre chopper-based delivery system has demonstrated a successful approach to recycling waste continuous fibres. The novel technique has shown that highly aligned short glass fibre and short carbon fibres prepregs and composites can be manufactured.

8   Future Work

The method described in the current report, produces aligned and reproducible prepregs, but it will be important to deliver good quality prepregs. Future work to follow on from this report should be aimed at controlling the following areas to improve the current process: (i) the prepreg hand-lay-up technique; (ii) chopper head set-up of the feeder roller, rubber anvil and chopper-head; (iii) fibre delivery rate; and (iv) uniform fibre application on the resin film.

This system also lends itself to investigations to expand on the current technique and introduce new parameters into the system: (i) the influence of longer length fibres, (ii) the increase in rate of prepreg production, (iii) build up hybrid composites containing glass fibre and carbon fibres and (iv) develop the short-fibre composites to integrate small diameter optical fibres to enable damage detection.

Overall it is critical that the purpose of any future experimental methods should aim to: (a) improve on the manufacturing performance in terms of efficiency, (b) maintain or improve on the current prepreg quality and (c) successfully recycle waste continuous fibres using the fibre chopper system.

9   Appendices

9.1   Recycling

The implementation of European legislation in the composite industry requires that 85% of composite waste must be recycled and reused by 2015 [1]. The increasing pressure from the EU landfill directive [61] and UK landfill tax [62] encourage a diversion from landfill. Landfill is traditionally one of the largest forms of waste disposal for FRPC. With taxes rising by 33% to £32 per tonne for 2008 and increasing £8 per year until 2010 as well as EU directives for disposal of waste [62] landfill costs are rapidly on the increase. Consequently there is an urgent need to develop techniques to reuse, recycle or redevelop preforms and composites. This will reduce the current disposal rate of preforms and composites, as 95% were buried in landfill sites in the UK [1], while alternative routes such as reuse and mechanical recycling account for the remainder [63].

The volume of waste produced by the whole composite market was estimated to the 156,000 tonnes in 2000, with approximately 70% from end-of-life waste and the remaining 30% from production; with projections doubling by 2015 [64].

Environmental factors are one of the more critical factors affecting the composite industry, due to the lack of clear recycling routes available. To make recycling procedures as easy and cost effective as possible, composite waste needs to be recovered in as clean and pure a condition as is feasible. However this can be difficult to achieve from the adhesion of fibres to resin. The process to clean and label materials can be a costly and labour intensive procedure where the effects can also lead to contamination. The safe and green disposal of composites is an increasing concern to many of the composite producers and users when products begin to reach their service end of life.

Current production of carbon fibre tow is at a global rate of 27,000 tonnes each year, as well as costing upwards of £10,000 per tonne if new [65] so recyclability of carbon fibre tows and composites is an advantage. Key factors which are limiting recycling process methods are techniques to remove the epoxy resin whilst maintaining the fibre quality and properties. A method such as pyrolysis, thermally degrades the epoxy resin by a reduction reaction, that is now used by Recycled Carbon Fibre (UK). Chemical removal of the epoxy matrix is also being investigated (University of Nottingham) which uses a solvent to effectively strip the fibres but maintain the strength and stiffness they originally had [65]. Typical applications that will benefit from recycling carbon fibre could be for light weight body panels, chassis etc in the automotive sector as well as marine, aerospace and other industries [65].

A report from Lucintel (Dallas Texas) [17] has stated that the demand for short-fibre thermoplastic composites has steadily increased, passing $4.3 billion in 2008. Glass fibre usage has reached the regional of 2.3 million tonnes worldwide per year [66] with the UK producing 240,000 tonnes of composite products in 2000 [31]. With production values increasing each year and the EU legislation to reduce the amount of composite waste in landfill recycling techniques are necessary. These changes over time have lead to increased demand to improve recyclability of waste fibres which has introduced many techniques that fabricate aligned short-fibre thermosetting composites.

Recycling techniques of composite waste can be grouped into four main categories [67]:

- Primary recycling – conversion of waste into material having properties which are equivalent to the original material.

- Secondary recycling – conversion of waste to material which has inferior properties to the original material.

- Tertiary recycling – conversion of waste into chemicals and fuel.

- Quaternary recycling – conversion of waste into energy by incineration.

The most attractive recycling option is to recycle waste into material with equivalent properties that are comparable to the original material. Successful composite recycling requires incentives, infrastructure, recycling techniques and market commitment [67]. Current preform recycling efforts are dominated through two main techniques: (i) comminution techniques where preforms are ground, chipped, or flaked into a powder size that can be used as a filler material for polymer processing; and (ii) thermal techniques which can recover fibres to be then chopped into short-fibres to produce sheet-moulded compounds (SMC) or dough-moulded composites (DMC). Thermal techniques can also recover energy and chemical compounds from the polymer materials.

10 References

[1] GPRMC. EU Waste legislation becoming more severe, Press release 2001 <www.gprmc.be/PressReleases.htm> viewed 20/1/11.

[2] Cantwell, W.J., Morton, J. The impact resistance of composite materials: A review. *Journal of Composites* 1991: 22:347-362.

[3] Hull, D., Clyne, T.W. *An introduction to composite materials*. Cambridge University press, 1992 Ed 2.

[4] Nam-Jeong, L., Jang, J. The effect of fibre-content gradient on the mechanical properties of glass-fibre-mat/polypropylene composites. *Composites Science and Technology* 2000:60:209-217.

[5] Stewart, R. Carbon fibre composites poised for dramatic growth. <http://www.reinforcedplastics.com/view/1464/carbon-fibre-composites-poised-for-dramatic-growth/> viewed 12.4.11.

[6] Tarr. A. Polymer basic. Basic principles of materials 2007. <http://www.ami.ac.uk/courses/topics/0209_pme/index.html> viewed 10.11.11.

[7] Piggot. M. R. Load bearing fibre composites. Kluwer. 2002:2:251-253.

[8] Bora, M.O., Coban, O., Sinmazcelik, T., Gunay, V. Effect of Fiber Orientation on Scratch Resistance in Unidirectional Carbon-Fiber-Reinforced Polymer Matrix Composites. *Journal of Reinforced Plastics and Composites* 2010:29:1476 – 1490.

[9] Wong, D.W.Y., Lin, L., McGrail, P.T., Peijs, T., Hogg, P.J. Improved fracture toughness of carbon fibre/epoxy composite laminates using dissolvable thermoplastic fibres. *Composites Part A: Applied Science and Manufacturing* 2010:41:759-767.

[10] Composites-by-design. bridging the gap between art & technology with carbon fibre. Composite Processes. The Manufacturing Process. Rendering courtesy Verisurf Software <http://composites-by-design.com/?page_id=61> viewed 03.05.11.

[11] Pandita, S.. Smith, C.. S-Gale, N., Paget, M., Allen, J.M., Fernando, G.F. "Clean" Filament Winding: A New Manufacturing Process' 2007.

[12] Starr, T.F. Pultrusion for engineers. Woodhead publishing Ltd. Pg 24-26.

[13] Cantwell, W. J, Morton, J. Detection of Impact Damage in CFRP Laminates. *Composite Structures* 1985:3:241-257.

[14] Harper, L.T., Turner, T.A., Martin, J.R.B., Warrior, N.A. Fiber Alignment in Directed Carbon Fiber Preforms - Mechanical Property Prediction. *Journal of Composite Materials* 2010:44:931-951.

[15] Short, G.J., Guild, F.J., Pavier, M.J. Delaminations in flat and curved composite laminates subjected to compressive load. *Composite Structures* 2002:58:249–258.

[16] Curtis, P.T., Bader, M.G., Bailey, J.E. The stiffness and strength of a polyamide thermoplastic reinforced with glass and carbon fibres. *Journal of Materials Science* 1978:1:377-390.

[17] Lucintel. Six short-fiber thermoplastics suppliers are analyzed, with SABIC and DuPont identified as market leaders. Composites World <http://www.compositesworld.com/news/lucintel-report-assesses-short-fiber-thermoplastics-market > 2009 viewed 11.01.11.

[18] Milewski, J.V. "Short Fiber Reinforcement: Where the Action is *Plastics Compounding*. 1979:17-37.

[19] Taib, R.M. Cellulose fiber-reinforced thermoplastic composites: processing and products characteristics. Thesis. Virginia Tech, Blacksburg 1998:123.

[20] Mouhmid, B., Imad, A., Benseddiq, N., Benmedakhène, S., Maazouz, A. A study of the mechanical behaviour of glass fibre reinforced polyamide 6, 6: Experimental investigation. *Polymer testing* 2006:25:544-552.

[21] Harper, L.T., Turner, T.A., Martin, J.R.B., Warrior, N.A. Fiber Alignment in Directed Carbon Fiber Preforms - A Feasibility Study. *Journal of Composite Materials*. Published online 15.10.08.

[22] Flemming, T., Kress, G., Flemming, M. A new aligned short-carbon-fiber-reinforced thermoplastic prepreg. *Journal of Advanced Composite Materials* 1995:5:151-159.

[23] Fu, S.Y., Lauke, B.. Effects of fiber length and fiber orientation distributions on the tensile strength of short-fiber-reinforced polymers. *Composite Science Technology* 1996:56:1179-1190.

[24] Thomason, J. The influence of fibre length and concentration on the properties of glass fibre reinforced polypropylene: 5. Injection moulded long and short fibre polypropylene. *Composite.Part A* 2002:33:1641-1652.

[25] Choi, N. S., Takahashi, K. Stress fields on and beneath the surface of short-fibre-reinforced composites and their failure mechanisms. *Composites Science and Technology* 1992:43:237-244.

[26] Tsuji, N., Springer, G,S., Hegedus, I. The Drapability of Aligned Discontinuous Fiber Composites. *Journal of Composite Materials* 1997:31:428-465.

[27] Bowen, C.R., Dent. A.C., Nelson, L. J., Stevens, R., Cain, M.G., Stewart. M. Failure and volume fraction dependent mechanical properties of composite sensors and actuators. *Journal of Mechanical Engineering Science* 2006:220:1655-1663.

[28] Epaarachchi, J., Ku, H., Gohel, K. A simplified empirical model for prediction of mechanical properties of random short fiber/vinylester composites. *Journal of Composite Materials* 2010:44:779-788.

[29] MacLaughlin, T. F., Barker, R. M. Effect of modulus ratio on stress near a discontinuous fibre. *Experimental Mechanics* 1972:12:178.

[30] Tucker, C.L., Liang, E. Stiffness prediction for unidirectional short-fiber composites: review and evaluation. *Composite Science and Technology* 1999:59:655-671.

[31] Harper, L.T., Turner, T.A., Martin, J.R.B., Warrior, N.A. Fiber alignment in directed carbon fibre performs – a feasibility study. *Journal of Composite Materials* 2009:43:57-74.

[32] Fu, S.-Y, Lauke, B, Mäder, E, Yue, C.-Y, Hu, X. Tensile properties of short-glass-fiber and short-carbon-fiber-reinforced polypropylene composites. Composites Part A: Applied science and Manufacturing 2000:31:1117-1125.

[33] Price, C.D., Hine, P.J., Whiteside, B., Cunha, A.M., Ward, I.M. Modelling the elastic and thermoelastic properties of short-fibre composites with anisotropic phases. *Composites Science and Technology* 2005:66:69-79.

[34] Hine, P. J., Duckett, R.A., Davidson, N., Clarke, A.R. Modelling of the elastic properties of fibre reinforced composites. I: orientation measurement. *Composites Science and Technology* 1992:47:65-73.

[35] Zak, G., Haberer, M., Park, C. B., Benhabib, B. Mechanical properties of short-fibre layered composites: Prediction and experiment. *Rapid Prototyping Journal* 1999:6:107-118.

[36] Sirkis, J. S., Lo, Y. L., Nielsen, P. L. Phase-strain model for polarimetric strain sensors based on fictitious residual strains. *Journal of Intelligent Material Systems and Structures* 1994:5:494-500.

[37] Charrier, J. M., Ciplijauskas, R.V., Doshi, S. R., Hamel, F.A. ANTEC 1986:939-943.

[38] Itoh, T., Hirai, H., Isomura, R. *Journal of Japan Institute of Light Metals* 1998:38:620-625.

[39] Yamashita, S., Hatta, H., Sugano, T., Murayama, K. Fiber orientation control of short-fibre composites: experiment. *Journal of Composite Materials* 1989:23:32-41.

[40] Bozarth, M. J., Gillespie Jr, J.W., McCullough, R,L. ANTEC 1986:568-572.

[41] Jackson, W. C, Advani, S.G, Tucker, C.L. Predicting the orientation of short fibers in thin compression mouldings. Journal of Composite Materials 1986:20:539-557.

[42] Kacir, L., Narkis, M., Ishai, O. Oriented short glass-fiber composites: Preparation and statistical analysis of aligned fiber mats. *Polymer Engineering Science* 1975:15:525-537.

[43] Edwards, H., Evans, N.P. Advances in Composite Materials; proceeding of the third international conference on composite materials 1980:2:1620-1635.

[44] Hannant, D.J., Spring, N. Magazine of Concrete Research 1974:26:47-48.

[45] Richter, H. Advances in Composite Materials; proceedings of the third international conference on composite materials 1980:1:387-398.

[46] Papathanasiou, T.D., Guell, D.C. Flow induced alignment in composite materials. Woodhead publishing 1997.

[47] Guell, D. C., Graham, A.L. Improved mechanical properties in hydrodynamically aligned, short-fibre composite materials. *Journal of Composite Materials* 1996:30:2-12.

[48] Fara, S., Pavan, A. Fibre orientation effects on the fracture of short fibre polymer composites: on the existence of a critical fibre orientation on varying internal material variables. *Journal of Materials Science* 2004:10:3619-3628.

[49] Calverty, P., Lin, T.L., Martin, H. Extrusion freeform fabrication of chopped-fibre reinforced composites. *High Performance Polymers* 1997:9:449-456.

[50] Sanomura, Y., Kawamura, M. Fiber orientation control of short-fiber reinforced thermoplastics by ram extrusion. *Polymer Composites* 2003:24:587-596.

[51] Sanomura, Y., Hayakawa, K., Mizuno, M., Kawamura,M. Effects of process conditions on Young's modulus and strength of extrudate in short-fiber-reinforced polypropylene. *Polymer Composites* 2007:28:29-35.

[52] Peng, J., Lin, L.T., Calvert, P. Orientation effects in freeformed short-fiber composites. *Composites Part A: Applied Science and Manufacturing* 1999:30:133-138.

[53] Chirdon, W. M., O'Brien, W. J., Robertson, R. E. Fraunhofer diffraction of short-fiber-reinforced composites aligned by an electric field. Electrostatics. *Dental Materials* 2006:22:107-11.

[54] Dodworth, A. Bentley motors develops unique directional carbon fibre preforming process for chassis rails. SPE Automotive Composites Conference & Exhibition 2009.

[55] Turner, T.A., Warrior, N.A., Pickering, S. High performance composite materials from recycled carbon fibre. National composite network 2007. <http://ncn-uk.co.uk/DesktopModules/ViewDocument.aspx?DocumentID=691> viewed 24.06.11.

[56] Hassan, A., Yahya, R., Yahaya, A.H., Tahir, A.R. M., Hornsby, P. R. Tensile, impact and fiber length properties of injection-molded short and long glass fiber-reinforced polyamide 6,6 composites. *Journal of Reinforced Plastics and Composites* 2004:23:969-986.

[57] ASTM D2584 (2002).

[58] ASTM D2734 (2003).

[59] ASTM D3039 (2008).

[60] Jameson, N.L. Production and evaluation of aligned short-fibre composites. Final Year Project. University of Birmingham. 2010.

[61] Waste: Commission calls time on sub-standard landfills in the EU. 1999 <http://europa.eu/rapid/pressReleasesAction.do?reference=IP/09/1154&format=HTML&aged=0&language=EN&guiLanguage=en> viewed 27.02.11.

[62] Landfill tax 2010 <http://archive.defra.gov.uk/environment/waste/topics/index.htm#landfill> viewed 31.05.11.

[63] GPRMC JEC- Press release: the green FRP label 2003 <http://www.gprmc.be/PressRelease.htm> viewed 19.1.10.

[64] Harbers, F. Green recycling label- The step towards closing the loop, 3rd automotive seminar France 2002.

[65] Marsh, G. Recycling carbon fibre composites. Reinforced Plastics.com 22.04.09.

[66] NNFCC 2007 <http://www.nnfcc.co.uk/metadot/index.pl?id=2718> viewed 25.0411.

[67] Halliwell,S. End of life options for composite waste. Recycle, reuse or dispose? National composite network best practice guide 2006 <http:/ww.netcomposites.com/> viewed 31.05.11.